JOINT TRANSPORTATION
RESEARCH PROGRAM
INDIANA DEPARTMENT OF TRANSPORTATION
AND PURDUE UNIVERSITY

Self-Healing Cementitious Composites (SHCC) with Ultrahigh Ductility for Pavement and Bridge Construction

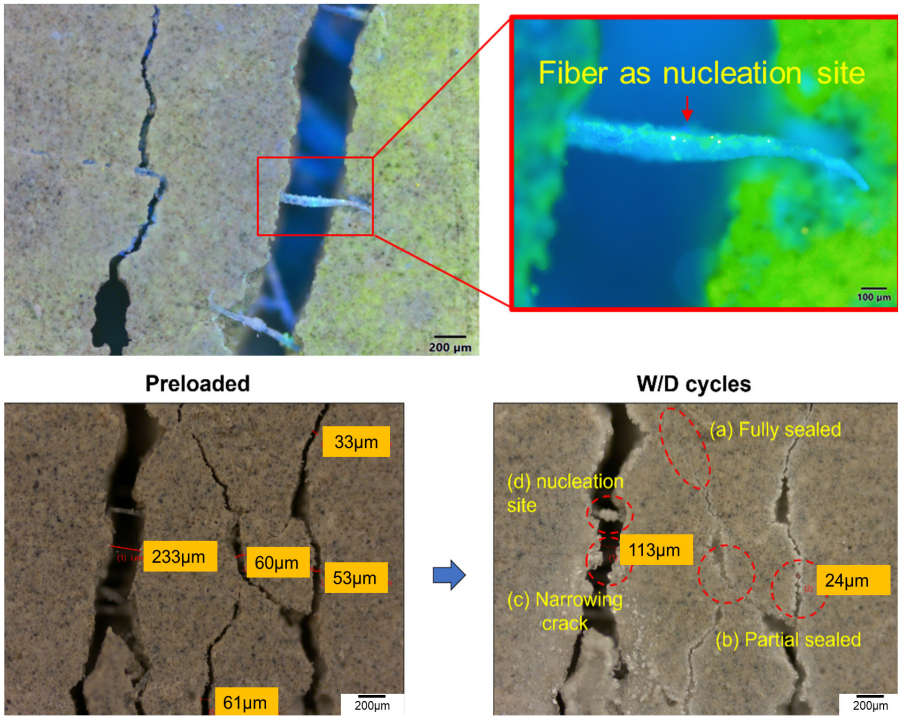

Cihang Huang, Yen-Fang Su, Na (Luna) Lu

SPR-4326 • Report Number: FHWA/IN/JTRP-2021/36 • DOI: 10.5703/1288284317403

RECOMMENDED CITATION

Huang, C., Su, Y.-F., & Lu, N. (2021). *Self-healing cementitious composites (SHCC) with ultrahigh ductility for pavement and bridge construction* (Joint Transportation Research Program Publication No. FHWA/IN/JTRP-2021/36). West Lafayette, IN: Purdue University. https://doi.org/10.5703/1288284317403

AUTHORS

Cihang Huang
Graduate Research Assistant
Lyles School of Civil Engineering
Purdue University

Yen-Fang Su
Graduate Research Assistant
Lyles School of Civil Engineering
Purdue University

Na (Luna) Lu, PhD
ACPA Professor
Lyles School of Civil Engineering
Purdue University
(765) 494-5842
luna@purdue.edu
Corresponding Author

JOINT TRANSPORTATION RESEARCH PROGRAM

The Joint Transportation Research Program serves as a vehicle for INDOT collaboration with higher education institutions and industry in Indiana to facilitate innovation that results in continuous improvement in the planning, design, construction, operation, management and economic efficiency of the Indiana transportation infrastructure. https://engineering.purdue.edu/JTRP/index_html

Published reports of the Joint Transportation Research Program are available at http://docs.lib.purdue.edu/jtrp/.

NOTICE

TECHNICAL REPORT DOCUMENTATION PAGE

1. Report No. FHWA/IN/JTRP-2021/36	2. Government Accession No.	3. Recipient's Catalog No.
4. Title and Subtitle Self-Healing Cementitious Composites (SHCC) with Ultrahigh Ductility for Pavement and Bridge Construction		**5. Report Date** December 2021 **6. Performing Organization Code**
7. Author(s) Cihang Huang, Yen-Fang Su, and Na (Luna) Lu		**8. Performing Organization Report No.** FHWA/IN/JTRP-2021/36
9. Performing Organization Name and Address Joint Transportation Research Program Hall for Discovery and Learning Research (DLR), Suite 204 207 S. Martin Jischke Drive West Lafayette, IN 47907		**10. Work Unit No.** **11. Contract or Grant No.** SPR-4326
12. Sponsoring Agency Name and Address Indiana Department of Transportation (SPR) State Office Building 100 North Senate Avenue Indianapolis, IN 46204		**13. Type of Report and Period Covered** Final Report **14. Sponsoring Agency Code**

15. Supplementary Notes

Conducted in cooperation with the U.S. Department of Transportation, Federal Highway Administration.

16. Abstract

Cracks and their formations in concrete structures have been a common and long-lived problem, mainly due to the intrinsic brittleness of the concrete. Concrete structures, such as rigid pavement and bridge decks, are prone to deformations and deteriorations caused by shrinkage, temperature fluctuation, and traffic load, which can affect their service life. Rehabilitation of concrete structures is expensive and challenging—not only from maintenance viewpoints but also because they cannot be used for services during maintenance. It is critical to significantly improve the ductility of concrete to overcome such issues and to enable better infrastructure quality. To this end, the self-healing cementitious composites (SHCC) investigated in this work could be a promising solution to the aforementioned problems.

In this project, the team has designed a series of cementitious composites to investigate their mechanical performances and self-healing abilities. Firstly, various types of fibers were investigated for improving ductility of the designed SHCC. To enhance the self-healing of SHCC, we proposed and examined that the combination of the internal curing method with SHCC mixture design can further improve self-healing performance. Three types of internal curing agents were used on the SHCC mixture design, and their self-healing efficiency was evaluated by multiple destructive and non-destructive tests. Results indicated a significant improvement in the self-healing capacity with the incorporation of internal curing agents such as zeolite and lightweight aggregate. To control the fiber distribution and workability of the SHCC, the mix design was further adjusted by controlling rheology using different types of viscosity modifiers. The team also explored the feasibility of the incorporation of colloidal nano-silica into the mix design of SHCC. Results suggest that optimum amounts of nano-silica have positive influence on self-healing efficiency and mechanical properties of the SHCC. Better hydration was also achieved by adding the nano-silica. The bonding strength of the SHCC with conventional concrete was also improved. At last, a standardized mixing procedure for the large scale SHCC was drafted and proposed.

17. Key Words	18. Distribution Statement
self-healing, fiber reinforced cementitious composite, internal curing, rheology, colloidal nano silica	No restrictions. This document is available through the National Technical Information Service, Springfield, VA 22161.

19. Security Classif. (of this report)	20. Security Classif. (of this page)	21. No. of Pages	22. Price
Unclassified	Unclassified	62 including appendices	

EXECUTIVE SUMMARY

Introduction

The formation of cracks in concrete structures is commonly observed due to the intrinsic brittleness of the concrete. Concrete structures, such as rigid pavement and bridge decks, are prone to deformation and deterioration caused by shrinkage, temperature fluctuation, and traffic load, which can affect the service life of the structure. The rehabilitation of the concrete structure can be expensive and challenging since they are in continuous service. Therefore, it is critical to develop self-healing cementitious composites (SHCC) with ultra-high ductility to potentially overcome the aforementioned issues.

In this project, the team designed a series of cementitious composites to investigate their mechanical performance and self-healing ability. First, various types of fibers were investigated to improve the ductility of the designed SHCC. To enhance the self-healing of SHCC, we tested if the combination of the internal curing method with SHCC mixture would improve self-healing performance. Three types of internal curing agents were used on the SHCC mixture design, and the self-healing efficiency was evaluated by using multiple non-destructive tests. The results indicate a significant improvement in the self-healing capacity with the incorporation of the internal curing agents. To control the fiber distribution and workability of the SHCC, the mix design was further adjusted by controlling the rheology using different types of viscosity modifiers. The team also explored the feasibility of the incorporation of nano-silica into the mix design of SHCC. Better hydration was achieved by adding the nano-silica. Moreover, the bonding strength between the SHCC and conventional concrete layer was further improved. The results suggest that a certain amount of nano-silica would positively influence self-healing efficiency and the mechanical properties of the SHCC. Finally, a standardized mixing procedure for the SHCC was also developed.

Findings

We have conducted a comprehensive investigation of a series of self-healing cementitious composites with various mix designs. Extensive experiments were performed to investigate the effectiveness of different variables, such as fibers properties, internal curing agents, and various additives in SHCC. The findings of this project are detailed as follows.

1. *Findings related to different fibers.*

    - Mechanical and crack width control ability of six different types of fibers, PVA (Polyvinyl Alcohol) Fiber, Strux 90/40, Masterfiber Mac Matrix, Fiberforce 650, Suf-Strand SF and Forta-Ferro One, were evaluated with SHCC design. Experimental results showed that SHCC samples with various fibers incorporated exhibited pseudo-strain-hardening behavior during the loading process due to the bridging effect of the fibers.
    - Among the six mixtures tested, samples with PVA (Polyvinyl Alcohol) fiber exhibited higher mechanical strength performance. For compressive strength, the PVA-SHCC performed 10% to 165% higher than others; for tensile strength results, the PVA-SHCC exceeded other sets by 24% to 65%; for flexural strength, the PVA-SHCC behaved 5% to 101% higher than SHCC incorporated with other fibers.
    - Analysis of the flexural deflection shows that the crack width control ability of the PVA fiber is stronger than other fibers. PVA fiber can control the propagation of the crack width by generating multiple narrowed cracks, while fewer cracks were formed in the sample with macro-fibers. It is also observed that PVA-SHCC exhibited a lower flexural strain capacity compared with others, which could be due to the shorter length of PVA that makes it easier to be pulled out during the loading.
    - Based on the experimental result, PVA fiber is the most suitable fiber for the design of SHCC since it can lead to higher mechanical strength and smaller crack width, which is favorable for self-healing.

2. *Findings related to internal curing aggregates.*

    - Two types of internal curing aggregates, Zeolite, and lightweight aggregate were used and evaluated with SHCC. Mechanical test results indicate that when internal curing aggregates were used, the samples showed over 15% compressive strength improvement for the cementitious composites sample with zeolite and a 6% improvement with lightweight aggregate.
    - The use of the zeolite could increase the healing ratio from around 2.0% to over 5.0% after the self-healing of 7 wet/dry cycles (28 days) based on two non-destructive tests. Results of the experiment suggest that the optimal zeolite replacing ratio for sand may be around 15 wt%. The self-healing performance of SHCC incorporated with lightweight aggregate was compared with the zeolite. The results indicate that the lightweight aggregate improved the healing efficiency of the SHCC, but the improvement was not as significant as zeolite.
    - Pore structure analysis suggests that the zeolite has a finer pore size compared to lightweight aggregate (LWA). During the self-healing period, zeolite is capable of slowly but continuously supplying water to cementitious materials. The continued water supply led to a better autogenous self-healing performance.
    - Experimental results provide solid evidence that the internal curing aggregates can enhance healing efficiency by providing water internally to accelerate the autogenous healing.

3. *Findings related to superabsorbent polymer (SAP).*

    - Properties of the SAP were investigated and their robustness evaluation shows that the SAP can be influenced by the superplasticizer, hydration accelerator, and fly ash. However, only a minor influence of less than 10% was observed. Therefore, it can be concluded that SAP is relatively robust under the designed environmental conditions.
    - During the experiments, a dramatic reduction in the water flow rate from 0.2 g/s to 0.02 g/s was observed within 60 seconds of the test when the SAP was incorporated. Experimental results indicate that SAP is an effective material for sealing the cracks in concrete materials.
    - Evaluation of the influence of the SAP on the rheology of cement paste shows that as the dosage of the SAP increased from 0% to 0.24 wt% of cement, the plastic viscosity showed a dramatic improvement of over 56%.

This suggests that the incorporation of the SAP may be able to improve interfacial friction between fiber and matrix and further enhance the fiber distribution.

- Mechanical tests for the SHCC incorporated with SAP indicate that incorporating the SAP particles reduced the 7-days compressive and flexural strength of the sample by over 25% and 20%, respectively, which was due to the large voids left by the dried SAP particles. It was also found that with a small dosage of the SAP, the 7-days tensile performance of the SHCC was slightly improved by around 13.8%. This may be due to the improvement of fiber distribution and that the void created by the SAP could act as flaws that triggered the formation of multiple cracks. However, with a higher dosage of SAP, the tensile strength was decreased again because of the large quantity of voids.

4. *Findings related to viscosity modifying admixtures (VMA).*

   - Three types of viscosity modifying agents were used, and the properties of the SHCC were evaluated. The viscosity results indicated that compared with thickening-type VMA, the binding-based VMA can better increase the viscosity of fresh SHCC. The increase of the viscosity of SHCC can prevent segregation, which improves the interfacial properties between fiber and matrix and fiber distribution.
   - Mechanical tests results suggest that VMA 450 (binding type) can effectively enhance the ductility of SHCC due to the improvement of the fiber-matrix interface quality and the fiber distribution.

5. *Findings related to the nano-silica based SHCC.*

   - The team investigated the mechanical properties and self-healing performance of SHCC incorporated with colloidal nanosilica. The experimental result shows that colloidal nanosilica can significantly improve mechanical strength. For the compressive strength result, the nanosilica-based SHCC can reach over 5,500 psi at 90 days. Flexural strength results indicate that SHCC with nanosilica showed 7% to 9% higher flexural strength than the reference set. Tensile results of SHCC suggest that the nanosilica-based SHCC had a higher tensile strength of over 500 psi.
   - Self-healing evaluation suggests that the incorporation of nanosilica presents a positive impact on autogenous healing of the SHCC. The result of the resonant frequency test indicates that under the wet/dry cycle condition, the RF recovery ratio of nanosilica-based SHCC can recover 15% or above for 28 days. After the designed self-healing period, the tensile testing revealed that the SHCC sample with E5 colloidal nano silica (CNS) can reach a higher tensile strength and stiffness retention ratio than the reference SHCC sample.

6. *Large scale SHCC sample testing.*

   - To study the feasibility of utilizing designed material in real field application, the team prepared the SHCC mixture on a large scale. The workability assessment by slump and J-ring tests indicates that the designed SHCC with VMA possesses excellent workability and passing ability which is comparable with self-consolidating concrete (SCC).
   - Layered structure beam was designed and tested to further study the flexural performance of SHCC/concrete composite. Different layer ratios between SHCC and concrete were designed, and the result suggests that as the ratio of the SHCC layer increased, a higher modulus of rupture (MOR) could be achieved. Specifically, the SHCC and concrete ratio of 3:1 can achieve the optimal flexural performance.
   - A standardized mixing procedure for the large scale SHCC was developed based on the large batch mixing. In the standardized procedure, it is suggested that extra attention needs to be made to check the inner wall of the mixer to ensure any agglomerate of the cementitious materials could be mixed and dispersed by the mixer. In addition, any additives that may counterweigh the effect of the VMA should be added after the well-mix of the PVA fibers.

Implementations

The objective of this project is to develop ductile self-healing cementitious composites (SHCC), which can be used in concrete applications especially for link-slab. The SHCC was delivered to INDOT as a reference for the design of concrete materials with ultra-high ductility and self-healing ability that can reduce the need for conventional rehabilitation.

- To ensure the quality of the fiber distribution and the ductility of the SHCC, PVA fiber with short fiber length, high tensile strength, and aspect ratio was chosen. Better mechanical properties and crack width control ability can therefore be expected.
- The internal curing method was applied into the design of the SHCC to further improve the self-healing performance. Internal curing aggregates with high porosity and small pore size, such as zeolite, performed better in the improvement of the healing efficiency. Optimal sand replacing ratio for zeolite is around 15 wt%.
- Superabsorbent polymer (SAP) can effectively seal the crack within a short period; however, it has a negative influence on the mechanical performance of the SHCC.
- Viscosity modifying admixtures (VMA) can effectively improve the fiber distribution and fiber-matrix interface of the SHCC, especially when a higher water to cement ratio is used. The experimental result indicates VMA 450 (binding type) with a dosage of 1% performed the best in SHCC with a water to cement ratio of 0.35, in terms of ductility.
- Addition of the colloidal nanosilica can further improve the mechanical and self-healing performance of the SHCC. The test result suggests 0.6 wt% of cement as the optimal dosage. Also, the bonding strength between the SHCC and conventional concrete layer was increased with the addition of the nanosilica.
- SHCC mixture design with VMA has been proved to possess satisfied workability and passing ability, which is comparable with self-consolidating concrete (SCC).
- The combination of the SHCC with conventional concrete can improve the flexural performance of the beam sample. A higher flexural strength with high modulus of rupture (MOR) can be achieved.
- Different strategies for the design of the SHCC can be adopted based on certain applications. For a concrete patching project, it is more desirable to have SHCC with a better curing quality and higher bonding strength. Therefore,

it is recommended to incorporate the internal curing agent and colloidal nanosilica, which are proven to lead to better curing and bonding performance. A lower PVA fiber content of 1 vol% may be used to reduce the cost. On the other hand, if SHCC is used for a link slab application, ductility and the self-healing ability are favorable. Thus, a higher dosage of the PVA fiber, such as 2 vol% can be used. Internal curing agents such as zeolite can be incorporated to further improve the self-healing performance.

Limitations and Future Studies

The extensive experiments conducted in this project have laid the foundation for the design of ultra-high ductility self-healing cementitious composites (SHCC). This project proved the effectiveness of using internal curing agents to improve the self-healing performance of the designed cementitious composite. The properties of the SHCC can be adjusted by selecting different types of fibers, internal curing agents, and VMA based on specific requirements. Nevertheless, there are still several limitations as discussed below.

- Although the properties of the designed SHCC have been systematically evaluated in the laboratory and in the relatively large batch, the performance of the specimen prepared by in-field batch mixing equipment still needs to be verified.
- For the long-term durability, limited research has been done for the SHCC, such as freeze-thaw, chloride penetration, corrosion resistance, and alkali–silica reaction (ASR) resistance.

CONTENTS

LIST OF FIGURES

LIST OF TABLES

1. INTRODUCTION

1.1 Background

Cracks always occur in conventional concrete infrastructures such as bridge construction, particularly the link-slab application due to structural deflection, concrete shrinkage, and temperature variation. Significantly, combined with the freeze-thaw condition and the use of deicing salt in northern regions, the damage of concrete structures caused by cracks is further amplified. The existence of the cracks in concrete shortens the service life of the structure by generating a pathway for harmful compounds to invade concrete from the external environment. Additionally, concrete infrastructures, such as bridges and highway pavement, are always in continuous service, making the repair or replacement even harder. To address this problem, it is necessary to design ductile concrete with the ability to self-heal the cracks. The ductility could prevent the concrete materials from sudden failure; simultaneously, the self-healing ability could prevent the event of cracks propagation and elongate the service life of the concrete materials.

The presence of water is one of the most critical factors governing the efficiency of autogenous healing in concrete. The concept of incorporation of the internal water reservoir in concrete materials has been well developed for internal curing and shrinkage migration. The internal curing method has been widely used to supply water internally to eliminate early age shrinkage. Thus, the combination of internal curing and autogenous healing has the potential to enhance autogenous healing performance.

This study proposes to develop fiber-reinforced self-healing cementitious composites (SHCC) with ductility that can be used in bridge applications such as link-slab. The designed material has the necessary self-healing ability to heal the cracks within one season to eliminate the potential issues of reinforcement corrosion and crack propagation.

1.2 Objective

This program aims to develop ductile self-healing cementitious composites (SHCC), which enables the healing of formed cracks within one season cycle to eliminate the potential deterioration of concrete infrastructure. The self-healing performance of the concrete is evaluated with the incorporation of three different types of internal curing agents with various mix designs, including lightweight aggregate, zeolite, and super-absorbent polymer (SAP). A hypothesis is proposed that the incorporation of the internal curing agents can improve the self-healing behavior of the designed concrete and evaluated in this project. Various types of fibers are examined to optimize the mechanical properties of the material. The rheological properties of the SHCC are adjusted, and the nano-silica is used to improve the properties of the designed material. As such, this project provides a recommendation for the design guidelines of the cementitious composite with self-healing ability and excellent mechanical performance, which can be used in concrete application, especially for link-slab.

1.3 Organization of the Report

This report consists of seven chapters. This first chapter introduces the background and objective of this research. The second chapter reviews previous research for the design of high-performance concrete, including the design of self-healing cementitious composite, properties of fiber reinforced concrete, internal curing method, and the rheology control of the concrete materials. The third chapter evaluates and compares various types of fibers that can potentially use in SHCC. The fourth chapter reports the self-healing performance of the SHCC with the incorporation of the internal curing agents. The fifth chapter presents the rheology adjustment of the SHCC by different methods. The sixth chapter reports the further improvement of the SHCC by using nano-silica. The seventh chapter includes the large batch mixing and testing of the SHCC, and a standardized mixing procedure is provided. The last part of this report presents a conclusion and recommendation for the design of the SHCC.

2. LITERATURE REVIEW

Concrete is widely used in construction projects. Concrete structures can be designed to have a service life as long as several decades. However, cracking in concrete can lead to the deterioration of the structure. The formation of cracks can be attributed to a variety of reasons. Timely repairs and rehabilitation which can prevent further deterioration are necessary for the concrete structure. However, those works could be extremely expensive, not to mention infrastructures such as bridges, tunnels, and pavement require continuous service that can further increase the difficulty of the repair or rehabilitation.

To address the above-mentioned issues, concrete with the ability to self-heal the crack has been proposed and studied. The idea for self-healing concrete is that after the formation of cracks, concrete itself can regenerate solid substances that can block the cracks and even recover its mechanical strength.

2.1 Self-Healing of Concrete

Autogenous healing of the concrete is associated with the physical or chemical processes that occur in the cementitious matrix, as shown in Figure A.1 (Yang et al., 2009). By analyzing the healing product in the crack mouth, newly formed C-S-H gel (Jacobsen et al., 1995) and calcium carbonate were found (Edvardsen, 1999), which implies that the main mechanisms of the autogenous healing are the secondary hydration, carbonation of calcium hydroxide and the crystallization of portlandite ($Ca(OH)_2$) (Huang et al., 2016; Keskin

et al., 2016). Solid healing products can block the cracks and prevent the entrance of aggressive agents. As a result, the further deterioration of the concrete can be prevented, which ensures the service life of the structure (Yang et al., 2009). Among different autogenous healing mechanisms, secondary hydration has been proved to be highly responsible for the recovery of the mechanical properties of the concrete structure. The newly formed healing products from secondary hydration possess a strength property that is able to re-connect the crack face and concrete debris together (Snoeck, 2015).

One of the most important factors that can affect the efficiency of the self-healing is the selection of cementitious materials. Previous research indicates that partially replacing cement with fly ash and/or blast furnace slag can significantly improve the healing performance of the concrete (Termkhajornkit et al., 2009; Yang et al., 2009). The underlying mechanism is that compared with cement clinker, fly ash and slag possess a lower reactivity, leading to a decrease in the early age hydration rate. Therefore, a larger amount of unreacted cementitious materials can be reserve for secondary hydration. It is also worth noting that the pozzolanic reaction of the fly ash and slag requires the existence of the calcium hydroxide. And it is known that calcium hydroxide is one of the hydration products of the cement. Thus, the replacement of the cement by the fly ash or slag should be controlled and limited to ensure that a sufficient amount of the cement will be hydrated to produce calcium hydroxide which can be used for secondary hydration of the fly ash or slag (Zhang et al., 2014).

Different exposure conditions have been studied by various researchers (Hung et al., 2017; Roig-Flores et al., 2016; Sisomphon, 2013). Hung et al. (2017) evaluated the healing performance of cementitious composites under three different curing conditions: lab-controlled dry, water submersion and natural weathering with high humidity. The result shows that the samples cured in a lab-controlled environment exhibited limited healing performance, compared with the other two curing environments with water supply (Hung et al., 2018). A similar conclusion was also found in other research (Jiang et al., 2015; Ma et al., 2014). Thus, it can be seen that in order to achieve sufficient autogenous healing in cementitious material, water supply is of vital importance. During the autogenous healing process, water can act as a carrier for the fine particles and ions, and it is also indispensable for the chemical reactions. Previous research found out that the healing efficiency in wet/dry cycles is higher than that in complete water submersion. This may be due to the wet curing can provide water for secondary hydration, while the CO_2 is available for the precipitation of calcium carbonate during dry conditions. Therefore, the combination of secondary hydration and the carbonation during the wet/dry cycles can lead to a higher autogenous healing efficiency (Ma et al., 2014).

In addition to the mixture design and curing condition, the crack width is another factor that can significantly influence the healing efficiency. The width of the crack can directly determine the amount of healing products that are required to plug the crack (Gagné & Argouges, 2012). The internal tensile stress caused by the shrinkage, external loading, or thermal expansion may lead to the intensive propagation of the crack width. If the crack width can be controlled during the loading process, the autogenous healing performance can be improved. Therefore, fibers have been introduced to the development of self-healing concrete (Yang et al., 2009). The fiber can act as bridges inside the concrete material and limit the propagation of the crack mouth. In addition to the crack width control, the reinforced fiber can also act as nucleation sites for the secondary hydration and the carbonation of calcium hydroxide. According to the microscopic observation, the healing products were found on the bridging fiber across the crack (Homma et al., 2009).

Based on the mechanisms of the autogenous healing, it is an intrinsic ability of cementitious material; with proper design, the concrete material can possess self-healing ability without aggressively increasing the cost and construction difficulty (Van Tittelboom & De Belie, 2013).

2.2 Fiber-Reinforced Concrete

Concrete is a complex composite material composed of fine and coarse aggregate bonded with cement mortar. The border between different particles, especially the mortar-aggregate interface, is typically the weak spot of the concrete material (Akçaoğlu et al., 2004). The crack may therefore tend to generate at the weak spot during the service life of the concrete. Without timely repair, those cracks may propagate and cause further deterioration of the concrete structure. It can be expected that a crack with a larger width requires a larger amount of solid products in order to reach completed sealing (Yıldırım et al., 2015). Therefore, the control of crack width has the potential to further improve the efficiency of autogenous healing (Mihashi & Nishiwaki, 2012). To address this issue, researchers have used fiber as reinforcement to control the crack width in concrete material (Nishiwaki et al., 2012; Qian et al., 2010). Generally, the tensile strength of the fiber used in the concrete industry is much higher than that of the hardened concrete matrix. The fiber can improve the post-cracking behavior of the concrete material by transferring the stress between crack faces and controlling the increase of the crack width (Bischoff, 2003; Paipetis et al., 1999). In addition, previous studies indicated that fiber can be used to produce concrete material with increased toughness and durability performance (Kuder & Shah, 2010; Lau & Anson, 2006).

In fiber-reinforced concrete, upon the formation of the crack, embedded fibers with random distribution can act as bridges to limit the propagation of the crack

and transfer the stress across the mouth of the crack (Cattaneo & Biolzi, 2010; Kaufmann et al., 2019). As a consequence, the strength and durability of the concrete with the incorporation of fiber as reinforcement are generally higher than the plain concrete (Ding & Kusterle, 2000). Nowadays, various fiber types, such as steel fiber, glass fiber, carbon fiber, and PVA fiber, etc., have been developed and used in the concrete industry. Different parameters of the fiber, such as length and aspect ratio, can significantly affect the performance of the fiber-reinforced concrete (Afroughsabet et al., 2016).

The fiber geometry can intensively influence the concrete properties. In the Doo-Yeol Yoo et al., (2015) study, the increase of the fiber length effectively enhanced the flexural deflection capacity of the cementitious composite (Yoo et al., 2015). In fiber-reinforced concrete, the completed pull out of the fibers can be considered as the main reason for the concrete failure. And the pull-out effect of the fiber can be determined by the bonding condition between the fiber and matrix. It can be expected that a longer fiber generally leads to an increase in the bonding area between fiber and the matrix, which results in an improvement in the ductility of the concrete (Yoo et al., 2015). Therefore, tailoring the fiber length can potentially affect the mechanical performance of the concrete. In addition, the researchers noticed that the increase in the fiber length could potentially lead to fiber entanglement and poor distribution, which may lead to a more porous structure (Yoo et al., 2014). It was reported that concrete material with longer fiber exhibited a lower compressive strength compared with those with shorter fiber (Chen & Carson, 1971). A similar experimental result was also found in Noushini et al's study, where the increase of the length of the PVA fiber enhanced the strain capacity of the sample while the improvement in splitting tensile strength of the concrete was not observed (Noushini et al., 2013). Based on previous work, it can be concluded that the length of the fiber can effectively influence the mechanical performance of the designed concrete. However, a balance exists between the positive and negative effects of using longer or shorter fibers. Apart from the fiber length, previous studies showed that the aspect ratio of the fiber is another primary factor that can affect the mechanical properties of the concrete. It was reported that the increase in the aspect ratio could lead to higher compressive strength and toughness (Eren & Celik, 1997). In Hameed et al.'s study, it was proposed that a larger aspect ratio of the fiber could result in a better control of the crack propagation. Therefore, the increment of the compressive and flexural strength can be expected when fiber with a higher aspect ratio is used (Hameed et al., 2009).

According to the literature review, it can be seen that the parameters of the fiber may affect the properties of the concrete material in a different way. Therefore, during the mixture design of the fiber-reinforced cementitious material, the selection of the fiber needs to depend on the specific requirement or application.

2.3 Internal Curing for Concrete Material

To design high-performance concrete, people generally increase the content of the cementitious material to produce a denser and stronger cementitious matrix. However, even though the low water to cement ratio benefits the strength of the concrete, it also increases the risk of the early age shrinkage cracks formation (Cusson & Hoogeveen, 2007). During the hydration process, the loss of water and relative humidity decrease leads to self-desiccation that generates internal stress. Under the constraint condition, the internal stress can cause the formation of cracks, which may lead to the early age failure of the concrete. For concrete with relatively high water to cement ratio, the external curing method can supply moisture and mitigate shrinkage. However, when it comes to the concrete with low water to cement ratio, a low permeability caused by the dense matrix does not allow the transfer of external water from the surface to the interior of the material (Bentz & Snyder, 1999). Therefore, external curing has limited efficiency in shrinkage reduction for the concrete with high binder content (Bentz et al., 2005).

In order to mitigate the potential damage caused by shrinkage in concrete with low water to cement ratio, the internal curing method has been developed; the schematic is shown in Figure A.2 (de la Varga et al., 2012). Pre-wetted internal curing agents with high water absorption capacity are used to serve as water reservoirs to supply extra water from the inside of the concrete material (Ma et al., 2019). It has been proved that the pre-wetted internal curing agent can releases the water once held in its structure during the hydration and prevent the autogenous shrinkage of high-performance concrete (Bentur et al., 2001).

2.3.1 Internal Curing Aggregates

In the application of the internal curing method, selection of the internal curing agent is of vital importance. The internal curing agent can not only affect the shrinkage reduction efficiency but also the mechanical properties of the concrete. Pre-wetted porous aggregates were initially used to partially replace the sand in high-performance concrete to serve as the internal curing agent. The porosity of the internal curing aggregates is generally responsible for the absorption capacity. High absorption capacity can potentially increase the effectiveness of the internal curing by carrying a larger amount of extra water. In addition, the size distribution of the pores inside the internal curing aggregate also influences the internal curing efficiency (Henkensiefken et al., 2009a; Ma et al., 2019). The previous study indicated that the pores in internal curing aggregate need to be larger than those in the cementitious matrix so that the water carried by the

aggregate will be preferentially released and consumed by the hydration process (Bentz et al., 2001).

Various types of internal curing aggregates have been studied and used in high-performance concrete materials (Dixit et al., 2019; Masum & Manzur, 2019; Tu et al., 2018). Among them, expanded lightweight aggregate is one of the most frequently used internal curing agents. It has been proved that complete elimination of the shrinkage may be expected when 25% of the normal-weight aggregate is replaced by lightweight aggregate (Bentur et al., 2001). The large pore with a diameter of greater than 1 μm in lightweight aggregate can be saturated within a short time and exhibit low water retention ability (Ma et al., 2019). During the early age hydration process, those large pores are capable of releasing most of their absorbed water at high relative humidity. Thus, it is an effective internal curing agent to reduce early age shrinkage by providing water to replenish the empty pores caused by self-desiccation (Castro et al., 2011). On the other hand, clinoptilolite zeolite, a porous aluminosilicate mineral, was reported to have nm-sized pores capable of storing water down to low relative humidity levels (Ghourchian et al., 2013; Zhang et al., 2018). The previous study indicated that the incorporation of pre-wetted zeolite could result in a shrinkage reduction of over 30% (Zhang et al., 2017). In Ghourchian et al.'s study, the internal curing efficiency of the zeolite is compared with expanded lightweight aggregate. It is reported that the 24 hours absorption capacity of the zeolite is around 41.8% higher than the lightweight aggregate. The mercury intrusion porosimetry test evaluated the size distribution of the pores. The result showed that lightweight aggregate possessed a coarse pore structure, while a large volume fraction of the nano-pore existed in the zeolite. For the absorption/desorption behavior, the lightweight aggregate was capable of releasing more than 95% of its absorbed water at a relative humidity of 90%, while zeolite retained around 90% of the water under the same environmental condition. Therefore, it is more likely for the zeolite to store part of its absorbed water instead of releasing it for early age hydration. Consequently, due to the high water retention capacity of the zeolite, lesser reduction of shrinkage could be expected when the zeolite is used as an internal curing agent (Ghourchian et al., 2013).

For the mechanical properties of the concrete incorporated with internal curing aggregate, a balance exists between the side effect of the porous structure of the internal curing aggregate and the positive effect of the internal curing. The high porosity of the internal curing aggregate may negatively affect the strength of the concrete, while a higher degree of hydration caused by the extra water carried by the curing agent has a positive effect on the mechanical properties of the concrete (Bentz & Weiss, 2011). In previous studies, both decrease and increase in strength caused by internal curing have been observed. It was reported that the use of the internal curing method resulted in a decrease of the early age compressive and tensile strength of the concrete, mostly due to the porous structure and larger particle size of the lightweight aggregate (Şahmaran et al., 2009). On the contrary, an increase in the long-term compressive strength was observed in Bentz's study. It was concluded that in the designed high-performance blended cement mortar, the improvement in the hydration overcame the negative influence of the porous structure of the internal curing agent, which resulted in an increase of the concrete strength (Bentz, 2007). Similar result was also found in other studies (de la Varga et al., 2012; Van et al., 2014).

2.3.2 Superabsorbent Polymer (SAP)

After the invention of the internal curing method, some concerns have been reported about the use of porous aggregates, requiring the pre-soaking prior to mixing. This could be difficult to handle in the field applications due to the lack of reasonable control over the absorption capacity of the curing aggregate. Also, the incorporation of the porous aggregate will lead to the decrement of the mechanical properties due to the incorporation of porous components (Jensen & Hansen, 2001). Therefore, superabsorbent polymers (SAP), which can be added in the cement mixtures in the form of dry powders, were proposed as a new type of internal curing agent to prevent the shrinkage of concrete and has been widely studied (Mechtcherine et al., 2006; 2014). SAPs are a group of cross-linked polymers with the ultra-high water absorption capacity of hundreds of times of their own weight (Kong et al., 2015). SAPs are able to absorb water and expand to form an insoluble gel that acts as a barrier to the flow of the water. Afterward, SAPs can release the absorbed water within the concrete and prevent shrinkage when the surrounding humidity drops. The water absorption mechanism of SAP is mainly the osmotic pressure arising from the difference in the concentration of ions between the gel and the surrounding solution (Lee et al., 2018). In the application of internal curing, crosslinked poly-acrylic/acid-acrylamide molecule is the most commonly used type of SAP (Zhu et al., 2015). In Jensen and Hansen's study, a high-performance cementitious composite blended with silica fume was designed with a water to cement ratio of 0.3 (Jensen & Hansen, 2002). In this reference sample without the addition of SAP, shrinkage deformation was observed up to 3,700 μm/m at the age of 21 days. However, when SAP was added at a rate of 0.3 and 0.6 wt% of binder, it was observed that the internal relative humidity of the concrete was effectively increased during the early age of the hydration process. The test result indicated that a 0.6 wt% of SAP addition could fully eliminate the shrinkage (Jensen & Hansen, 2002). Similar result was also found in other studies, which proved that SAP could be used as an effective internal curing agent (Just et al., 2015; Mechtcherine et al., 2006).

In Hasholt et al's (2012) paper, it was reported that the overestimate of SAP water absorption capacity could result in an incorrect mixture design, where the extra water added for internal curing is too large. As a consequence, the increase of the actual water to cement ratio may result in a decrease in the concrete strength (Hasholt, 2012). In Lee et al's (2018) study, it was observed that the concentration of the cations and the alkalinity of the environment could intensively influence the swelling behavior of the SAP. The study found out that the calcium ions are capable of binding with carboxylate groups in the acrylate chains of the SAP, which further decreases the absorption capacity of the SAP (Lee et al., 2018). Similarly, Zhu et al. (2015) reported that a stiff shell structure was formed when the SAP sample was immersed in the Al^{3+} solution. The presence of the barrier layer directly reduces the water absorption capacity of the SAP by hindering the water transportation between the SAP and the solution (Zhu et al., 2015). Therefore, it can be concluded that the behavior of the SAP can be affected by environmental conditions. It is necessary to understand the robustness of the SAP to optimize the mixture design when SAP is used as an internal curing agent.

2.4 Summary

According to the literature review, the healing of cracks with smaller width requires less amount of solid product, which is more likely to be completed healed. Therefore, the efficiency of the autogenous healing performance could be improved by incorporating fibers to control the crack width propagation. On the other hand, according to the mechanisms of autogenous healing, it can be noticed that water is a critical factor for the autogenous healing of concrete materials. A sufficient self-healing phenomenon can only be observed when external water is available. However, the external water supply is not continuous and unstable. Thus, developing a method that can avoid the limitation of the external water supply will be beneficial to the autogenous healing efficiency. Internal curing is a well-developed method that supplies additional water for cementitious material to eliminate early age shrinkage. Internal curing agents with high water absorption capacity can be used as internal water reservoirs for cement hydration. Thus, with proper design, the internal curing agent has the potential to supply water for autogenous healing. Various types of internal curing agents have been studied. Among them, porous aggregates and superabsorbent polymer (SAP) have been widely used. However, as the direct experimental evidence is lacking, it is still unclear if the healing performance can be enhanced by the internal curing method. In addition, inadequate studies have been performed on the robustness of the SAP in the fresh concrete mixture, which may potentially negatively affect the mechanical properties of the concrete materials.

3. EFFECT OF DIFFERENT CONFIGURATIONS OF FIBERS

3.1 Objective

According to the literature review, it can be seen that the parameters of the fiber can affect the properties of the concrete material in a different way. Therefore, during the mixture design of the fiber-reinforced cementitious material, the selection of the fiber needs to depend on the specific requirement or application. To study the influence of fiber parameter on the mechanical properties of the SHCC, PVA fiber (Polyvinyl Alcohol) and five different types of macro-fibers approved by the Indiana Department of Transportation (INDOT) (Strux 90/40 fiber, Fiberforce 650, TUF-Strand SF, Forta-Ferro One and Masterfiber Mac Matrix fiber) were used to reinforce the designed cementitious composite, as shown in Figure A.3. The material properties of the fibers are shown in Table A.1.

The ingredients that used in the mixture included Type I Ordinary Portland cement (OPC, Buzzi Unicem, USA), Grade 100 blast furnace slag (Skyway cement company LLC, USA), Class C fly ash (fly ash direct, ltd.- Joppa Power Plant, USA), natural sand and tap water. The mix composition is listed in Table 3.1. In order to achieve high mechanical performance, relatively low water to binder ratio of 0.35 was used. Two percent volumetric fraction of fiber was incorporated to control the crack width and enhance the ductility of the designed material.

The cementitious materials, sand, and internal curing aggregates were firstly dry mixed for 3 minutes at low speed to reach a uniform state. After that, water was added and mixed for 3–5 minutes until the mixture reached good fluidity and uniformity. Finally, the fibers were slowly added into the mixture at a low mixing speed within 1 minute, followed by a medium speed mixing for 3 minutes to achieve good fiber dispersion. The fresh cementitious materials were then cast into 50 mm cubic molds for the compressive test, 240 mm $\times$ 60 mm $\times$ 15 mm plate for the four-point bending test, and dog-bone specimens (Figure 3.1) for uniaxial tensile test, respectively. The samples were de-molded after 24 hours and cured in a 100% relative humidity chamber for 28 days.

3.2 Experimental Method

A Universal Tensile Machine (MTS Insight 10) was used to conduct the mechanical tests. The 28th day compressive and flexural strengths for each mixture were determined by five cubic and plates samples according to ASTM C109 and ASTM D6272, respectively. The test setup for the flexural test is shown in Figure A.4. The deflection of the sample was monitored by a linear variable displacement transducer (LVDT). For the uniaxial tensile test, a customized fixture was used, as shown in Figure A.5. The loading rate was controlled at 0.5 mm/min to simulate the quasi-static

TABLE 3.1
Mixture design (by weight of cement)

Mix	OPC-I	Blast Furnace Slag	Fly Ash	w/b*	Fiber (Volume %)	Sand
PVA-SHCC	1	0.15	0.15	0.35	2	0.80
Strux 90/40-SHCC	1	0.15	0.15	0.35	2	0.80
MasterFiber-SHCC	1	0.15	0.15	0.35	2	0.80
Fiberforce 650-SHCC	1	0.15	0.15	0.35	2	0.80
TUF-Strand SF-SHCC	1	0.15	0.15	0.35	2	0.80
Forta-Ferro One-SHCC	1	0.15	0.15	0.35	2	0.80

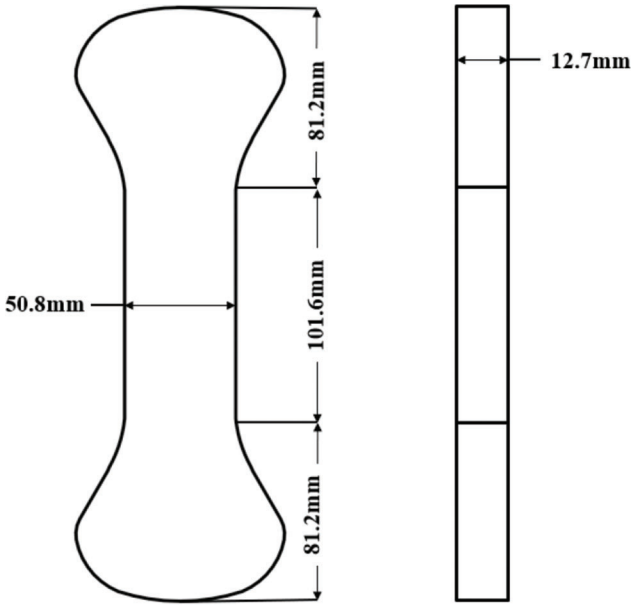

Figure 3.1 Dog-bone specimen for uniaxial tensile loading.

loading condition. The result of the mechanical tests was averaged from the five replicates of each mixture.

3.3 Result and Discussion

3.3.1 Mechanical Properties

Mechanical properties of the designed cementitious composite with different types of fiber are shown in Figure 3.2, 3.3, and 3.4. It can be observed that PVA-SHCC exhibited a higher strength level at 28 days compared with other mixtures with macro-fibers. For compressive strength (Figure 3.2), the sample with PVA fibers exhibited a strength of 8,800 psi, which was 10%–165% higher than other mixtures. Still, it is worth noting that samples with Tuf-strand, Masterfiber and Fortar fiber also showed a relatively high strength performance of around 7,980 psi. As for the uniaxial tensile test (Figure 3.3), the incorporation of PVA fiber led to the highest uniaxial tensile strength of 506 psi, while all the other samples with macro-fibers showed similar strength of around 435 psi, which was 20% lower than the PVA-SHCC. For the flexural test (Figure 3.4), samples with PVA, fortar-ferro and Strux 90/40 fiber exhibited a similar strength level of around 1,160 psi, while the Masterfiber-SHCC, Tuf-Strand-SHCC and Fiber-Force-SHCC showed a lower flexural strength of less than 1,015 psi. The analysis of the flexural strain is discussed in 3.3.2.

It can be observed from the result that, overall, the sample with PVA fiber exhibited better mechanical performance. There are three underlying reasons for this phenomenon. Firstly, PVA fiber has a higher tensile strength. Upon the formation of the crack during the loading process, PVA fiber can transfer a higher level of stress across the cracks for propagation. Therefore, the structural integrity could remain intact at a higher stress level. Secondly, PVA fiber has a short length of 0.3 inches, compared with macro-fibers with a length of over 1.5 inches. When longer fiber is used, the fiber entanglement is more likely to happen during the mixing process. Thus, the poor distribution of the fiber could lead to the worse mechanical performance of the concrete material. Thirdly, the aspect ratio of the fibers can affect the mechanical strength of the concrete. Various studies have proved that a higher aspect ratio of the fiber potentially leads to a higher strength of the concrete material (Costa et al., 2012; Eren & Celik; Marar et al., 2001). It was reported that a high aspect ratio could delay the debonding of the fiber from the cementitious matrix during the loading process (Köksal et al., 2008). Since the aspect ratios of the PVA is much higher, better mechanical performance can, therefore, be expected for the sample with PVA fiber.

3.3.2 Crack Width Control Ability of the Fibers

During the flexural test, the midspan deflection of the sample was monitored by a linear variable displacement transducer (LVDT). According to ASTM-D6272, the flexural strain was calculated by Equation 3.1).

$$Strain = \frac{4.70 * D * d}{L^2} \qquad \text{(Equation 3.1)}$$

Where D is the maximum midspan deflection (in), d is the depth of the beam (in), and L is the support span of the sample (in).

The flexural stress-strain curves of the tested material are shown in Figure 3.5. It can be observed that the sample incorporated with PVA fiber showed a stronger flexural strength, while the use of macro-fibers generally led to a higher flexural strain capacity but lower

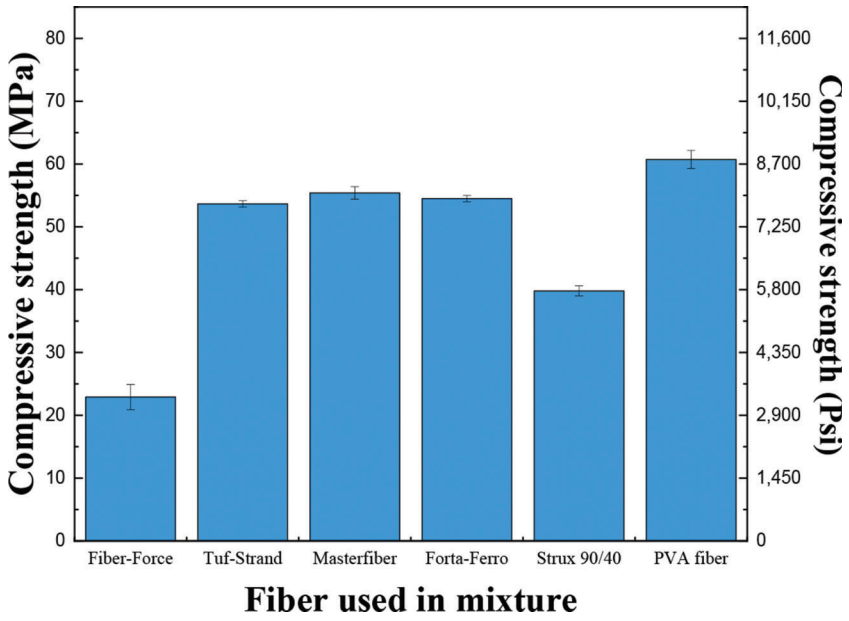

Figure 3.2 Compressive strength results of SHCC incorporated with various fibers.

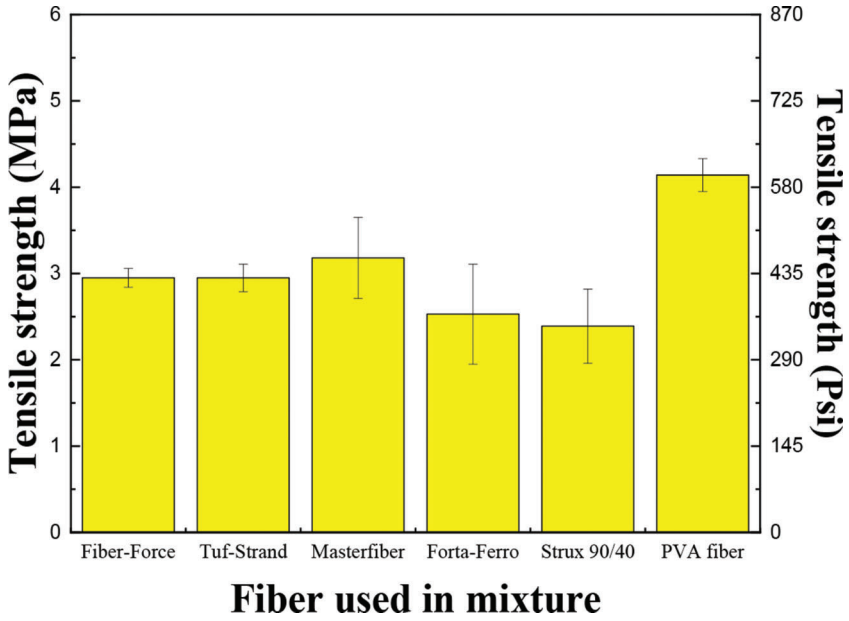

Figure 3.3 Tensile strength results of SHCC incorporated with various fibers.

strength level. Unlike the brittle behavior of the conventional concrete, all mixtures tested in this study exhibited relatively high ductility during the loading process. Among which, the sample with PVA fiber, Strux 90/40, Tuf-strand, and Forta-Ferro fibers showed pseudo-strain-hardening behavior during the loading process, which means that the post-cracking strength of the sample was higher than the first-cracking strength. This phenomenon can result in the formation of multiple cracks that were bridging bridged by the fibers. As can be seen in the stress-strain curve, every sudden drop of the flexural stress represents the formation of a new crack (Ranade et al., 2011). In Figure 3.5, after the formation of a crack, the stress dropped and then continued to increase, rather than drastic decrease and leads to the failure. This phenomenon is because the fibers across the crack successfully acted as bridges to transfer the stress, which prevented the uncontrollable crack propagation.

As for the crack width control ability, it can be observed from Figure 3.5 that when macro-fiber was used, samples with Forta-Ferro, Strux 90/40 fiber and Tuf-strand fiber, 5 cracks were formed in the matrix during the flexural loading, while fewer cracks can be observed in the sample with FF650 and MasterFiber. The limited number of cracks in the matrix indicates

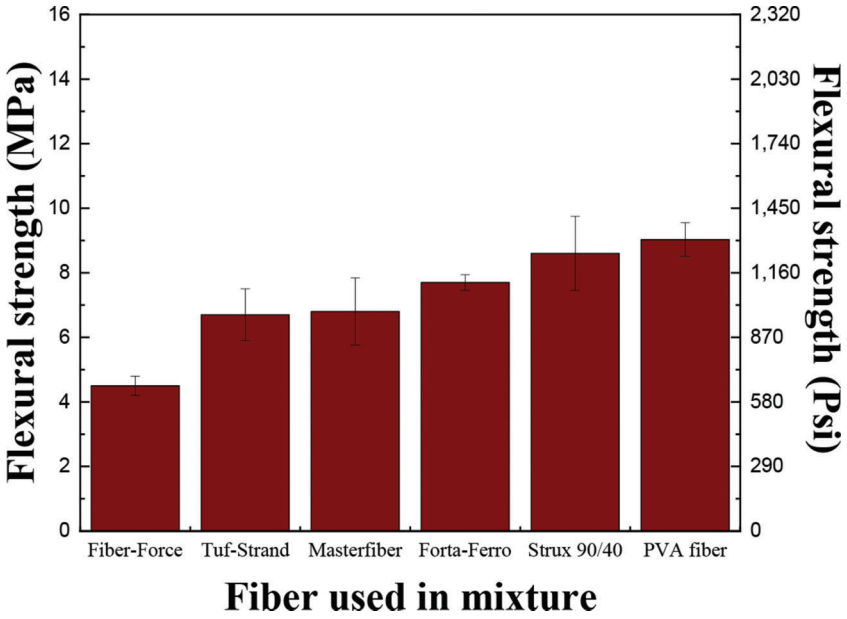

Figure 3.4 Flexural strength results of SHCC incorporated with various fibers.

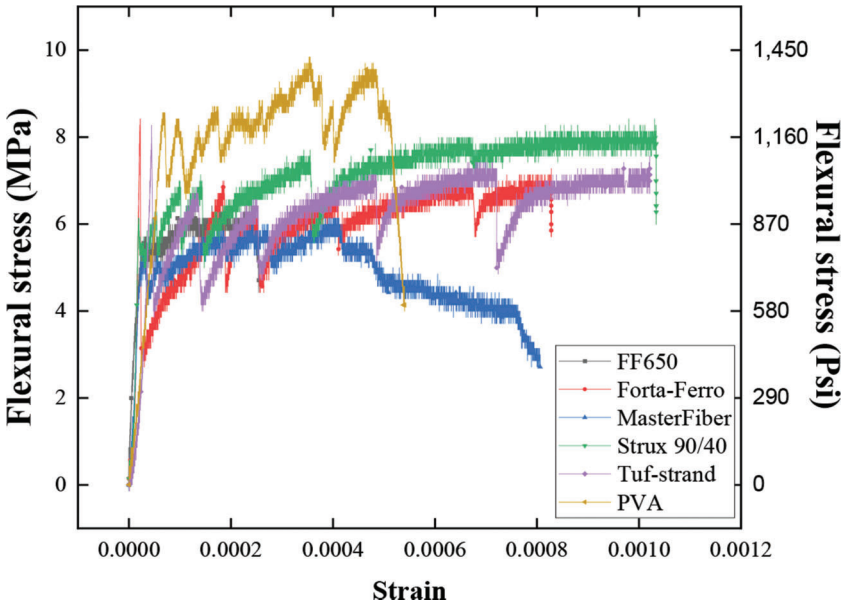

Figure 3.5 Stress-strain curve of SHCC with various fibers.

that the crack could propagate without effective limitation throughout the loading process. A wider crack opening can thus be expected. On the other hand, when PVA fiber was used, a formation of more than 10 cracks can be observed from the flexural stress-strain curve. The formation of cracks in the sample with PVA fiber was continuous and evenly distributed throughout the loading process. Therefore, for the sample with PVA fibers, a better crack width control performance can be expected. In addition, a lower flexural strain capacity could also be observed in the PVA-SHCC. The shorter length of the PVA fiber is favorable for the fiber distribution but also makes it easier to be pulled out during the test, thus resulted in a lower strain capacity.

3.4 Summary

In this section, different types of fibers were used in the designed cementitious composite. Experimental results show that the SHCC designed with fiber can result in pseudo-strain-hardening behavior during the loading process. Among six mixtures, samples with PVA fiber exhibited higher mechanical strength. For compressive strength, the PVA-SHCC performed 10% to 165% higher than others; for tensile strength results,

the PVA-SHCC exceeded other sets for 24% to 65%; for flexural strength, the PVA-SHCC behaved 5% to 101% higher than SHCC incorporated with other fibers. The analysis of the flexural deflection shows that the crack width control ability of the PVA fiber is stronger than the macro-fibers, since PVA fiber is stronger with higher aspect ratio and has a shorter length which less prone to entangle. The existence of the PVA fiber can control the propagation of the crack width by generating multiple cracks, while less cracks could be formed in the sample with macro-fibers. It is also observed that PVA-SHCC exhibited a lower flexural strain capacity compared with others, which could be due to the shorter length of PVA that makes it easier to pull out during the loading. In this project, the goal is to develop a high-performance cementitious composite with self-healing ability. It is favorable to choose a fiber with stronger crack width control ability which could limit the propagation of the cracks and potentially increase the efficiency of the self-healing. Therefore, PVA fiber is more suitable for this specific purpose and will be used in the following study about the evaluation of the autogenous healing performance.

4. INTERNAL CURING AGENT-BASED SHCC

4.1 Objective

Based on the literature review, it has been concluded that water is one of the indispensable factors that affect self-healing. However, due to the limited supply of free water inside the hardened concrete, most of the products contributing to the self-healing process (such as calcium hydroxide and calcium carbonate) can only form on the outer surfaces of the elements and are thus vulnerable to leaching. As such, the concept of internal curing is introduced to serve as internal water reservoirs to enhance self-healing efficiency. In this project, a hypothesis is proposed that the incorporation of the internal curing agent can improve the self-healing performance of the designed concrete. This theory is examined in this chapter by a series of tests, and a recommendation for the mixture design is provided.

4.2 Experimental Method

Three types of internal curing agents, Zeolite, lightweight aggregate, and SAP are used and evaluated. Among them, the zeolite and lightweight aggregate are expected to serve as internal water reservoirs which can supply water internally. And the SAP is incorporated to act as the internal sealing agent that could swell and block the crack from the inside.

In the first part of this study, zeolite was firstly used to verify our theory. Then, the lightweight aggregate was incorporated to compare with zeolite, and the mechanism of the influence of the internal curing agent on self-healing was investigated.

4.3 Effect of Using Zeolite in SHCC

4.3.1 Mixture Composition of Zeolite-SHCC

The compositions of mixtures used to prepare SHCC specimens are shown in Table 4.1. These included the ordinary (Type I) Portland cement (OPC, Buzzi Unicem USA), grade 100 slag cement (SC, Skyway Cement Company), Class C fly ash (FA, Fly Ash Direct Ltd.-Joppa Power Plant), silica sand (AGSCO Corporation), and polyvinyl alcohol (PVA) fibers (NYCON Corporation).

The water absorption capacity of the clinoptilolite zeolite (KMI Zeolite Inc, USA) particles was test as 18%. In this study, the zeolite was used to replace part of the silica sand. Figure 4.6 presents the particle size distribution of zeolite and silica sand. The water absorption capacity of zeolite is 18%. To have a thorough understanding of the influence of the internal curing aggregate on the performance of the self-healing, the replacing ratios for the sand were designed from 0% to 30%. All mixes have the w/b of 0.32 and 2% volumetric fraction of PVA fiber.

4.3.2 Mechanical Test

The SHCC samples were cured in the moisture-curing room for 10 days to decrease the probability of the shrinkage cracking. Then, the samples were moved to an environment-controlled chamber with $23 \pm 2^{\circ}C$ and 50% RH for another 40 days until testing. Mechanical properties, including compressive test and splitting tensile test, were conducted. Three 50 mm cubes evaluated the compressive strength of specimens from various mixtures according to ASTM-C109. For the splitting tensile test (ASTM-C496), 100 mm × 200 mm

TABLE 4.1
Compositions of concrete mixtures (proportions expressed as fraction of cement weight)

Mix	OPC	SC	FA	Zeolite	Silica Sand	w/b[1]	PAV Fiber (Volume %)	Zeolite Replacement (%)[2]
Z_0	1	0.15	0.15	0	0.80	0.32	2	0
Z_75	1	0.15	0.15	0.06	0.74	0.32	2	7.5
Z_150	1	0.15	0.15	0.12	0.68	0.32	2	15
Z_225	1	0.15	0.15	0.18	0.62	0.32	2	22.5
Z_300	1	0.15	0.15	0.24	0.56	0.32	2	30

[1]Water-to-binder ratio.
[2]Level of replacement of sand by zeolite (weight %).

cylindrical specimens were used. Three-cylinder and cubic specimens were prepared for each mixture. The strength measurements were averaged from the three replicates of each mixture.

4.3.3 Self-Healing Evaluation by Non-Destructive Test

The SHCC samples were pre-damaged at the age of 50 days and then exposed in the wet/dry condition to evaluate the self-healing performance. To induce the pre-damage in the specimens (100 mm × 200 mm cylinders), the loading was applied in the circumference direction of the sample using splitting tensile method. The pre-loading of the specimens was applied 80% of the ultimate splitting tensile strength of each mixture to avoid the different degrees of the damage (or pre-cracks) among the specimens. After the pre-damage, the specimens were exposed to healing cycles (4 days per cycle) with 2 days in a high moisture environment (100% RH) and 2 days in a moderate humidity environment (50% RH) for 7 cycles (28 days). The design of the wet/dry cycles intends to simulate the natural environment where the external water supply is limited.

After the healing period, the self-healing process of the specimens was evaluated via two non-destructive tests (NDT), including resonant frequency (RF) and ultrasonic pulse velocity (UPV) tests. According to ASTM C215, the torsional mode was adopted to consider the geometric shape of the cylinder specimens for RF measurement. The RF measurement setup consisted of a piezoelectric oscilloscope (GrindoSonic MK5, Penn Tool Co.), a vibration detector, a wooden ball, and sponge support, as shown in Figure 4.7

UPV test (NDE 360 Platform, Olson Instruments) was conducted according to ASTM-C597. The device was calibrated with a reference aluminum bar before testing. To eliminate human errors during the measurement, a custom-designed wooden frame was utilized, as shown in Figure 4.8. The transducers were pushed to contact both sides of the cylinder surface with a constant force from springs. The high vacuum coupling agent was applied to erase the air void on the interface between sensors and samples.

The sound samples were measured for RF and UPV before pre-damage. After imposing the 80% tensile loading to pre-damage the samples, the RF and UPV test were conducted again. To attain the self-healing performance in cementitious materials, RF and UPV were conducted after 1st, 3rd, and 7th wet/dry cycles (4, 12, and 28 days after pre-damaged).

4.3.4 Properties of Zeolite-SHCC

4.3.4.1 Mechanical performance. Figure 4.1 presents the compression results of various zeolite replacing ratios of SHCC samples. As the figure shows, compressive strength grows slightly as the zeolite content increases. The sample without zeolite incorporated has a strength of 69.2 MPa, while the high zeolite content (30%) raised to 80 MPa. The compressive strength gains around 15% due to the extra water released from the internal curing agent for continuous hydration, which enhances the strength of the matrix. Thus, the improvement of the degree of hydration is reflected in the increase of compressive property.

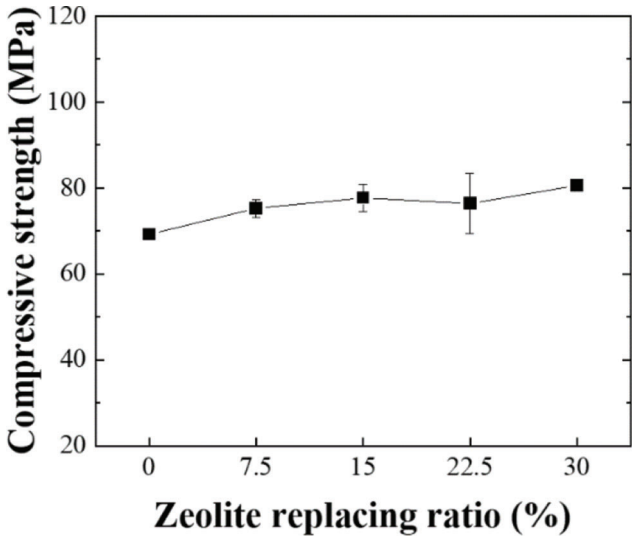

Figure 4.1 Compressive strength of different samples.

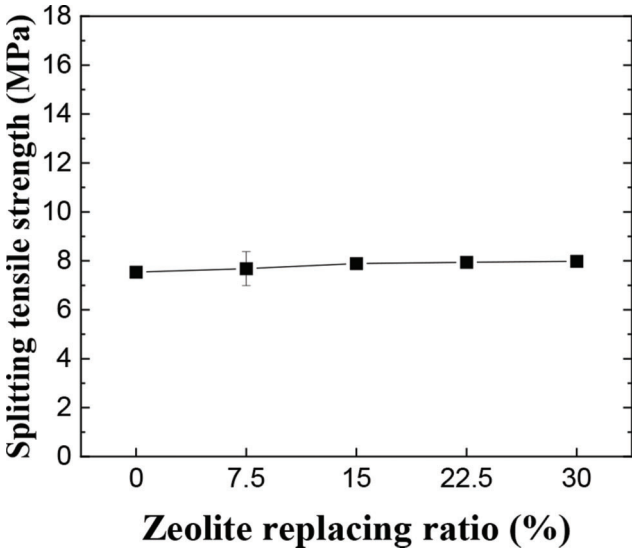

Figure 4.2 Splitting tensile strength of different samples.

Figure 4.2 presents the splitting tensile result of different SHCC samples. As can be seen that the tensile strength of the sample is range from 7.54 MPa to 7.98 MPa as the content of the zeolite increases. The result indicates that although zeolite is a high porosity materials, it would not affect the tensile performance with replacing ratio of up to 30%. The enhancement of tensile stiffness due to internal curing and incorporation of PVA fiber might compensate for the high porosity weakness.

4.3.4.2 Self-healing performance of zeolite-SHCC. The self-healing performance of SHCC samples was evaluated via a resonant frequency test and ultrasonic pulse velocity test at each age of interest. The NDT results of the sound sample were measured before the pre-damage imposed on the sample. The measurements were also conducted after the sample was pre-damaged and underwent different wet/dry cycles, including 1, 3, and 7 cycles.

$$\text{Recovery ratio } (\%) = \frac{\text{NDT}_{\text{Healed}} - \text{NDT}_{\text{Pre-damaged}}}{\text{NDT}_{\text{sound}}} \times 100\% \quad \text{(Equation 4.1)}$$

Figure 4.3(a,b) depict the recovery results of the resonant frequency test and ultrasonic pulse velocity test, respectively. It can be seen that the incorporation of the zeolite effectively improved the self-healing performance. It is no surprise that the recovery ratio of both RF and UPV is increased with the wet/dry cycles for all mixtures due to the further hydration of un-hydrated cementitious materials. The benefit of adding porous zeolite in cementitious materials is to increase the bulk absorption capacity of the sample, which leads to the sample to absorb and store part of the external water under wet curing conditions. Consequently, the stored water can be slowly released for continuous secondary hydration when the external water is unavailable. In addition, since the zeolite was pre-wetted before the mixing, it is also possible that part of the internal curing water was used for the healing of the crack.

In Figure 4.3(a), it can be noted that the recovery ratio of the 1st cycle increases with the zeolite replacing ratio increase; however, the SHCC with 30% zeolite incorporation shows less healing performance than others. After 3 cycles, the sample with 15% and 22.5% performed better recovery ratio than all other samples. It is worth to note that the RF recovery results of 30% sample growth rapidly from 1 cycle (4 days) to 3 cycles (12 days). The RF experiment result underwent 7 wet/dry cycles suggested that incorporating the internal curing agent improves the healing performance of the designed material, while the sample with 15% of zeolite performs the best and shows around 6% recovery ratio. However, the healing performance decreased with the zeolite replacing ratio increasing for the more zeolite incorporated sample of 22.5% and 30%.

The UPV results can be seen in Figure 4.3(b). After the first cycle, the UPV recovery ratio increases with the zeolite content up to 15%, and the healing performance decreases after incorporating more internal curing agents. The SHCC with 22.5% zeolite exhibits a better healing performance of 4.1% on the 3rd wet/dry cycle. The 7th wet/dry cycle result reveals that the increasing tendency of recovery rate reaches the maximum for the sample with 15% zeolite; nevertheless, it decreased afterward. The UPV result happened to have a similar trend with the RF outcome on the seven cycles, which implied that the optimal zeolite replacing ratio to improve self-healing performance might be around 15%.

We have noticed that the healing performance decreased after 15% incorporation. The phenomena may be attributed to the densification of the cementitious matrix of high zeolite content SHCC block the external water for secondary hydration, which is the so-called "blocking effect." To be more specific, part of the water stored in zeolite might be released during the early stage of hydration, which is expected as an internal curing effect. The extra water provided by the internal curing agent can enhance the hydration degree of cementitious materials and further densify the cement matrix. Consequently, a dense cement matrix would tend to block the water supply from the external environment, as Figure 4.4 shows. As mentioned above, it is important for the sample to absorb water from the external environment and use it for self-healing when the water supply is unavailable. A cement matrix with a high hydration degree may inhibit the ability of the sample to absorb and store water. Also, due to the dense matrix, the water release via an internal curing agent might not be able to transport to

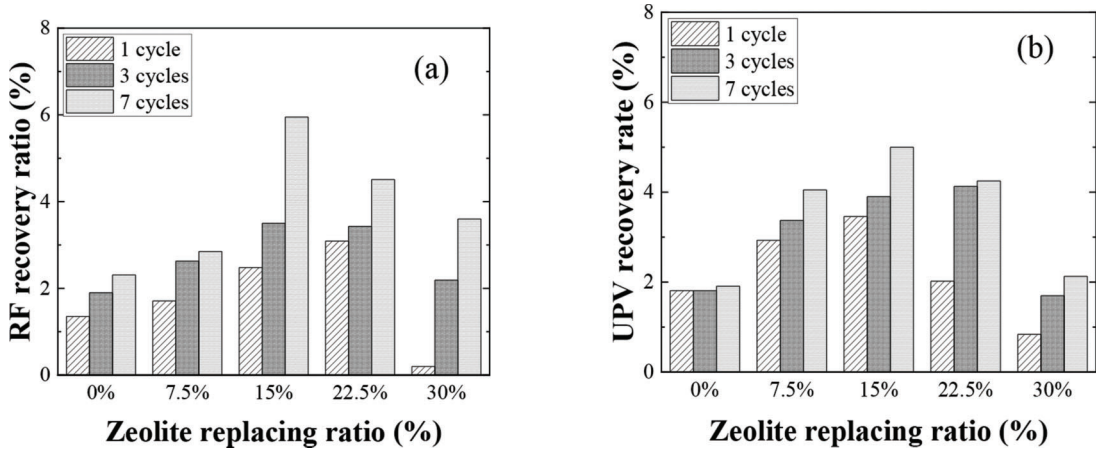

Figure 4.3 Self-healing performance at different Zeolite replacing ratios: (a) resonant frequency test and (b) ultrasonic pulse velocity test.

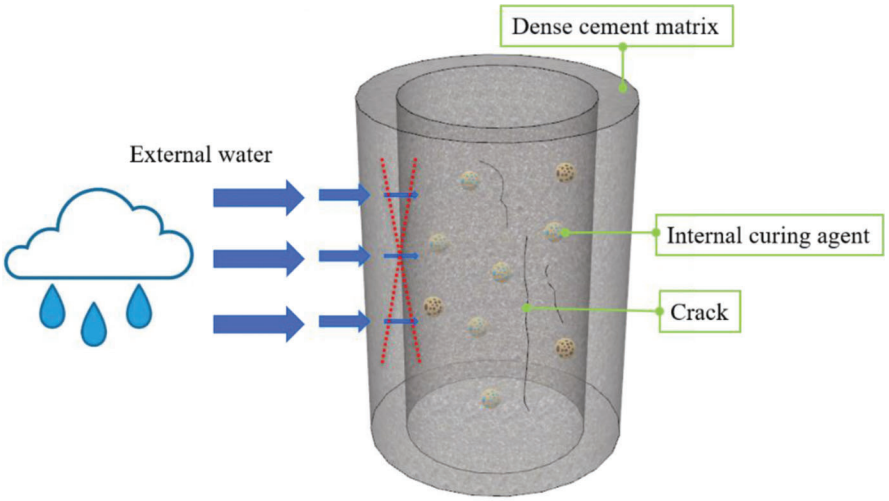

Figure 4.4 Schematic of blocking effect.

the crack for healing. Moreover, as the amount of the internal curing water carried by the zeolite increase, larger portion of the cement particles was consumed during the early age hydration. Consequently, less amount of the cement would be available for secondary hydration during the self-healing period. Thus, once the incorporation rate of the internal curing agent is higher than the balance point (15% in this study), the increase of the amount of the internal curing agent might lead to a negative effect.

The strength recovery factor is defined as $\sigma_{reloaded}/\sigma_{ultimate}$, where $\sigma_{reloaded}$ is the reloaded tensile splitting strength, and $\sigma_{ultimate}$ is the ultimate strength. After the non-destructive evaluations, the post-7-cycles SHCC samples were reloaded using a splitting tensile test. Figure 4.5 presents the tensile strength recovery factor of different SHCC samples after 7 wet/dry cycles. As shown in Figure 4.5, the recovery factor of all samples is higher than 0.73. The strength recovery factor of plain SHCC sample without zeolite incorporated is around 0.84. The 7.5% sample performed the best tensile recovery of 0.98. Nevertheless, as the zeolite content increase, the recovery factor decreased. It might occur due to the blocking effect, which limited the infiltration of external water into samples as discussed in the previous section. Also, due to the higher hydration degree of the sample with larger zeolite content, limited amount of the cement would be available after the pre-damaging process.

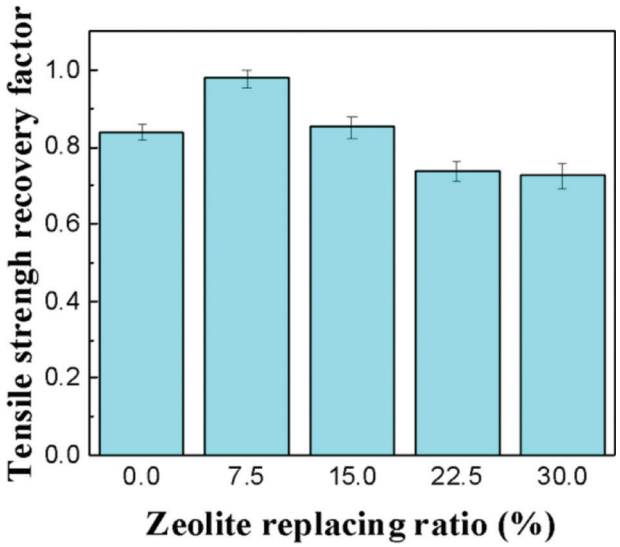

Figure 4.5 The tensile strength retention ratio of different SHCC sample after 7 cycles.

4.4 Effect of Using Lightweight Aggregates in SHCC

4.4.1 Mixture Composition of LWA-SHCC

To further study the mechanism of the influence of internal curing aggregates on the healing of the designed composite, lightweight aggregate was used as an internal curing agent and compared with zeolite. Table 4.2 presents the mixture design for the LWA-SHCC. Two sets of mixtures with zeolite were also designed to compare with the LWA-SHCC.

4.4.2 Mechanical Test

The fresh cementitious materials were then cast into 50 mm cubic molds for the compressive test, 240 mm × 60 mm × 15 mm plate for four-point bending test, and dog-bone specimens for uniaxial tensile test and self-healing evaluation, respectively. The samples were de-molded after 24 hours and cured in a 100% relative humidity chamber for 28 days.

4.4.3 Self-Healing Evaluations

To evaluate the autogenous healing performance of the sample, a designated level of damage was induced to

TABLE 4.2
Mixture design (by weight of cement) for the study of internal curing aggregates

Mix	OPC-I	Blast Furnace Slag	Fly Ash	w/b[1]	PAV Fiber (Volume %)	Zeolite	Lightweight Aggregate	Sand	Replaced (%)[2]
R_0	1	0.15	0.15	0.35	2	0	0	0.80	0
L_15	1	0.15	0.15	0.35	2	0	0.06	0.74	15
L_30	1	0.15	0.15	0.35	2	0	0.12	0.68	30
Z_15	1	0.15	0.15	0.35	2	0.06	0	0.74	15
Z_30	1	0.15	0.15	0.35	2	0.12	0	0.68	30

[1]Water-to-binder ratio.
[2]Internal curing agent replaced sand rate (weight %).

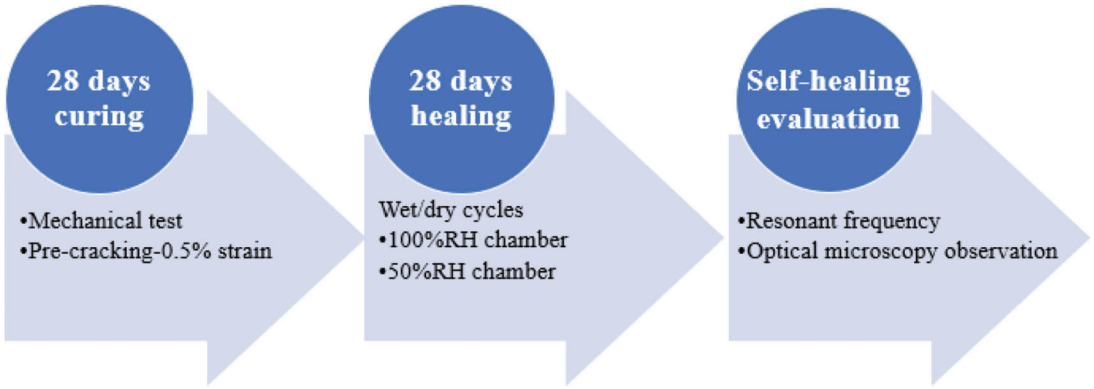

Figure 4.6 Experimental procedure for autogenous healing evaluation.

the sample. A tensile strain of 0.5% was chosen as the pre-loading level to induce cracking on the specimens. After the pre-loading, samples were exposed to wet/dry cycles to simulate the natural environment of raining and sunny, which has a discontinuous water supply. Each wet/dry cycle includes two days curing at 100% relative humidity, and another 2 days at 50% relative humidity. The total healing period was kept at 28 days (7 cycles).

The autogenous healing performance was evaluated through a resonant frequency test and optical microscope. The measurement of resonant frequency is based on ASTM C215 (Subcommittee C09.64, 2019). The cracks were examined through an optical microscope. By using image analysis software (Image J), the sealing of the crack mouth can be observed and quantified. For each crack on the specimen, test points were taken at an equal distance of 200 μm. Changes in the crack width for all the test points were analyzed before and after the healing period. The experimental procedure is shown in Figure 4.6.

4.4.4 Properties of LWA-SHCC

4.4.4.1 Mechanical performance. After 28 days of moisture curing, compressive and uniaxial tensile test were conducted. Figure 4.7, Figure 4.8, and Figure 4.9 present the compressive, flexural and uniaxial tensile test results, respectively. It can be observed that the incorporation of internal curing agents slightly

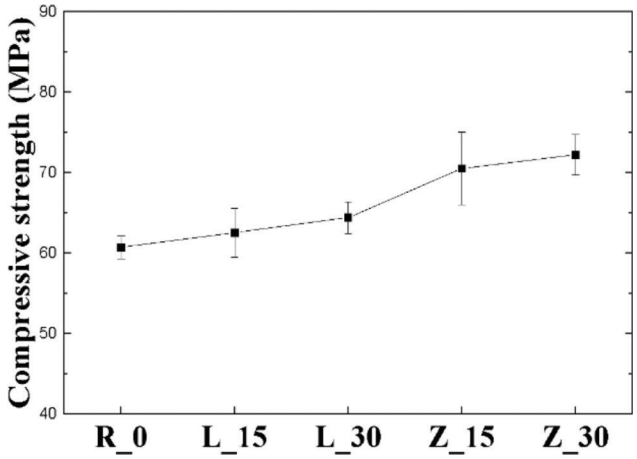

Figure 4.7 Result of 28 days compressive test.

increased the compressive and flexural performance while the tensile strength stayed almost consistent.

Moreover, by comparing the two types of internal curing agents, the sample with zeolite exhibited a more pronounced improvement in compressive and flexural strength. The phenomena may be attributed to the higher water absorption capacity of zeolite. A considerable amount of water was supplied by zeolite, leading to a denser cementitious matrix, which is favorable for mechanical behavior. When it comes to the uniaxial tensile test, the incorporation of zeolite or

LWA was expected to be detrimental to tensile performance because of the larger particle sizes of internal curing agents. The porous agents can act as flaws in the cement matrix when uniaxial tensile loading was applied. The higher hydration degree due to the internal curing compensated the negative effect of adding large internal curing agents.

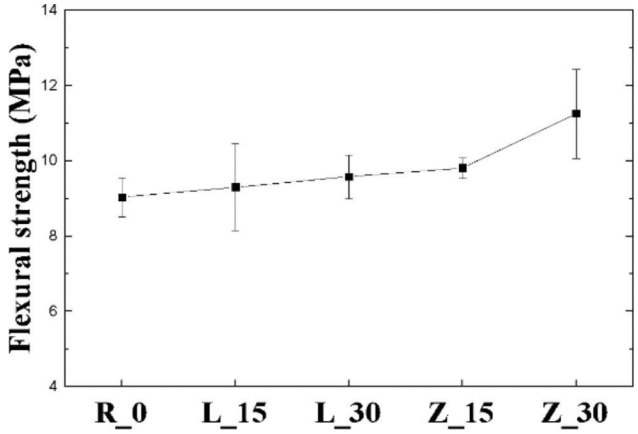

Figure 4.8 Result of 28 days flexural test.

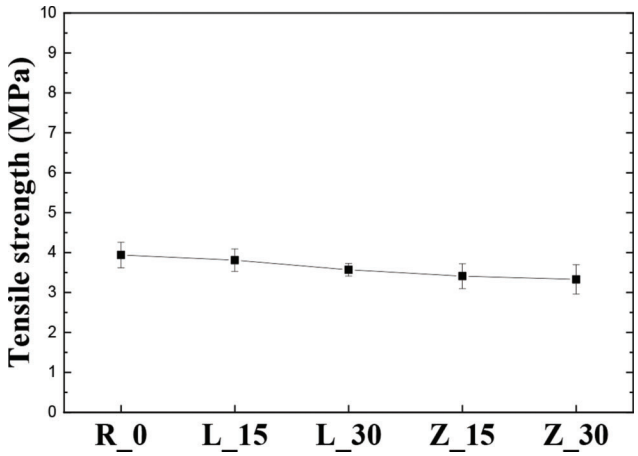

Figure 4.9 Result of 28 days uniaxial tensile test.

4.4.4.2 Self-healing performance. As shown in Figure 4.10, after 28 days of healing, all the samples showed certain levels of healing. Among this, samples with internal curing agents exhibited a more significant self-healing ability compared with the reference group. Specifically, while the R_0 had 12.6% of the recovery ratio, the samples L_15, L_30, Z_15, and Z_30 showed a higher recovery ratio of 18.3%, 23.8%, 25.3%, and 21.3%, respectively. The recovery ratio increased with the increase in the replacement level of lightweight aggregates. The effect of zeolite was somewhat more complicated. It had the highest recovery ratio at the replacement level of 15%, but there was a decrease in the recovery ratio at the replacement of 30%, which will be discussed later.

Morphology observation was performed by using an optical microscope. Figure 4.11 shows the healing of cracks throughout the wet/dry cycles. As the curing cycles increased, the healing of the micro-cracks can be observed. The optical microscopic image of cracks was compared before and after 7 wet/dry cycles of curing to further quantify and compare the healing efficiency. The crack width reduction ratio (Equation 4.2) was used to represent the healing extent of the crack mouth. The result is shown in Table 4.3.

$$\text{Reduction ration } (\%) = \frac{\text{Original crack width} - \text{Healed crack width}}{\text{Original crack width}} \times 100\% \quad \text{(Equation 4.2)}$$

According to the result of the morphology observation, all the mixtures showed complete sealing for crack widths below 20 μm due to the self-healing behavior.

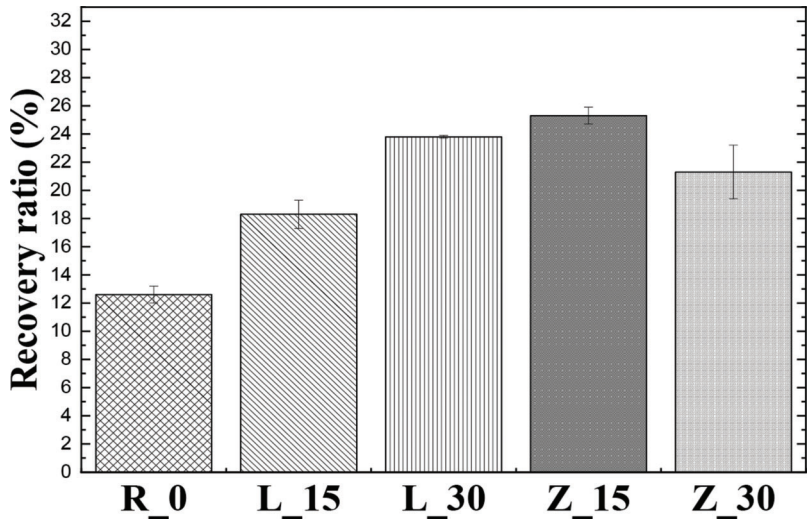

Figure 4.10 Recovery ratio of designed materials based on resonant frequency measurement.

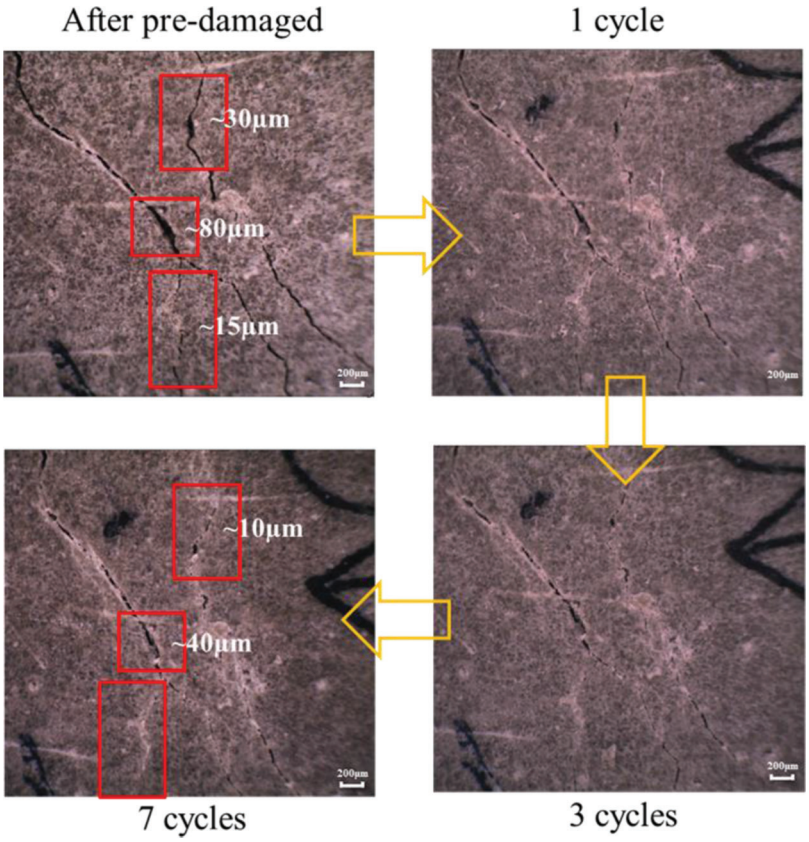

Figure 4.11 Healing of cracks throughout wet/dry cycles (from mixture R-0).

TABLE 4.3
Crack width reduction ratio of different mixtures

Crack Width Range (μm)	R_0	L_15	L_30	Z_15	Z_30
0~10	100	100	100	100	100
10~20	100	100	100	100	95.56
20~30	43.52	44.24	44.73	88.61	48.17
30~40	42.79	40.96	55.73	59.69	50.3
40~50	25.27	27.70	31.67	46.28	33.96
>50	20.85	34.09	23.64	49.09	31.28

For R_0, the reduction ratio dropped to around 40% at the crack width of 20~40 μm and remained at a low level of around 20% above 40 μm. With the incorporation of pre-wetted internal curing agents effectively increased the crack width reduction ratio for all crack width ranges. Z_15 achieved the best healing performance among all groups. The reduction ratio was almost two times higher than the other groups at 20~30 μm. Even above 50 μm, it still retained around 50% of the crack width reduction ratio.

4.4.4.3 Pore structure of the internal curing aggregates. Internal curing agents under saturated surface-dry (SSD) condition were tested to evaluate the water desorption kinetics by monitoring the change of the weight under different designed conditions. The normalized moisture content defined as $\frac{Mass\ Water}{48h\ Water\ Absorption}$, is used to quantify the extent of the water desorption. A normalized weight of 1.0 represents the saturated internal curing agent. The result of the water desorption kinetic test is shown in Figure 4.12. It can be seen that zeolite and LWA reached equilibrium after 8 hours at a relative humidity of 50%. Furthermore, 80% and 90% of their absorbed water were released, respectively. It is expected that since LWA and zeolite have been used to supply water to reduce the early age shrinkage, a high release rate of water is required under such a relative humidity level (Paul & Lopez, 2011). Afterward, when samples were moved to the chamber with 10% relative humidity, zeolite released another 10% of its absorbed water while

LWA stayed the same. The result implies that zeolite had a higher water retention capacity compared with LWA. It is likely that zeolite stored part of its absorbed water under the ambient environment and released it under extremely low humidity. In the self-healing process, this higher water retention capacity of zeolite could facilitate the continuous hydration of the cementitious materials, which leads to a higher healing efficiency.

Scanning electron microscopy (SEM) images of LWA and zeolite are shown in Figure 4.13. The highly porous structure can be seen for both zeolite and LWA, which suggests the high water absorption capacity. In general, the water absorption process in aggregate is caused by the capillary effect (Henkensiefken et al., 2009b). During the hydration process, the larger pores tend to lose the water first (Henkensiefken et al., 2009a). A finer pore structure can lead to a stronger capillary force that tends to retain the water. By comparing SEM images of LWA and zeolite, the size of the pores in zeolite is clearly smaller than LWA. Thus, a slower water release rate can be expected for zeolite, which verifies the water desorption results, as shown in Figure 4.12. In contrast, the open void and the connection between pores can be observed in LWA. Therefore, a high water-transport efficiency with rapid water absorption/desorption rate in LWA can be expected and was observed in Figure 4.12.

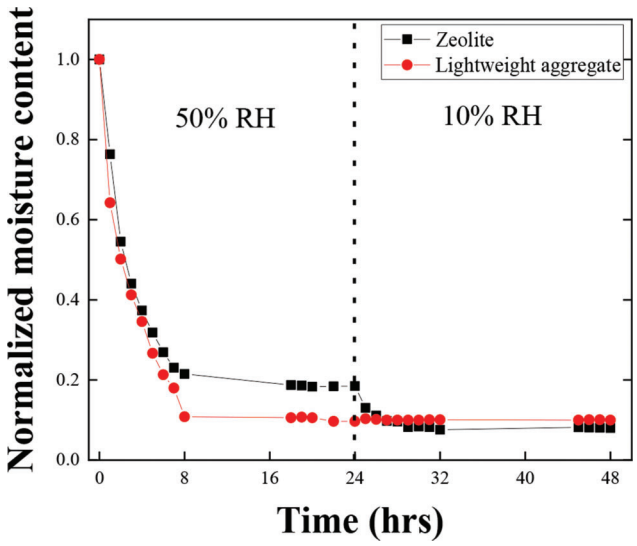

Figure 4.12 Water desorption behavior of internal curing agents.

4.4.4.4 Mechanism of the improvement in healing performance. After the self-healing period, samples were submerged into water to test the bulk absorption capacity. As shown in Figure 4.14, the sample with internal curing agents exhibited a higher absorption capacity compared with the reference mixture. It can be noticed that the result of the bulk absorption capacity exhibited a similar trend to the result of the self-healing evaluation (Figure 4.10), which is expected since a higher absorption capacity of the sample could increase the possibility of the un-hydrated cementitious materials been exposed to water and result in the self-heal of the sample. In addition, it can be seen that the bulk sample absorption capacity increased when the replacement ratio of LWA increased from 15% to 30%.

We observed that water absorption capacity correlates very well with the self-healing ability of studied systems, which coincides with our previous study (Su et al., 2020). A higher capacity of water storage capacity could result in better self-healing performance. The addition of porous zeolite and LWA tends to

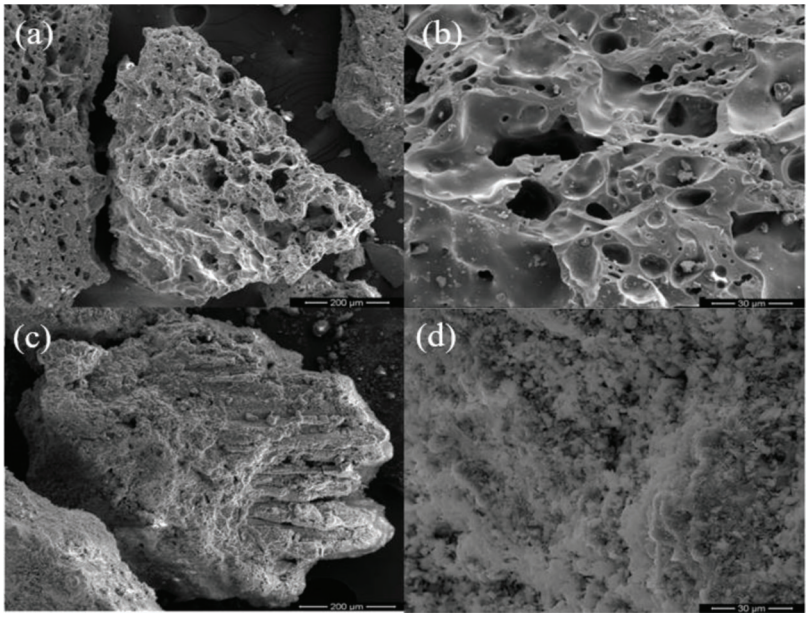

Figure 4.13 SEM images of internal curing agents: (a–b) lightweight aggregate and (c–d) Zeolite.

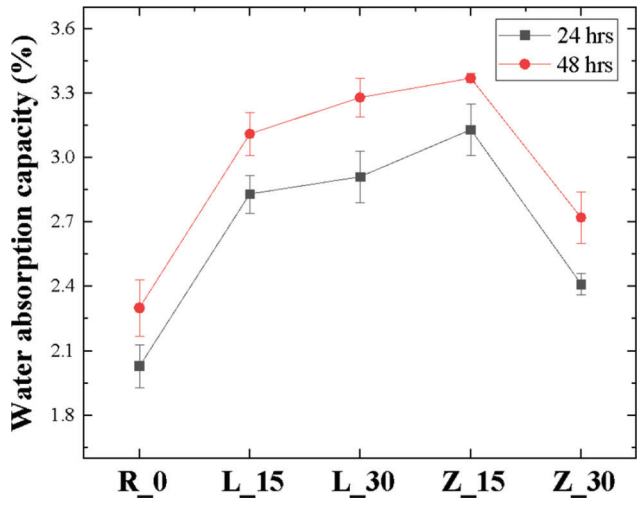

Figure 4.14 Bulk sample water absorption capacity.

increase the bulk absorption capacity of the sample (Figure 4.14), which makes it more likely to absorb and store part of the external water when it is under wet curing condition (Kou et al., 2014). Consequently, this part of the stored water can be slowly released for continuous secondary hydration and precipitation of the calcium carbonate when the external water is no longer available. Besides, if we took a closer look at the effect of zeolite when the content of zeolite increased from 15% to 30%, the water absorption capacity decreased, and its decreasing water absorption compromised the healing performance. Considering the water absorption capacities of zeolite and LWA are 18.00% and 13.64%, respectively, mixture Z_30 is expected to have the highest water absorption capacity. However, the test result shows that this is not the case. In fact, mixture Z_30 exhibited the lowest absorption capacity among all the samples with internal curing agents, even though the mechanical tests have already proven that Z_30 did have the most robust matrix due to a larger amount of internal curing water carried by 30 wt% of zeolite. The reason may be the existence of the balance between the incorporation of porous agent and internal curing effects. When the internal curing effect is under a certain threshold, the incorporation of a porous curing agent will increase bulk absorption capacity. In contrast, when the amount of internal curing water beyond that threshold, the increment in compactness of the matrix due to the internal curing effect starts to block the external water from absorbing by the bulk sample, the so-called water blocking effect, which leads to a lower absorption capacity (Su et al., 2020).

Based on the result of the internal curing agents' desorption test, as shown in Figure 4.12, zeolite has a higher water retention capacity compared with LWA. LWA tends to release all its absorbed water in the ambient environment, while zeolite can store part of it. Also, the SEM images show that zeolite has finer pores compared with LWA (Figure 4.13), leading to a slower water release rate. These features of zeolite are favorable for the improvement of self-healing since it is vitally essential for the internal curing agent to has the ability to supply water when the external moisture is limited continuously. The TGA measurement shows that samples incorporated with zeolite exhibited a higher degree of hydration, which confirms the stronger internal curing effect and secondary hydration. It can be noticed that, although Z_30 had a lower bulk sample absorption capacity than the mixtures with LWA (Figure 4.14), it still led to the comparable self-healing performance compared with LWA (Figure 4.10 and Table 4.3) owning to its high water retention capacity and slower water release rate (Figure 4.12).

4.5 Effect of Using Superabsorbent in SHCC

4.5.1 Experimental Design

According to the literature review, autonomous healing of the concrete is based on the artificially incorporated healing agents which allows the complete healing of cracks larger than several hundreds of micrometers, while the autogenous healing exhibited a less healing capacity of less than 100 μm.

In order to prevent the overestimation of the absorption capacity of the SAP in concrete mixture, the robustness of the SAP was evaluated. The SAP used in this study is a commercially available SAP Floset 27. Various dosages of the superplasticizer, hydration accelerator and fly ash were designed, and the absorption behavior of the SAP was tested by the filtration test and void size analysis.

A filtration test was performed to evaluate the influence of superplasticizer and hydration accelerator on the water absorption behavior of SAP. The concentration of the SP and accelerator were ranged from 0 to 2.0 wt% and 0 to 1.0 wt%, respectively. A constant mass of the SAP of 0.2 g was prepared for each test. The test setup is shown in Figure 5.4. The SAP was filtrated by a funnel after 15 minutes soaking in the 100 mL DI water with different concentrations of the superplasticizer or hydration accelerator. A pump was used to provide a constant pumping pressure to accelerate the filtration process. The absorption capacity of the SAP was calculated by Equation 4.2.

$$\text{Absorption capacity } (g/g) = \frac{m_{liquid}}{m_{SAP}} \quad \text{(Equation 4.2)}$$

Where m_{liquid} is the mass of the liquid that is absorbed by the SAP and the m_{sap} is the original mass of the SAP that adds into the solution.

Void size analysis was conducted to analyze the size of the pores that leave by SAP after it releases the absorbed water. The void size left by the SAP can be used as an index to represent the absorption behavior of the SAP during the mixing and curing process. Different dosages of superplasticizer, hydration accelerator, or fly ash were designed. Samples with four different fly ash to cement contents (FA/CEM) range

from 0 to 1.2 were prepared. Based on the technical data sheet provided by the manufacturers, the designed dosages for superplasticizer and accelerator were ranged from 0 to 2 wt% and 0 to 1.79 wt%, respectively. All the sample was incorporate with 0.25 w% of the SAP and the water to cement ratio was 0.4. The samples were de-molded after 24 hours and cured in the laboratory condition for 7 days.

After the curing, the samples were cut into 25.4 mm cubic by a diamond saw, and calcinated under 600°C for 1 hour to decompose the SAP particles. Then, acetone was used to clean the surface of the sample. To enhance the contract between the void and the matrix under the microscope, the surface of the sample was colored by black marker, and then pre-treated by the barium sulfate powder. To evaluate the average void size on the surface of the sample, the microscopic images were analyzed by the software Image J.

A water flow test was designed to evaluate the self-sealing performance of the SAP in concrete materials. Cement paste with 1 wt% of the SAP was cast into 76.2 mm (diameter) × 152.4 mm cylinder and cured in the laboratory environment for 7 days. A reference sample without the addition of SAP was also prepared. The water to cement ratio of the mixtures was 0.4. After the 7 days curing, splitting tensile loading was conducted to pre-crack the sample. The crack width was controlled by two steel rings as 0.16 mm. The experimental setup includes a water tank, PVC tube, rubber tube, balance and computer, as shown in Figure 5.5. The water tank can continuously supply water, while a rubber tube connected to the PVC tube controls the water level to make sure the constant of the water pressure to the testing sample. Balance and the computer are used to monitor and record the weight of water passing through the sample with time.

4.5.2 Result and Discussion

4.5.2.1 Robustness of SAP. Results of the robustness evaluation of SAP are shown in Figures 4.15, 4.16, and 4.17. For the filtration test, as can be seen in Figure 4.15(a) and Figure 4.16(a), the absorption capacity of the SAP decreased from 287.5 g/g to 102.6 g/g as the dosage of the superplasticizer increased from 0 to 2 wt%. On the other hand, when 1 wt% of the accelerator was used, a much more aggressive inhibition can be observed, where the absorption capacity of the SAP was decreased down to 8.4 g/g. Therefore, it can be concluded that the presence of the superplasticizer or hydration accelerator can effectively inhibit the swelling of the SAP particles. The result was further verified by the void size analysis, as shown in Figure 4.15(b) and Figure 4.16(b). During the mixing process, the dry SAP particles swelled by absorbing part of the mixing water. Afterward, the absorbed water was released for cement hydration as the relative humidity decrease, which caused the shrinkage of the SAP particles and generated empty voids inside the cementitious matrix. Therefore, the average void size can be used to analyze the absorption behavior of the SAP in fresh concrete. The incorporation of the superplasticizer or accelerator led to a smaller average void size, which indicates that the swelling of the SAP was inhibited by the additives that were incorporated. On the contrary, as shown in the Figure 4.17, the addition of the fly ash led to an increase in the average void size. This could be due to the low solubility of the fly ash compared with cement. Since the presence of cations such as Ca^{2+} and Al^{3+} was reported to have an inhibiting effect on the swelling of the SAP, the low solubility of the fly ash reduced the cation concentration of the pore solution, which promoted the absorption capacity of the SAP.

It is worth noting that even though the result of the filtration test shows that the superplasticizer and accelerator can aggressively reduce the absorption capacity of the SAP, only minor influence was observed from the void size analysis. Especially for the hydration accelerator, only 3.2% reduction was observed when the dosage of the accelerator was 1.79 wt%. Furthermore, the average void size was reduced for 10.0% when 2 wt% of the superplasticizer was used.

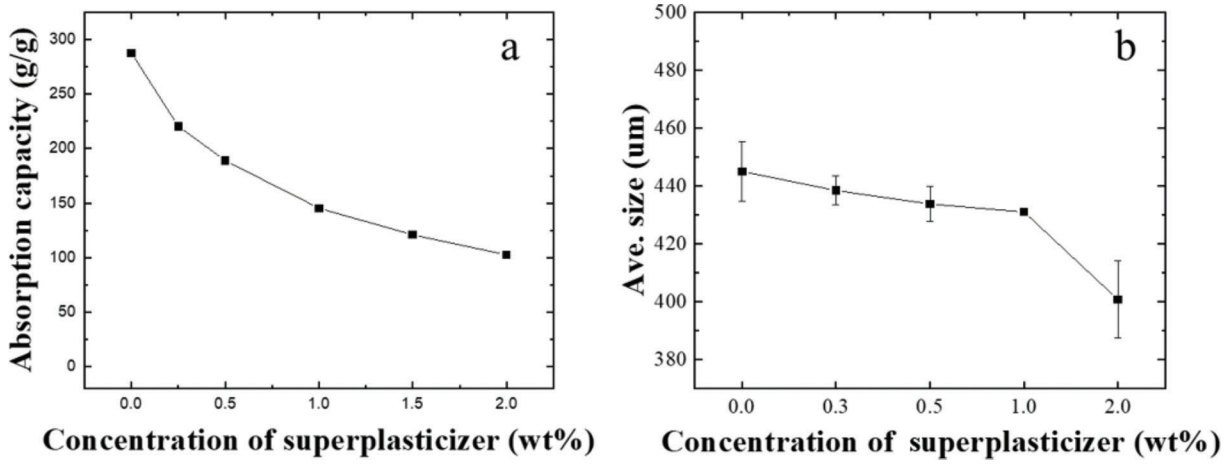

Figure 4.15 Evaluation of the SAP robustness under various superplasticizer dosage: (a) filtration test and (b) void size analysis.

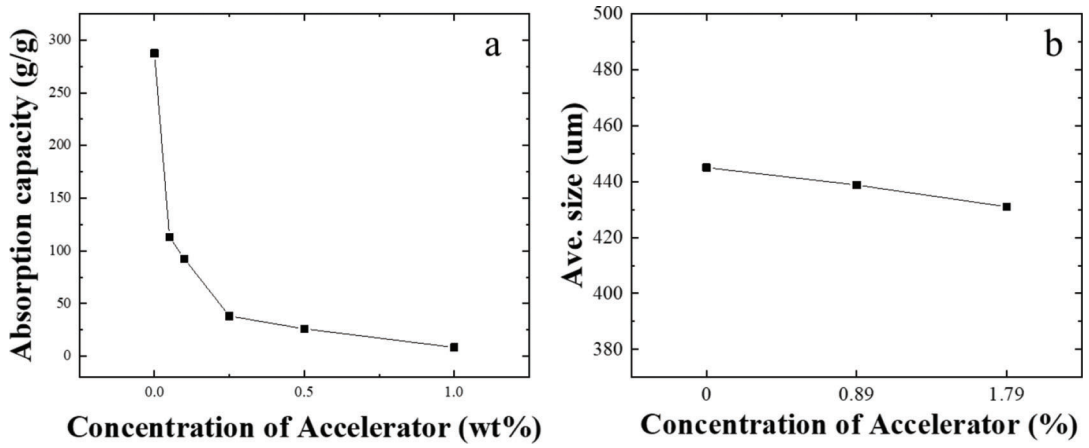

Figure 4.16 Evaluation of the SAP robustness under various hydration accelerator dosage: (a) filtration test and (b) void size analysis.

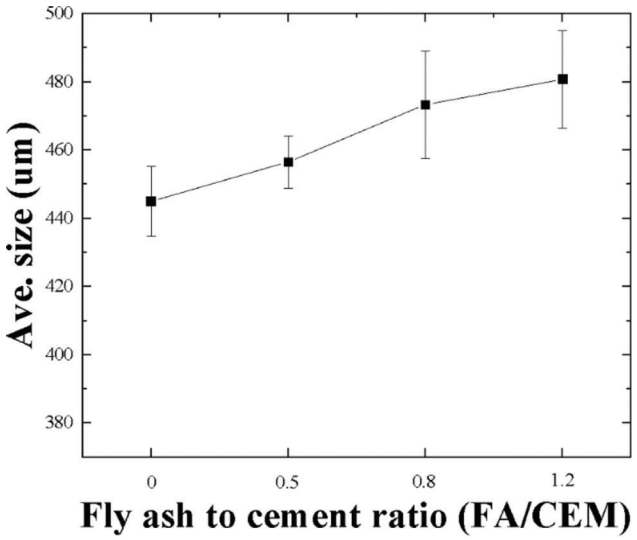

Figure 4.17 Evaluation of the SAP robustness under various fly ash content.

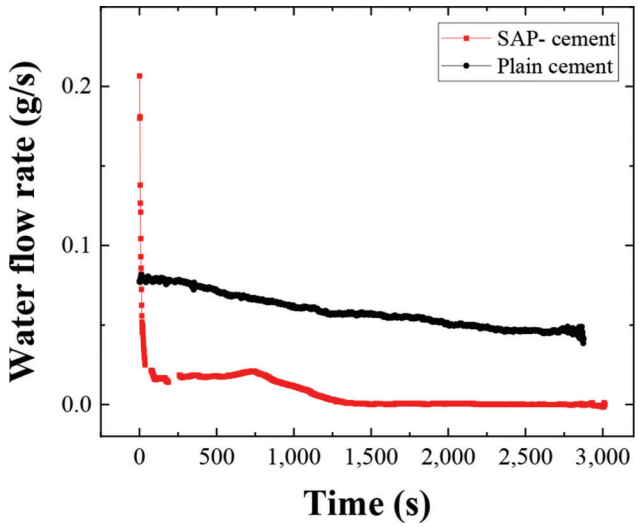

Figure 4.18 Water flow rate of the testing samples.

Similarly, when the fly ash to cement ratio was 1.2, only 8.1% increment on the average size was found. Therefore, it can be concluded that the SAP is relatively robust under various environmental conditions. However, during the mixture design with SAP, the use of superplasticizer, hydration accelerator and fly ash should be considered as a factor that may influence the efficiency of the internal curing.

4.5.2.2 Self-healing performance of SAP. According to the data recorded by the computer, the water flow rate can be calculated by the weight of water passing through the sample per unit time, as shown in Figure 4.18. The cumulative passing water with time was also acquired, as shown in Figure 4.19.

It can be observed from the result that the incorporation of SAP effectively controlled the seeping of the water compared with the plain cement sample. In Figure 4.18, it can be noticed that compared with the reference mixture, the sample with SAP has a higher water flow rate at the beginning. It could be due to the large pores left by drying SAPs that favor the passing of the water. However, it can be noticed that within 60 seconds, the water flow rate decreased from over 0.2 g/s to 0.02 g/s, which is already lower than the plain cement sample. In this process, there are two mechanisms for the reduction of the water flow rate. Firstly, once the SAPs embedded inside the cement paste come in contact with water, it will start to absorb water and prevent part of the water from passing through the sample. Secondly, after the SAP absorbs water, the swelling effect of the SAP can seal the crack and block the further seeping of the water. In Figure 4.19, it can be observed that the passing of water was effectively controlled for the sample with SAP. On the contrary, the water passing through the sample without SAP increased almost linearly with time. The total weight of the passing water was over 150 g after 3,000 s, which is 7 times higher than the sample with SAP. Therefore, it can be concluded that the self-sealing effect of the SAP

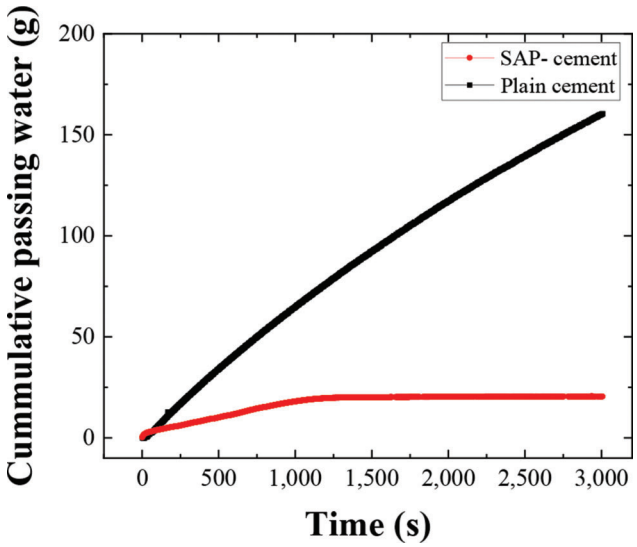

Figure 4.19 Weight of the cumulative passing water.

is capable of controlling the seepage of the external water. If the cracked concrete is exposed to the outdoor environment, such as precipitation or groundwater, SAP inside the concrete will form a soft gel that fills in the formed cracks, preventing the further water penetration, which is called self-sealing. The self-sealing occurs rather rapidly (usually within a few minutes in the presence of external water). Afterward, the water retained in SAP triggers the hydration and carbonation at the surface of cracks, leading to long-term self-healing.

4.6 Summary

In this chapter, effects of the incorporation of internal curing agents into the designed cementitious composite on the self-healing performance were tested. Experimental results show that the internal curing aggregates can enhance the healing efficiency by providing water internally to accelerate the autogenous healing.

In the evaluation of the internal curing aggregates, it was found that the cementitious composites with porous curing aggregate had better compressive strength than the reference sample. The extra water supplied by the pre-wetted zeolite or lightweight aggregate could enhance the degree of hydration to form more C-S-H gel and a strong cement matrix. The samples show an over 15% compressive strength improvement for the cementitious composites sample with zeolite and a 6% improvement with lightweight aggregate.

Evaluation of the self-healing performance shows that the addition of the internal curing aggregate improved the healing of the sample. The use of the zeolite could increase the healing ratio from around 2.0% to over 5.0% after 7 wet/dry cycles (28 days) based on two non-destructive tests. Results from the experiments suggests that the optimal zeolite replacing ratio for sand may be 15 wt%. In addition to zeolite, a conventional internal curing agent, the lightweight aggregate was also incorporated and the properties of the SHCC were compared with the zeolite. The results indicate that the use of the lightweight aggregate improved the healing efficiency of the SHCC, but the improvement was not as significant as zeolite. The pore structure analysis suggests that the zeolite has a finer pore size compared with LWA. During the healing period, it is capable of slowly but continuously supplying water to cementitious materials when the external water supply is unavailable. The continued water supply led to a better autogenous self-healing performance compared with lightweight aggregate.

Evaluation of the SAP indicated that the absorption behavior of the SAP could be influenced by the superplasticizer, hydration accelerator, and fly ash. However, only a minor influence of less than 10% was observed. Therefore, it can be concluded that SAP is relatively robust under the designed environmental conditions. For the self-sealing effect of the SAP, a dramatic reduction in the water flow rate from 0.2 g/s to 0.02 g/s was observed within 60 seconds of the test when the SAP is incorporated. In addition, the 5 hours cumulative passing water of the reference sample was 7 times higher than that with the incorporation of SAP. In summary, experimental results indicated the effectiveness of using SAP as a self-sealing agent in concrete materials.

5. RHEOLOGY CONTROL OF SHCC

5.1 Introduction

Rheological control is critical for optimize the fiber distribution and to realize the micromechanical design of SHCC. In fiber reinforced cementitious composite, a higher solid volume fraction can lead to a higher frictional force between fiber and other solid particles. Therefore, in the design of the high ductility cementitious composite, low water to cement ratio is generally used to ensure the fiber distribution and fiber-matrix interface. However, considering the economic efficiency and practical application, a relatively high-water content of 0.35 is used in the design SHCC. Thus, the quality of the fiber distribution would be a concern and affect the ductility of the SHCC. In this session, we discuss the efficiency of two approaches on rheology control, including the addition of SAPs and adjusted by various viscosity-modified agents. The mechanical performance of the SHCC was also evaluated and reported in this chapter.

5.2 Effect of SAP on the Rheology of SHCC

In this part of the study, we first present the influence of the SAP on the rheology properties of the cement paste. The plastic viscosity of the cement paste was calculated and discussed. Moreover, the mini-slump test was performed to identify the workability of SAP

based SHCC, and the mechanical properties of the sample were evaluated.

5.2.1 Materials and Methods

A commercially available SAP (Floset 27 CS) was chosen in this study. The selected SAP is a cross-linked copolymer of acrylamide and acrylate in a powder form with a mean particle size of 194 μm, as shown in Figure 5.11. The absorption capacity in the synthetic cement pore solution was measured using the tea-bag method, as described in (Mechtcherine et al., 2018). The synthetic cement pore solution was prepared based on previous work (Kjeldsen et al., 2006). As shown in Figure 6.1, the SAPs absorbed the synthetic cement pore solution and reached a plateau rapidly while the absorption of SAPs in DI water kept increasing, showing no sign of saturation within the investigated time range. The absorption capacity of the SAP in DI water was much higher than that in synthetic cement pore solution. It can be due to the existence of the cations such as Ca^{2+} that reduced the water retention capacity of the SAP (Kang et al., 2018). The plateau value in the cement pore solution is around 35 g/g, representing that 35 g of solution absorbed by the unit weight (1 g) of dry SAP powders, and SAPs reached 90% of the plateau value at 3 minutes after the SAPs first came into contact with the solution.

5.2.2 Rheological Measurements

As SAP absorbs the water and reduces the free water in the cement matrix, it will significantly alter the workability. It is necessary to evaluate the influence of SAP on the rheological properties. All rheological characterization was performed on a temperature-controlled, stress-controlled rotational rheometer with a 4-blade vane geometry set at a constant temperature of 25°C. The rheological test started with a pre-shearing to ensure that all the samples were at a reproducible reference state. The sample was left to rest for 120 s to allow for stress relaxation and followed by a linear shear ramp to obtain a flow curve. The shear stress response was recorded. From the flow curve, the yield stress and plastic viscosity were obtained using the Bingham model.

$$\tau = \tau_0 + \eta_{pl}\dot{\gamma}$$

Where τ is shear stress, γ is shear rate, τ_0 is dynamic yield stress, and η_{pl} is plastic viscosity.

5.2.3 Experimental Result

A downward portion of the curve was fitted with the Bingham model. The yield stress is the intercept with the vertical axis (when the shear rate is 0) and the plastic viscosity is the slope of the curve (constant throughout the shear rate range considered). The plastic viscosity and dynamic yield stress increase monotonically with the addition of SAP as shown in Figure 5.1. The result shows that as the dosage of the SAP increased from 0% to 0.24 wt% of cement, the plastic viscosity showed a dramatic improvement of over 56%. Based on the experimental result, the incorporation of the SAP could improve the fiber distribution since it can increase the viscosity of the mixture and the frictional force between fiber and other cementitious composite components during the mixing process. To further verify the influence of SAP on the performance of SHCC, mechanical tests were conducted and presented in Section 5.2.5.

5.2.4 Mini-Slump and Viscosity Test Results of SAP Based SHCC

To study the influence of the SAP on the fresh properties of the SHCC, mini-slump and viscosity tests were conducted. The mixture composition is shown in Table 5.1. After the raw materials were prepared, the cement, slag, fly ash, sand and SAP powder were dry mixed for 3 minutes. Then, water was added for the wet mixing for 3 minutes. After the wet mix, a partial of the

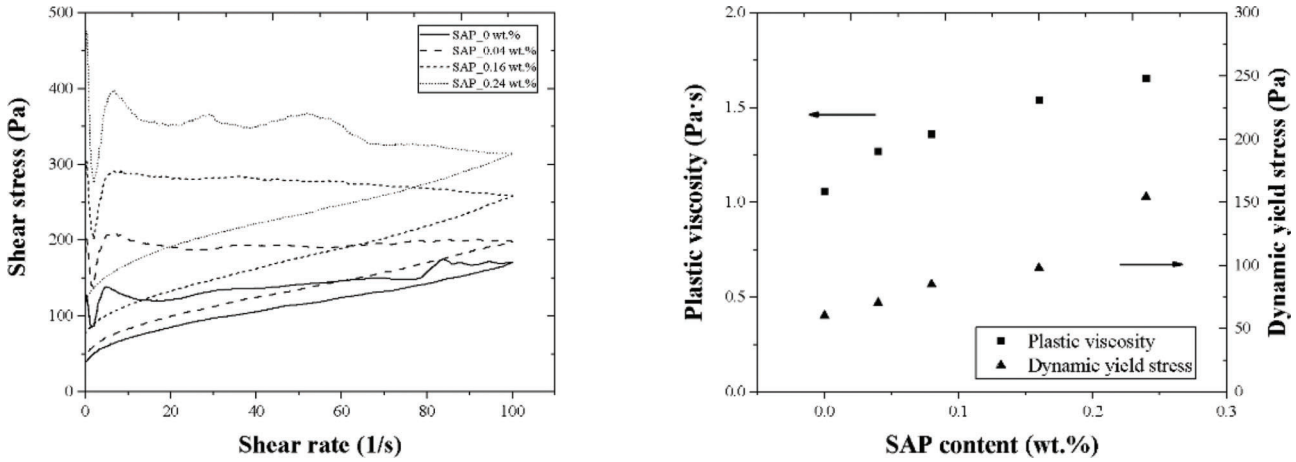

Figure 5.1 Flow curve of SAP cement (left), the effect of SAP on the plastic viscosity and dynamic yield stress of cement paste (right).

TABLE 5.1
Mixture composition for the evaluation of slump and viscosity of SAP-SHCC

Mix	OPC-I	Blast Furnace Slag	Fly Ash	w/b*	Fiber (Volume %)	Sand	SAP
2%PVA	1	0.15	0.15	0.35	2	0.8	0
2%PVA+0.166SAP	1	0.15	0.15	0.35	2	0.8	0.166
2%PVA+0.664SAP	1	0.15	0.15	0.35	2	0.8	0.664

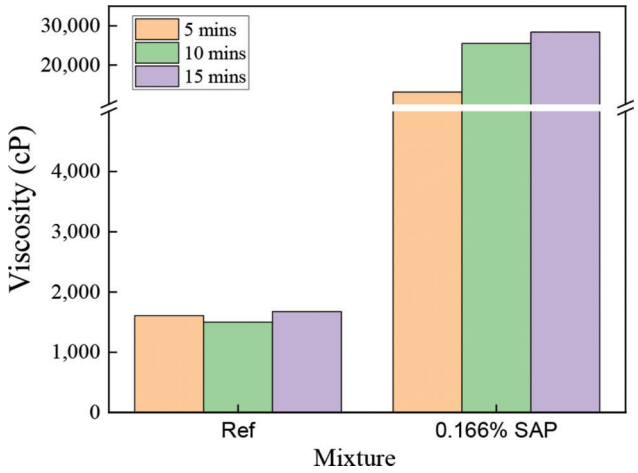

Figure 5.2 Viscosity evaluation of the SHCC based SAP.

Figure 5.3 Mini-slump test for SHCC with 0.664% SAP.

mortar was taken out for viscosity measurement until the 15th minute (after adding water). The rest of the matrix was constantly mixed for 2 more minutes before adding the fiber. As the SHCC were well mixed, the fresh SHCC was used for the mini-slump test. The results are shown in Figures 5.2 and 5.3 and Table 5.2.

It can be seen from the Figure 5.2 that the addition of the SAP effectively increased the viscosity of the SHCC mixture from around 1,800 cP to over 10,000 cP, which is favorable for the improvement of the fiber distribution. From Table 5.2, it can be found that the addition of the 0.166% SAP reduced the diameter of the mini-slump for 9.1%, which indicates the water absorption ability of the SAP could adjust the workability of the SHCC and prevent the overflow of the mixture due to the use of the fly ash. However, it can also be observed from Figure 5.3 that when the higher dosage of the SAP was used (0.664 wt%), the workability of the SHCC was un-satisfied, the viscosity and mini-slump of the SHCC with 0.664% SAP were unable to be measured due to the extreme low workability.

In this part of the study, the influence of the SAP on the fresh properties of the SHCC was investigated. It was found that SAP can effectively increase the viscosity and decrease the workability of the mixture using small dosage of 0.166 wt%, which shows potential in improving the fiber distribution. However, it was also observed that higher dosage of the SAP could lead to a poor quality of the mixture. It causes concern of the mechanical properties since SAP may negatively affect the hydration of the cementitious materials since it will absorb a large portion of the water and hinder the early age hydration. Therefore, in the following

TABLE 5.2
Result of the mini-slump test

Mixture	Ref	0.166%	0.644%
Diameter (inch)	6.188	5.625	–

study, the mechanical performance of the SAP based SHCC was examined. Extra water was designed and provided for the SHCC mixtures with SAP incorporation to ensure the early age hydration.

5.2.5 Mechanical Properties of SAP Based SHCC

5.2.5.1 Experimental design. To evaluate the influence of the SAP on the mechanical properties, SHCC mixtures incorporated with SAP were designed, as shown in Table 5.3. Since SAP is used as internal curing agent that absorbs large amount of free water during the mixing process, extra water was provided for the mixtures with SAP to ensure workability and early age hydration. 50 mm cubic, 240 mm × 60 mm × 15 mm plates, and dog-bone specimens were prepared for the compressive test, four-point bending test, and uniaxial tensile test, respectively. The sample was demolded after 24 hours and cured in the moisture room until testing age.

5.2.5.2 Result and discussion. After 3 and 7 days of the moisture curing, the samples were subjected to

TABLE 5.3
Mixture design for the evaluation of the mechanical properties of SHCC-SAP

Mix	OPC-I	Blast Furnace Slag	Fly Ash	w/b*	Fiber (Volume %)	Sand	SAP
2%PVA	1	0.15	0.15	0.35	2	0.8	0
2%PVA+0.166SAP	1	0.15	0.15	0.35+0.07	2	0.8	0.166
2%PVA+0.664SAP	1	0.15	0.15	0.35+0.07	2	0.8	0.664

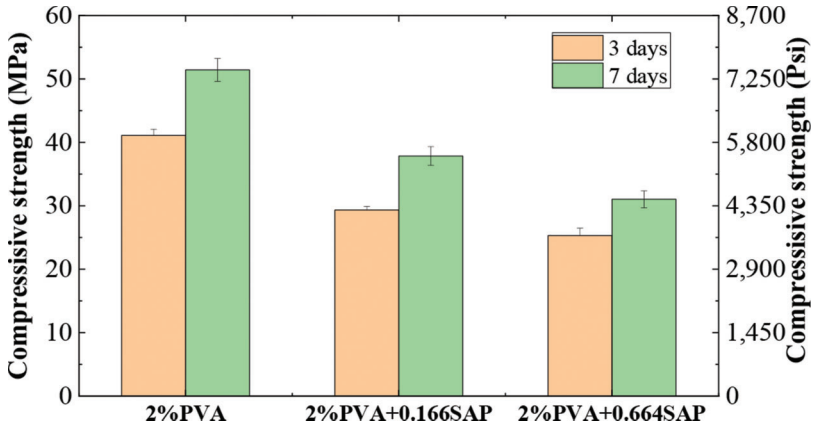

Figure 5.4 Compressive strength result for the SHCC-SAP.

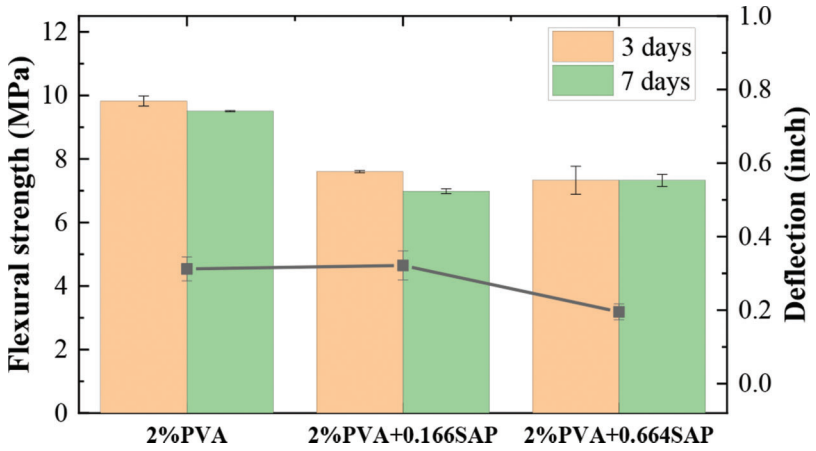

Figure 5.5 Flexural strength result for the SHCC-SAP.

mechanical testing. The results are presented in Figures 5.4, 5.5, and 5.6. It can be observed that the addition of the SAP decreased the compressive strength of the SHCC at both testing age of 3 and 7 days. When 0.166% of the SAP was used, the compressive strength of the sample was decreased for over 25%, while a higher dosage of the SAP could further decrease the strength for another 15%. The adverse influence of the SAP on compressive strength could be due to the increased porosity inside the matrix which was resulted in the swelling and shrinking of the SAP particles. The SAP particles absorbed water in the fresh mixture and the swelling effect increased its volume. Later, as the cement matrix got harden, releasing the absorbed water from the SAP left large pores inside the system. Therefore, a lower compressive strength can be expected. Similar phenomenon was also found from the flexural test, as the size of the pore and the porosity increased, the strength performance was adversely affected. In terms of the flexural deflection, the high dosage of the SAP incorporation reduced the ductility of the SHCC, while the addition of the 0.166% SAP performed similar as the reference sample. On the other hand, it can be noted that the uniaxial tensile strength of the sample with 0.166% SAP exhibited a slightly higher tensile strength and further increasing the dosage

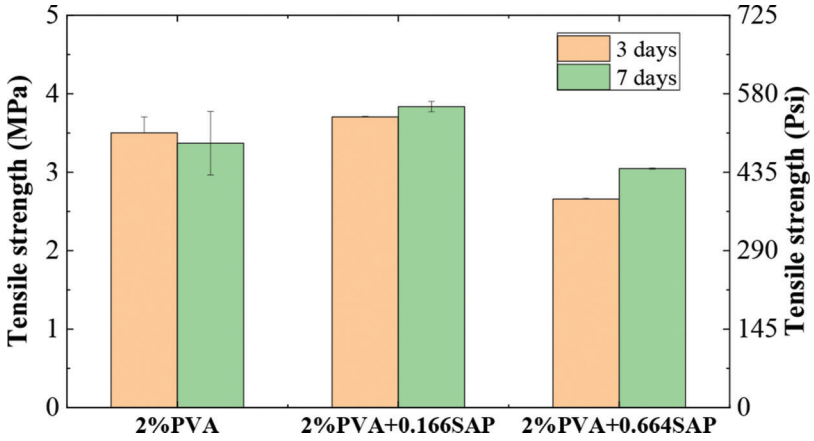

Figure 5.6 Tensile strength result for the SHCC-SAP.

TABLE 5.4
Experiment dosages of different VMA

	Reference	VMA 358 (~225 cP) (%)	VMA 362 (~570 cP) (%)	VMA 450 (~2,270 cP) (%)
VMA Percentage	0%	0.1	0.1	0.1
		0.2	0.2	0.2
		0.3	0.3	0.3
		0.5	0.5	0.5
		1.0	1.0	1.0

of the SAP resulted in a reduction of the tensile performance. This result was due to the voids left by the SAP and the improvement of the fiber distribution. The empty space that was occupied by the swelled SAP could acted as flaws in the matrix that can trigger the formation of multiple cracks. Initially, the strong SHCC matrix can generate limited number of cracks that were bridging by the fibers was discussed in the Section 3.1. The number of cracks was tightly related to the amount of fiber that can contribute to the ductility of the sample. The existence of the voids left by SAP particles increased the possibility of forming more cracks in the matrix during the loading process, which resulted in a better tensile performance. Moreover, as mentioned in Section 5.2.3, the increase on the viscosity of the mixture by SAP is favorable for the improvement of the fiber distribution which contributes to the higher tensile strength. However, as the dosage of the SAP increased, the existence of large number of voids started to negatively affect the performance of the sample, which resulted in a decrease of the tensile strength in the sample with 0.664% of the SAP.

5.3 Effect of VMA on Rheological Control of SHCC

5.3.1 Experimental Method and Design

To improve the fiber dispersion and increase the interfacial force between fiber and matrix, the commercially available viscosity modifying agents (VMA) were used to adjusting the rheological properties of SHCC. Three types of VMAs, including two thickening-type (methenamine based (VMA 358) and biphenyl-based (VMA 362) and binding types (methylpentane based, VMA 450) from BASF company, were utilized with the apparent viscosity of 225 cP, 570 cP, 2,270 cP, respectively. The SHCC samples were tested with different dosages of VMA (from 0.1% to 1%), as the table shown in Table 5.4.

Figure 5.7 presents the experimental logistic of the testing in this session. After the raw materials were prepared, the materials were dry mixed using the mixer for 3 minutes. Then, the water was added for the wet mixing for 3 minutes. Some mortar samples were taken out for viscosity measurement until the 15th minute (after adding water.) The rest of the matrix was constantly mixed for 2 more minutes before adding the fiber. As the SHCC were well mixed, the fresh SHCC were taken to test the mini-slump and cast in the flexural plate mold for the four-point bending test.

5.3.2 Result and Discussion

Figure 5.8 shows the results of viscosity measurements with various configurations of VMA. It can be seen that the VMA was able to increase the viscosity of the SHCC matrix. For VMA 358 and VMA 362, the viscosity of SHCC is located around 1,000 cP to 1,500 cP at 15 minutes. However, for SHCC with VMA 450, the viscosity measurement was exceeded 1,500 cP. Specifically, the viscosity reached 2,500 cP as the VMA 450 dosage increased to 0.3%. Figure 5.9 shows the viscosity results of 1% dosage of three types of

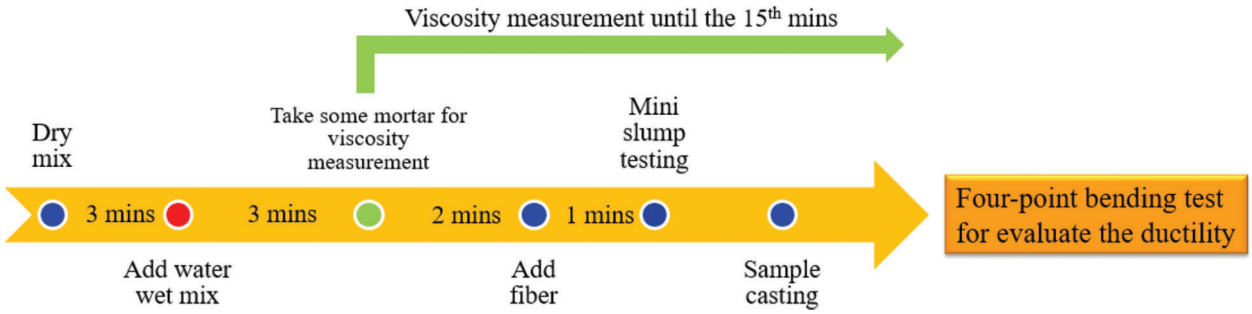

Figure 5.7 Experimental logistic of VMA-SHCC.

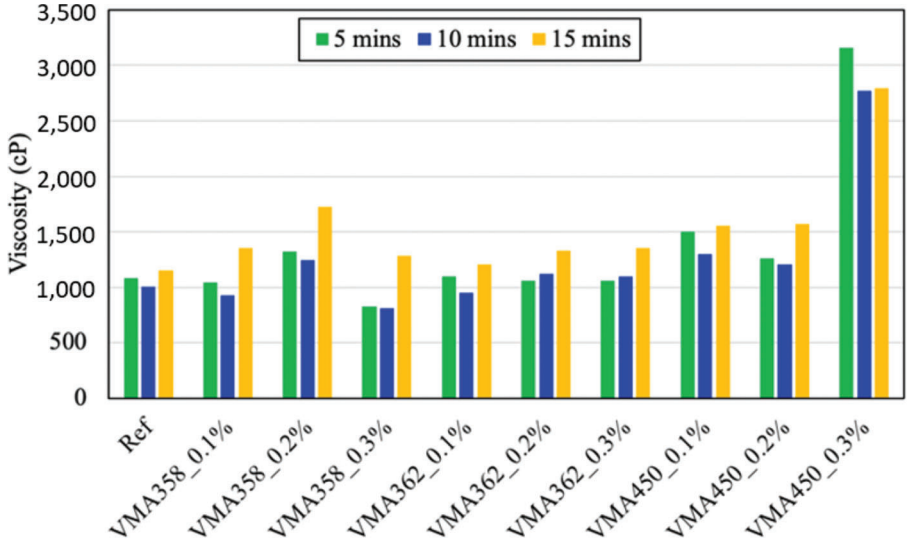

Figure 5.8 Results of viscosity measurements with various configuration of VMA.

VMA. It can be seen obviously that VMA 450 is more effective in enhancing the viscosity properties than the other VMAs with the measurement of around 50,000 cP.

Figure 5.10 shows the mini-slump results of PVA-SHCC with various dosages of VMA. As the figure indicated, the slump flow diameter results were decreased as the VMA added. However, the diameter of all samples was higher than 5 in, which indicated the SHCC were still remained the excellent workability. Figure 5.11 shows the mini-slump results of Strux-SHCC with various dosages of VMA. It can be observed that the VMA did not significantly affect the mini-slump flow result of SHCC contained Strux fiber, which implied that the addition of VMA did not influence the interfacial force between Strux fiber and matrix.

Figure 6.13 shows the results of flexural strength with various configuration of VMA-SHCC with PVA fiber. It can be seen that for SHCC incorporated with VMA 358, the flexural strength increased as the dosage of VMA as 0.1%, but the strength decreased as the VMA increased. For the sample with VMA 362, the flexural strength of SHCC deceased as the VMA dosage of 0.1%, and it increased as the dosage increased to 0.2%. For the SHCC sample with VMA-450, the flexural strength did not have significant changes. Figure 6.14 presents the results of flexural strength with various configurations of VMA-SHCC with Strux fiber. It can be seen that the flexural strength decreased with the increase with the VMA. During the experiments, we have noticed that the PVA- SHCC sample with VMA 450 shown strain hardening behavior since it can significantly increase the interfacial friction between matrix and fiber. Thus, the ductility of flexural testing results for the PVA-SHCC sample has been analyzed using the ductility index. Figure 6.15 illustrates the ductility index of PVA-SHCC with various dosages of VMA 450. The ductility index increased with the increase of dosage of VMA 450 owing to the improvement of interfacial properties.

5.4 Summary

To further improve the performance of the SHCC, this study investigated the influence of the SAPs and various viscosity-modified agents on the rheology properties of the SHCC. Moreover, the mechanical performance of the SHCC after rheology modification was evaluated. The key summaries are list below.

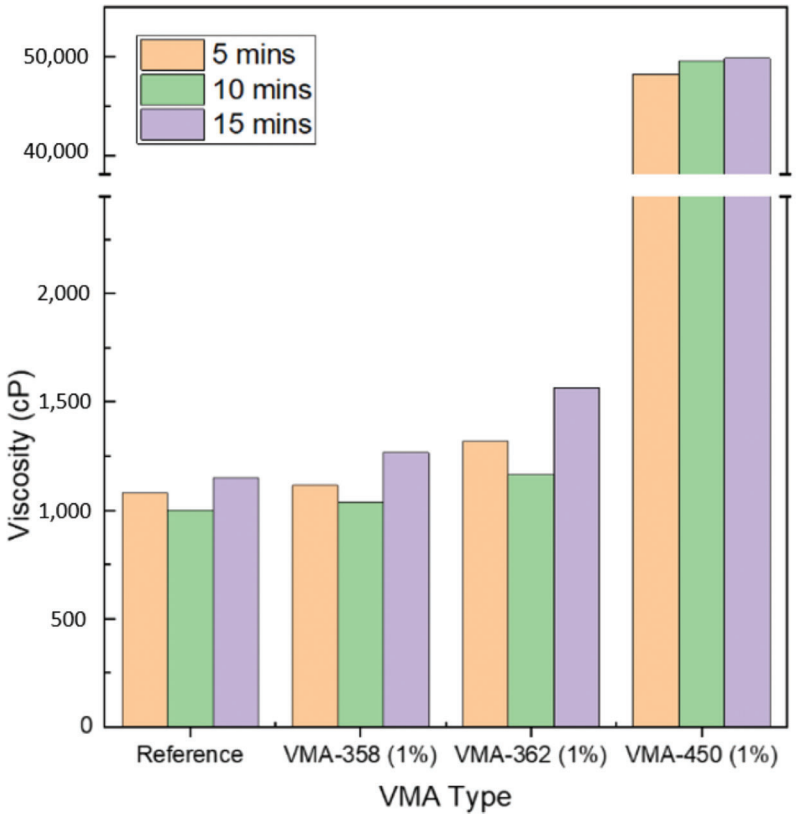

Figure 5.9 Comparison of the viscosity of three types of VMA (1%).

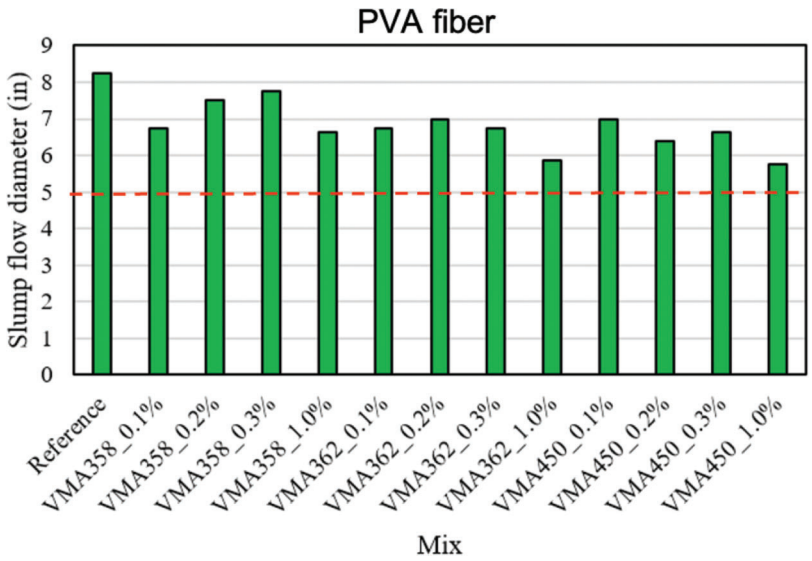

Figure 5.10 Results of mini-slump test with various configuration of VMA-SHCC with PVA fiber.

- Evaluation of the influence of the SAP on the rheology of cement paste shows that as the dosage of the SAP increased from 0% to 0.24 wt% of cement, the plastic viscosity showed a dramatical improvement of over 56%, which suggest that the incorporation of the SAP may be able to improve the fiber distribution since it may increase the frictional force between fiber and another component of the cementitious composite during the mixing process.
- Fresh properties of the SHCC could be adjusted by the use of the SAP. However, when a higher dosage of the SAP was used, it could negatively affect the quality of the mixture, especially at an early age due to the large water absorption capacity of the SAP particles. It is recommended that extra water need to be provided for the mixture with SAP addition in order to ensure the early age hydration of the cementitious materials.

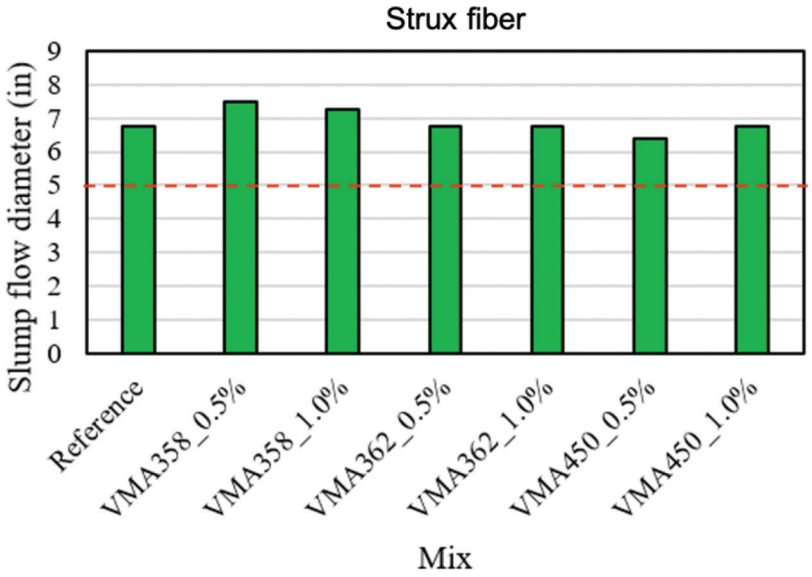

Figure 5.11 Results of mini-slump test with various configuration of VMA-SHCC with Strux fiber.

- Mechanical tests for the SHCC incorporated with SAP indicate that the incorporation of the SAP particles reduce the 7 days compressive and flexural strength of the sample by over 25% and 20%, respectively. The large voids left by the dried SAP adversely influence the matrix quality. On the other hand, it was also found that with a small dosage of the SAP, the 7 days tensile performance of the SHCC was slightly improved by around 13.8% due to the void created by the SAP could act as flaws which triggered the formation of multiple cracks. Also, the increase in the viscosity of the mixture by SAP is favorable for improving the fiber distribution, which contributes to the higher tensile strength. However, with a higher dosage of SAP, the tensile strength was decreased as the large quantity of voids started to affect the performance of the sample adversely. The evaluation of the SAP in SHCC suggests that the incorporation of the SAP may improve the fiber distribution in SHCC, but the adverse effect of the SAP on the cementitious matrix resulted in a worse mechanical performance.
- Three types of viscosity modify agents were used, including two thickening-type (methenamine based and biphenyl based) and binding type (methylpentane based). The viscosity results indicated that compared with thickening-type VMA, the binding based VMA can better raise the viscosity of fresh SHCC mortar. The increase of the mortar viscosity of SHCC can prevent segregation and improve the interfacial properties between fiber and matrix and fiber distribution. The mechanical strength results indicated that VMA has less impact on flexural strength; however, VMA 450 (binding type) can effectively enhance the ductility of SHCC due to the improvement of interfacial properties.

6. NANOSILICA BASED SHCC

6.1 Introduction

Colloidal nanosilica as reported can improve the rheological properties, mechanical properties, and durability of cementitious materials through refining the microstructure and pozzolanic reaction. In this session, we investigated whether the mechanical properties and self-healing performance of SHCC can be improved with the incorporation of colloidal nanosilica.

6.2 Mixture Design and Experiment Procedure

In this session, a series of nanosilica based SHCC experiments were performed. Four different mixes were conducted using ordinary Portland cement (OPC), class C-fly ash (FA), silica sand, PVA fiber, and colloidal nanosilica (CNS). The PVA fiber was kept 1% volume friction for all mixture. To ensure the interfacial friction between the mixture and fiber, the VMA 450 (BASF company) was added, and the ratio was kept at 1% by weight of cement to better performance, as reported in the previous chapter. The colloidal nanosilica (E5 nanosilica, Specification Products, USA) was varied from 0% (as reference group) to 1% by weight cement in SHCC. The composition of SHCC is shown in Table 6.1. The water to binder ratio was kept constants for all the mixes at 0.35.

During the mixing, dry powder form materials (OPC, FA, Silica sand) were mixed for 3 minutes. Half of the water was added first for wet mix. Another half of water was mixed with VMA and added for mixing 3 minutes. PVA fibers were added after the mortar was ready and mixed for 2 minutes. The liquid colloidal nanosilica was added the last as the vendor suggested and mixed for 2 more minutes. The SHCC were cast into the mold and cover with plastic sheet at 23°C laboratory environment for 24 hours. After 1 day, the specimens were demolded and placed in the curing chamber until the testing age.

Various experiments were conducted to evaluate the (1) mechanical properties and (2) self-healing performance of nanosilica based SHCC. For the mechanical

TABLE 6.1
Composition of SHCC with nanosilica (by cement weight)

Mix	OPC	FA	Silica Sand	CNS[1] (%)	VMA[1] (%)	PVA Fiber[2] (%)	W/B[3]
REF	1	0.5	0.8	0	1	1	0.35
0.3% E5 CNS	1	0.5	0.8	0.3	1	1	0.35
0.6% E5 CNS	1	0.5	0.8	0.6	1	1	0.35
1.0% E5 CNS	1	0.5	0.8	1.0	1	1	0.35

[1]By weight percent of cement.
[2]By volume percent.
[3]Water-to-binder ratio.

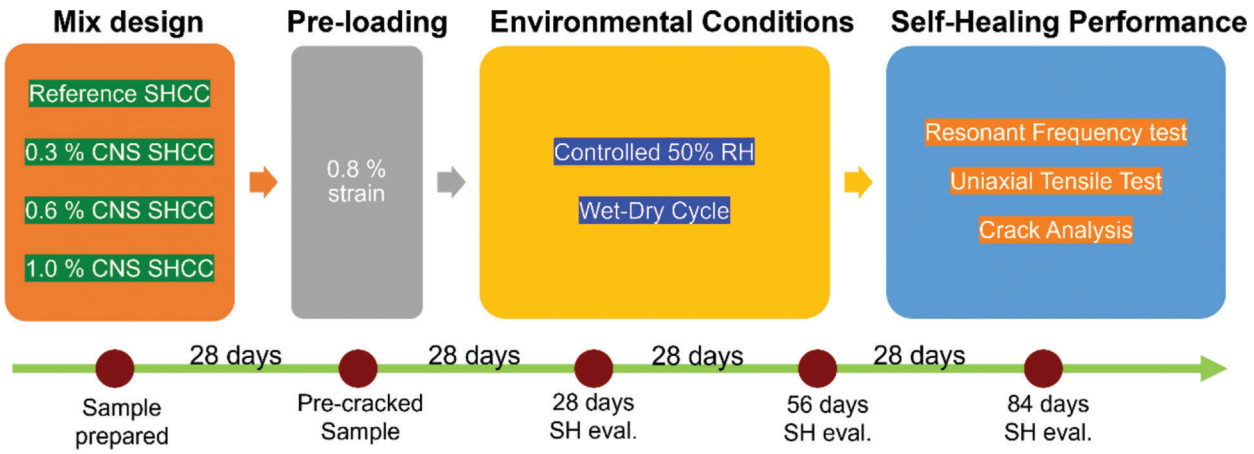

Figure 6.1 Experiment procedure of self-healing evaluation with nanosilica.

properties' evaluation, the samples were prepared for compressive testing (2" cubic specimen), direct tensile testing (dog-bone specimen), and three points flexural testing (plate specimen). The testing ages were 7 days, 28 days, and 90 days. The four shrinkage bars were also prepared for each SHCC set to assess its dry shrinkage from 3 days to 90 days per ASTM. The bond strength between new cast SHCC in corresponding with old concrete layer was also investigated in accordance with ASTM C1583. The pull-off testers (Proceq DY-225) were used for measuring the bond strength.

To investigate the self-healing performance of SHCC, the dog bone samples were prepared for conducting the resonant frequency test and direct tensile test. The procedure for evaluating the self-healing performance of the nanosilica based SHCC specimens is shown in Figure 6.1. The resonant frequency of intact SHCC dog bond samples was measured firstly. Then, the samples were preloaded through uniaxial tensile loading with the pre-strain level of 0.8% and took the measurement of the resonant frequency of pre-cracked samples as the baseline. Pre-cracked SHCC specimens were placed in two types of environmental conditions for assessing the self-healing performance, including wet-dry cycles (altered between immersed in water for 48 hrs and placed in 50%RH for 48 hrs) and a controlled chamber with the controlled temperature of 23 $\pm$ 2°C and humidity of 50 $\pm$ 5%RH. The wet-dry cycles condition is to simulate the sunny day and rainy day, and the controlled 50%RH condition is to consider the extreme condition of low humidity level. Self-healing evaluation was measured at 28 days (1 month), 56 days (2 months), and 84 days (3 months) using both resonant frequency test and direct tensile test.

6.3 Results and Discussion

6.3.1 Mechanical Performance

6.3.1.1 Compressive testing. The compressive strength results of nanosilica based SHCC were presented in Figure 6.2. It can be seen that for the early age (7 days), the compressive strength of four types of SHCC were higher than 4,500 psi. Among the four sets, SHCC with 0.6% E5 nanosilica shown highest compressive strength results of around 5,000 psi. For the 28 days, the trend of the compressive strength is clear that 0.6% E5-SHCC showed the highest compressive strength of over 6,200 psi due to the addition of nanosilica to accelerate the hydration. However, for the long-term results (90 days), the SHCC with nanosilica incorporation did not show significant increments (3%–5%) compared with 28 days results. Interestingly, the reference SHCC (without nanosilica) presented higher compressive strength increments of 10% compared with the other sets of

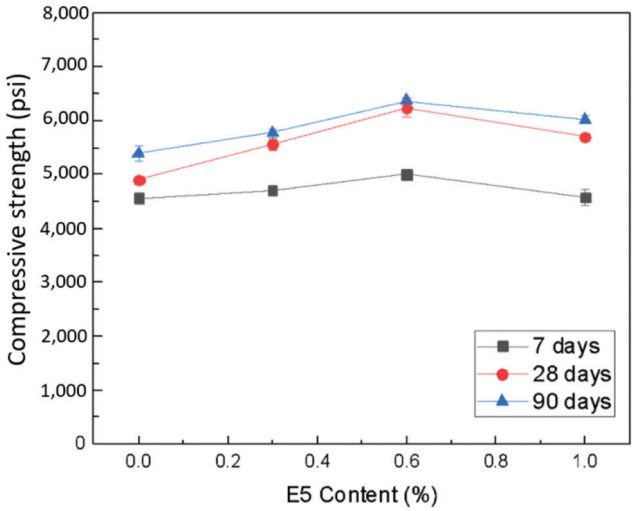

Figure 6.2 Compressive strength results.

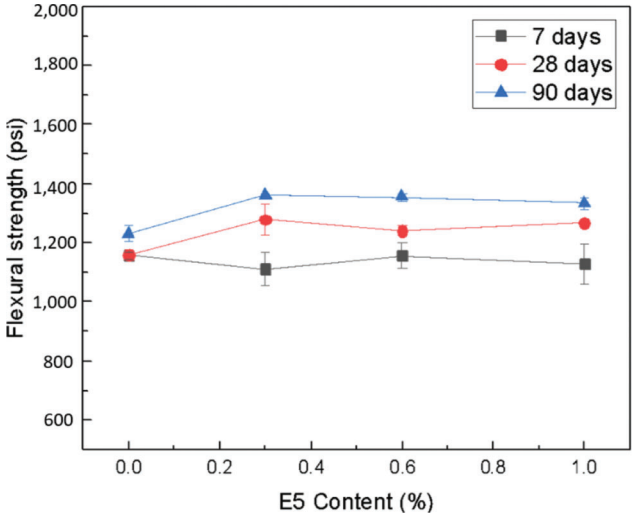

Figure 6.3 Four-points flexural test results.

nanosilica based SHCC. The reason might attribute to the nanosilica accelerated hydration before 28 days, thus, SHCC approximated the high degree of hydration earlier than the reference set.

6.3.1.2 Flexural testing. Figure 6.3 shows the flexural strength results of four-point bending test. It can be observed that the results of 7 days strength did not show significant difference for SHCC with various E5 CNS dosages. The results of 28 days strength indicate that SHCC with E5 nanosilica presents higher flexural strength than the reference set for 7% to 9%. The 90 days flexural strength results present a similar trend with 28 days data.

Figure 6.4 indicates the calculation of the ductility index for 28 days SHCC sample. The ductility index is defined as the ratio between the strain on the modulus of rupture (MOR) and the strain on a limit of proportionality (LOP), i.e., (Ductility index = $\delta_{MOR}/\delta_{LOP}$) (Hameed et al., 2009). This index can be used to

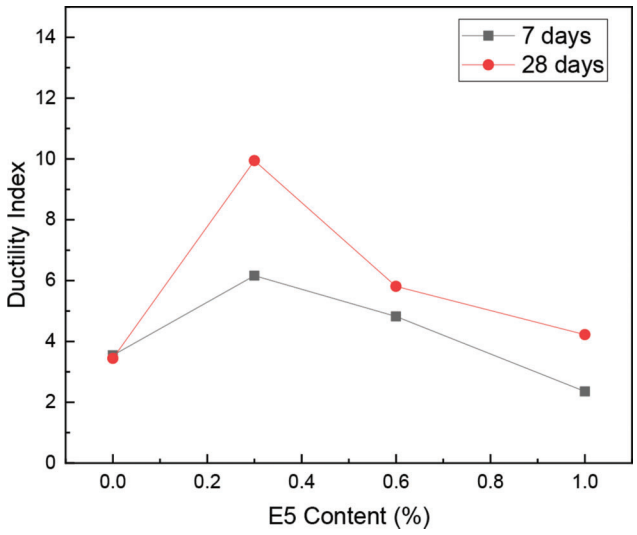

Figure 6.4 Ductility index.

determine the degree of ductility of the materials behaved strain-hardening property. As the figure is shown, SHCC with nano-silica incorporation present higher ductility than the reference set. It can be seen that 0.3% E5 SHCC presents the highest ductility, which might be the optimized CNS dosage to enhance the interfacial properties between matrix and fiber. Based on previous studies, it has to satisfy two micro-mechanics criteria–cracking energy and strength, to achieve the strain-hardening behavior. The SHCC matrix with 0.3% E5 CNS successfully optimized the fiber bridging strength stress to be larger than the stress across the crack tip. Thus, it will require more energy to de-bond the fiber and resulted in a higher flexural capacity. However, the extra CNS would not benefit the ductility performance of SHCC.

6.3.1.3 Tensile testing. Tensile strength results of SHCC samples are shown in Figure 6.5. It can be seen that the strength results at the age of 7 days did not show a significant difference (considered the error bar) for four mixtures with various dosages of E5 CNS. Nevertheless, at the age of 28 days, the nanosilica based SHCC show higher tensile strength results; specifically, for SHCC with 0.6% and 1.0% nanosilica, the tensile strength results are higher than 500 psi.

6.3.2 Drying Shrinkage

Dry shrinkage results of four SHCC mix from 3 days to 90 days were shown in Figure 6.6. As the figure indicated, the early age shrinkage of SHCC were located around 0.05% to 0.06% for 3 days and 0.07% to 0.08% for 7 days. The incremental of dry shrinkage tends to slow down after 28 days. It is hard to observe the correlation between dry shrinkage and nano silica content since the results of each set did not have a significant difference if considering the error bar. The reason could be due to the PVA fiber, which dominated

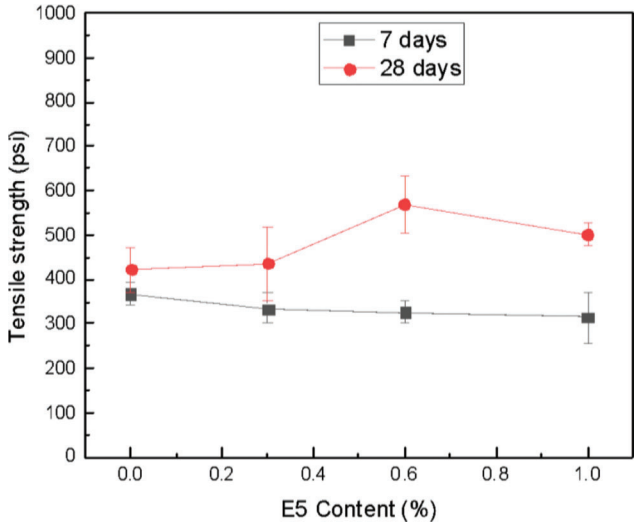

Figure 6.5 Tensile strength results.

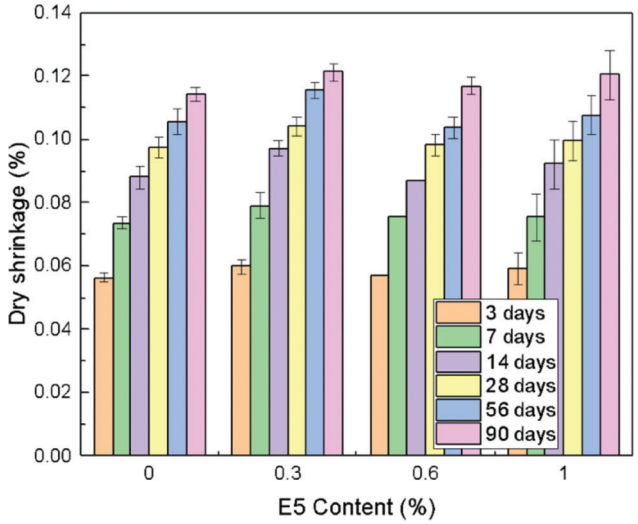

Figure 6.6 Dry shrinkage results of SHCC-E5.

the control of dry shrinkage, which was hardly affected by the addition of nanosilica in SHCC.

6.3.3 Bond Strength Testing

To evaluate the bond strength between SHCC and concrete, pull-off testing was performed. The 2 inches of concrete layer were prepared and cured for 35 days as substrate. Two types of sample configurations were prepared including reference SHCC-to-concrete, 0.3% E5 CNS-SHCC-to-concrete. The thickness of the upper layer is 4 inches. The pull-off testing was conducted at three different ages of the new casting upper layer for 3, 7, and 28 days. Figure 6.7 reveals the results of bond strength for different types of upper layers. It can be observed that the bonding strength between the upper layer and substrate layer increased over time. For early age results, 0.3% E5 SHCC showed higher bonding strength than Reference SHCC due to the accelerated

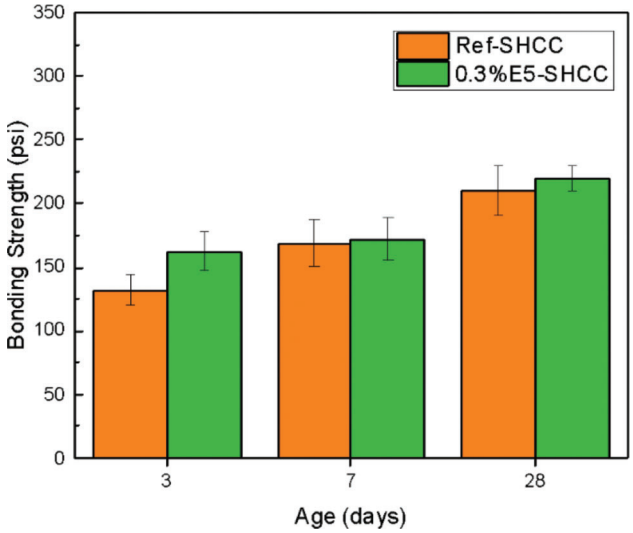

Figure 6.7 Bond strength results of SHCC-E5.

reaction of nanosilica, which improve the interfacial adhesion between concrete and SHCC.

6.3.4 Self-Healing Evaluation

Several experiments were conducted to assess the self-healing performance of SHCC with various dosages of nanosilica, including resonant frequency test, direct tensile test, and microscope crack analysis. Furthermore, scanning electron microscope (SEM) was performed to understand the morphology and hydration degree after self-healing period.

6.3.4.1 Resonant frequency test. A resonant frequency test was performed per ASTM C215 to evaluate the self-healing performance of SHCC samples. The results are shown in Figure 6.8. As can be seen that under the wet/dry cycle condition, the RF recovery ratio of reference SHCC is higher than SHCC with E5 CNS at early cycles (7-cycles). This might be due to the reference sample (without colloidal nano silica incorporated) contained more remaining unhydrated particles. On the other hand, nano silica with the high surface-area-to-volume ratio increases chemical reactivity during hydration of cementitious materials; thus, the higher portion of cement particles were consumed at its early stage. However, after 14 cycles (56 days), the CNS based SHCC gradually caught up in the RF recovery ratio, especially for SHCC samples with a higher dosage of colloidal nano silica (i.e., 0.6% and 1%). Among three sets of colloidal nano silica based SHCC, the sample with 0.6% CNS showed a higher recovery ratio than the other sets.

Figure 6.9 reveals the results of the resonant frequency recovery ratio for the sample under the dry condition. As the figure illustrates, SHCC sample with CNS incorporated presents a higher RF recovery ratio, particularly, 0.6% E5-SHCC showed the highest recovery ratio than other samples.

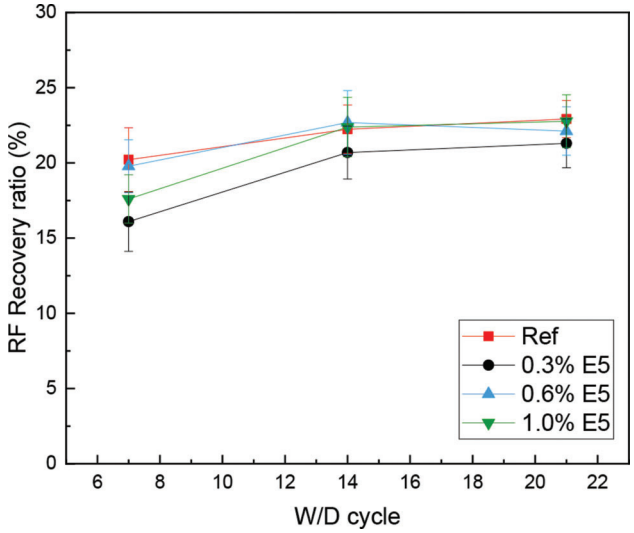

Figure 6.8 Results of resonant frequency test (SHCC exposed to W/D cycle).

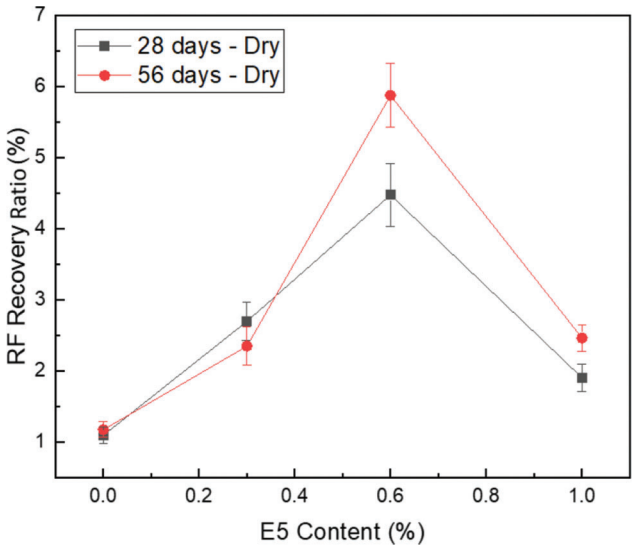

Figure 6.9 Results of resonant frequency test (SHCC exposed to 50% RH dry condition).

One of the possible assumptions is attributed to the "water holding effect" of colloidal nano silica floc network, which would be able to retain some water for long-term reaction even under low humidity environmental conditions. Previous literature (Yoo et al., 2014) indicated that once silica sol contacts with cement particles, they tend to gel instantly. The silica gel is a three-dimensional network that allows ions and water to slowly diffused in and outward the system (Cusson & Hoogeveen, 2007). Thus, the water evaporation of the CNS based SHCC was reduced and resulted in further hydration inside SHCC and a higher RF recovery ratio.

6.3.4.2 Direct tensile test. The pre-crack SHCC sample was exposed to two designated environmental conditions and re-loading at the age of interest. Figure 6.10 illustrates the tensile strength retention ratio (a) and tensile stiffness retention ratio (b) of SHCC with various dosages of colloidal nano silica after W/D cycles conditioning. The tensile strength and stiffness retention ratio was the proportion between maximum stress (σ)/stiffness (k) under pre-loading and re-loading conditions which is defined as:

$$\sigma_{re-loading} \text{ or } k_{re-loading}/\sigma_{pre-loading} \text{ or } k_{pre-loading} \ (\%)$$

It can be observed that the colloidal nano silica-based SHCC samples performed a higher tensile strength retention ratio than the reference set. Specifically, 0.6% E5 and 1% E5 SHCC samples showed better tensile strength retention ratio of the value higher than 90% compared with other sets. This result echoes the mechanical testing results from the previous session. The reason might be attribute to the densification of the matrix with higher dosages of colloidal nano silica, which strengthens the ITZ between SHCC matrix and PVA fiber. Figure 6.10(b) plots the results of the tensile stiffness retention ratio of SHCC samples. It is obvious that the SHCC sample with E5 CNS can reach higher tensile stiffness than reference sample with the ratio higher than 100%. The continued pozzolanic reaction during the W/D cycles period resulted in a finer C-S-H phase and densified the microstructures (Bentz & Snyder, 1999) of colloidal nano silica based SHCC to achieve even higher stiffness compared with the sample before W/D cycle conditioning.

Figure 6.11(a,b) exhibit the tensile strength and stiffness retentions ratio of SHCC samples under the controlled 50% RH conditions, respectively. It can be seen that even without the external water supply, the tensile performance of SHCC still increased over time. Specifically, those samples with colloidal nano silica incorporation performed an exceptional stiffness retention ratio than the reference SHCC. Comparing the two healing conditions, it is interesting that there is no significant difference in tensile strength (Figure 6.10(a) and Figure 6.11(a)) and stiffness (Figure 6.10(b) and Figure 6.11(b)) retention ratio between the sample under W/D cycle and dry condition. The reason might be most fibers are not broken or pulled out under the pre-cracking level; hence, all the pre-cracked SHCC specimens are still able to show satisfactory retained tensile strength and stiffness.

6.3.4.3 Crack analysis. Conditions of cracks after exposing SHCC sample to designated environmental conditions were evaluated. Figure 6.12 compares the microscope images for SHCC samples after preloaded and several W/C cycles. In general, the W/D cycles conditions was effective for activating the self-healing of SHCC sample due to the suppling of water. For the cracks with a width less than 30 μm, they were able to seal completely after two W/D cycles as (a) location in Figure 6.12. It can be observed that the cracks were

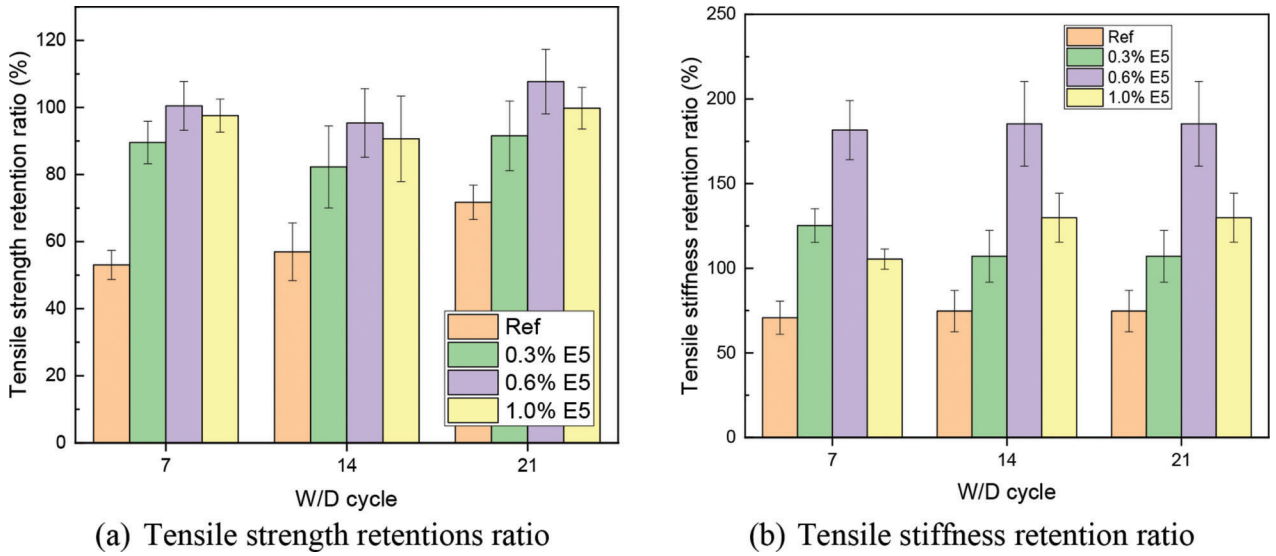

Figure 6.10 Results of tensile strength and stiffness retention ratio test (SHCC exposed to W/D cycles).

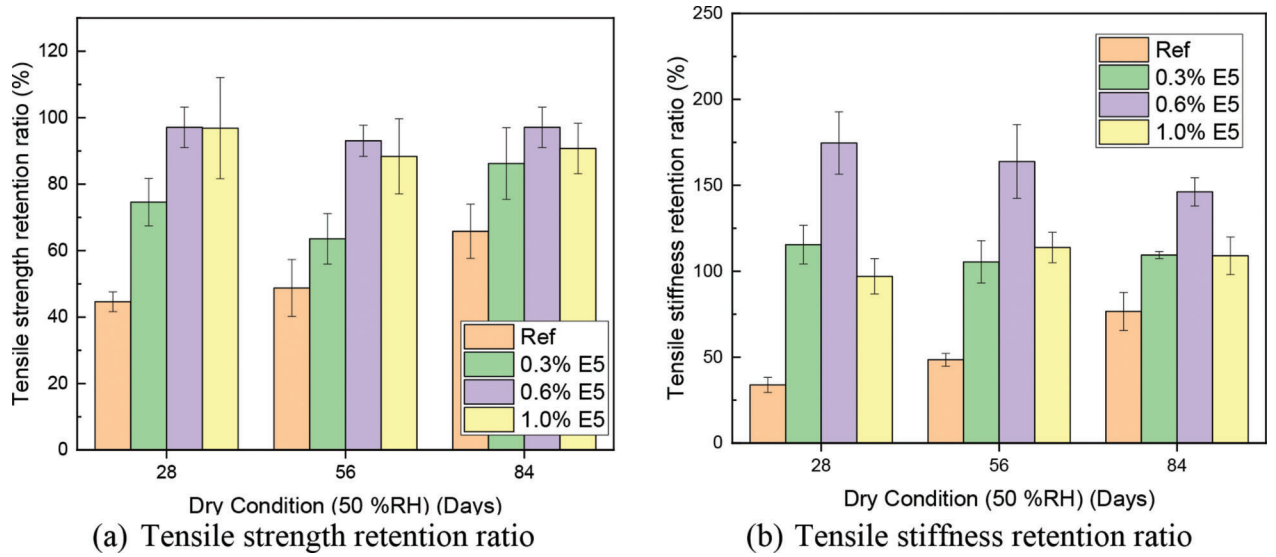

Figure 6.11 Results of tensile strength and stiffness retention ratio test (SHCC exposed to dry conditions).

partially sealed with a width around 50 μm, as (b) spots indicated in the figure. Yang et al. (2009) suggested that for those crack widths larger than 150 μm, it can barely observe the autogenous healing of SHCC; however, we have observed the crack narrowing from 233 μm to 113 μm after two W/D cycles conditions as shown at the spot (c) in Figure 6.12. As suggested by literature (Feng et al., 2019), the PVA fiber can be the nucleation site for growing the healing precipitants, which was also observed in this figure at (d) area.

Figure 6.13 illustrates the average crack recovery ratio after several W/D cycles for different SHCC samples. It can be seen that reference SHCC shows higher average crack recovery ratio than nanosilica based SHCC since Ref SHCC might retain more unhydrated cementitious particles for further hydration. Also, crack sealing of Ref SHCC might mostly be due to the formation of calcite ($CaCO_3$) or re-crystallization of portlandite leached from the bulk paste, which is more easily observed on the surface. On the other hand, it has been noticed that the 0.6% and 1% E5-SHCC shows a lower average crack recovery ratio compared with 0.3% E5 sample and Ref SHCC sample, it might be because of the crack width of these samples were not favorable for healing. Yang et al. (2009) found there is no or less recovery for the crack width larger than 150 μm. Thus, if we look into the probability of the crack width for different samples as Figure 6.14 shown, it can find that the probability of a large width crack (larger than 150 μm) of 0.6% and 1% E5-SHCC is higher than 0.3% E5 set and reference set. Specifically, in the crack width range of 300 μm to 400 μm, the probability for SHCC sample of 0.6% and 1% E5 mix is higher than 5%.

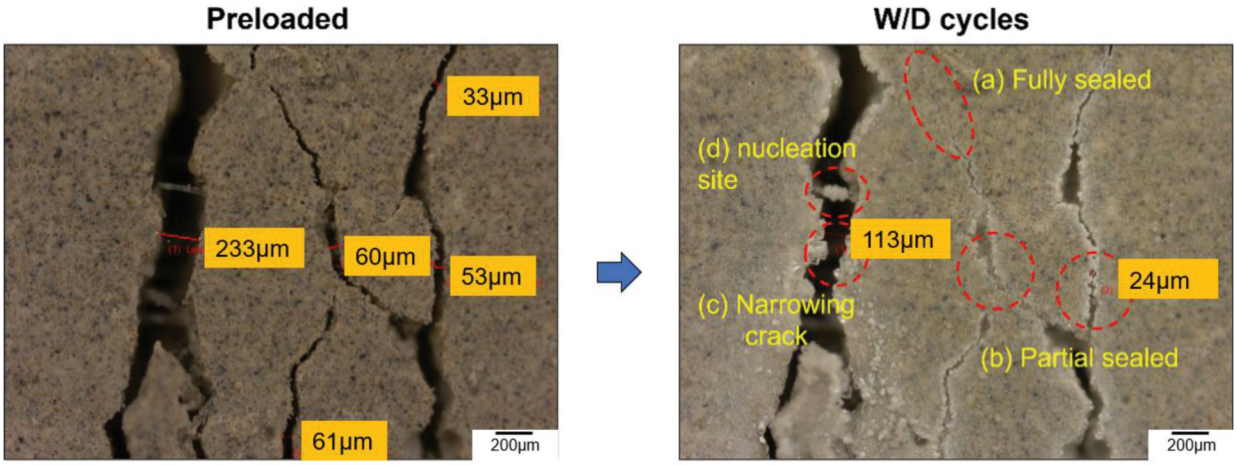

Figure 6.12 Representative microscope images for sample (0.3% E5 SHCC) after preloaded and two W/C cycles.

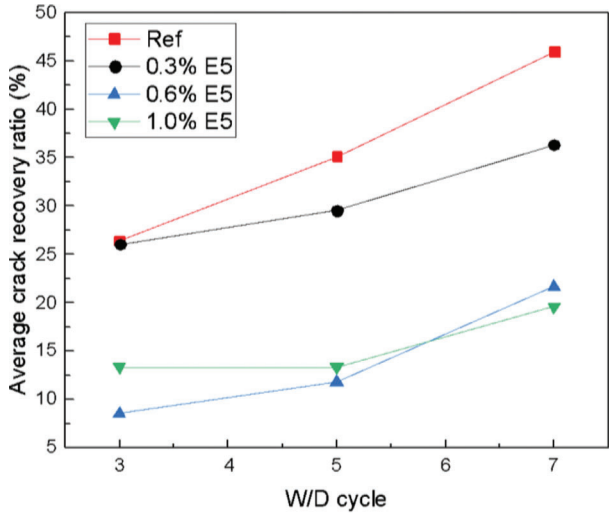

Figure 6.13 Results of average crack recovery ratio for SHCC under W/D cycle curing condition.

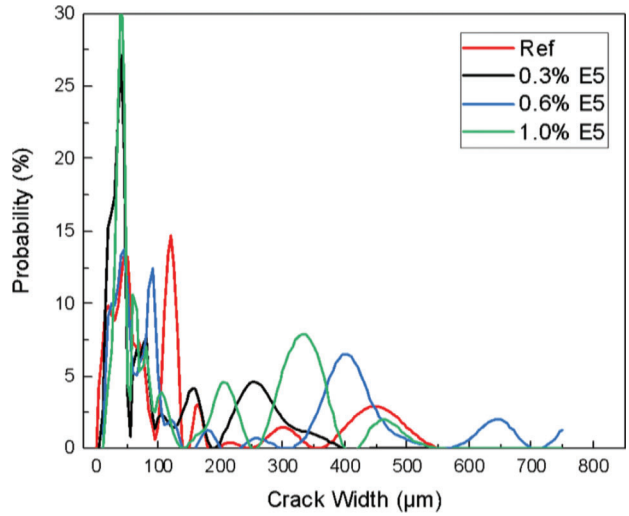

Figure 6.14 Probability of SHCC crack width after three-points bending test.

6.3.4.4 SEM image analysis of unhydrated cementitious materials. To understand the morphology and hydration condition of SHCC samples after the healing period, the scanning electron microscope (SEM) was used. The surface of SHCC sample was coated with platinum to enhance the surface conductivity before SEM analysis, then the surface was observed by using a scanning electron microscope. Figure A.11(a–d) displays the representative SEM images for different types of SHCC samples after 21 wet-dry cycles. In the SEM images, the components are identified based on the shapes and gray levels. The main area with grey color represents the cementitious paste, and the sand in the image appears as a shade of darker gray. The unhydrated cementitious particles are the brighter whitish grains. And the black sphere-shaped regions are the cross- of the PVA fibers. From the SEM images, it can be observed that all the samples were well-hydrated, and the cementitious matrix was dense after the designed curing period. It is observed that the unhydrated cementitious particles were smaller when various dosages of the CNS were incorporated. This may be due to the internal curing effect, and the nano seeding effect of the CNS improved the hydration of the cementitious materials, which led to a higher hydration degree and smaller size of the unhydrated cementitious particles.

Afterward, the images were further analyzed through Image J software to identify the average size of unhydrated cementitious particles. More than five images were used for each data point for different conditions (7 cycles and 21 cycles). It can be observed that the averaged particle size of the unhydrated cementitious materials decreased with the increase of colloidal nano silica content (Figure 6.15). Notably, the particles area of 1% E5 CNS-SHCC sample is smaller than 160 μm^2. This evidence further verifies the benefits of long-term hydration promotion of CNS in SHCC.

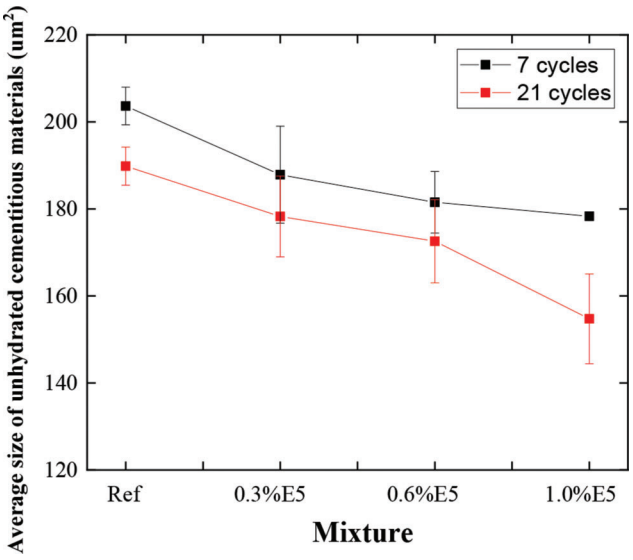

Figure 6.15 Average area of unhydrated cementitious materials of different SHCC samples.

6.4 Summary

In this session, the mechanical properties and self-healing performance of nanosilica based SHCC were compared with the reference SHCC. For the mechanical properties, compressive testing, tensile testing, flexural testing, and pull off testing were conducted at different age of interest. A shrinkage bar test was also performed to monitor the dry shrinkage for up to 90 days. On the other hand, the self-healing performance was assessed through the non-destructive resonant frequency and destructive tensile tests. Microscopy images of SHCC samples after being exposed to designated environmental conditions were taken to analyze cracks' condition. SEM images were also taken for the evaluation of the cementitious hydration. Based on the experimental results and the analysis from this session, conclusions can be drawn as follows.

1. The incorporation of colloidal nanosilica can significantly improve the mechanical properties of SHCC. For the compressive strength results, the nanosilica based SHCC can reach over 5,500 psi at 90 days. Flexural strength result indicate that SHCC with E5 nanosilica shown higher flexural strength than reference set for 7% to 9%. Tensile results of SHCC suggest that the nanosilica based SHCC show higher tensile strength of over 500 psi. Also, SHCC with nanosilica incorporation presents higher ductility than the reference set as reflected on the ductility index. Specifically, the additional ratio of 0.6% by weight of cement can achieve the best mechanical strength performance which might be the optimal dosage.
2. The bonding strength between SHCC and old concrete layer was assessed through pull-off testing. The pull-off testing was conducted at three different ages of the new casting SHCC upper layer for 3, 7, and 28 days. The results indicate that the bonding strength between the upper layer and substrate layer increased over time. Due to the accelerated reaction of nanosilica, 0.3% E5 SHCC shown higher bonding strength than Reference SHCC at the early age, which attributed to the improvement of the interfacial adhesion between concrete and SHCC.
3. Self-healing evaluation suggests that the SHCC with nanosilica incorporated presents a positive impact for autogenous healing of the pre-cracked sample. Resonant frequency test results indicated that under the wet/dry cycle condition, the RF recovery ratio of nanosilica based SHCC can recover 15% or above for 28 days. The tensile testing revealed that the SHCC sample with E5 CNS could reach higher tensile strength and stiffness retention ratio than the reference SHCC sample. Based on the microscope image analysis of cracks, all the SHCC has shown crack recovery after wet-dry cycles conditions (28 days). Specifically, 0.3% E5 can reach higher than 30%. However, the crack sealing of Ref SHCC might mainly be due to the formation of calcite ($CaCO_3$) or re-crystallization of portlandite leached from the bulk paste, which is mostly on the surface and easier to be observed by the microscope. Therefore, the crack recovery ratio is higher than colloidal nano silica based SHCC.

7. LARGE SCALE SHCC SAMPLE TESTING AND THE MIXING PROCEDURE

To study the feasibility of utilizing designed material in the real field application, large SHCC samples were prepared. The flexural performance of the SHCC was evaluated through the flexural bending testing per ASTM C78. A suitable mixing and casting method for the production of SHCC on a large scale was also identified. A standard operating procedure was developed based on this study.

7.1 A Standardized Procedure for Large Batch SHCC Mixing

The preparation of the SHCC in large scale requires a specific procedure and sufficient mixing to ensure a satisfactory fiber distribution. Therefore, a standardized procedure was proposed for the SHCC mixing in large batch.

1. Prepare all the dry ingredients except PVA fiber (cement, SCMs, fine aggregates, etc.) and pre-mix for 5 minutes using slow mixing speed.
2. Add the VMA into the prepared mixing water, then stir for 3 minutes to dissolve the VMA into the water. If this step is unable to accomplish due to the large volume of the water, transfer a sufficient part of the mixing water into a container and do the stirring with VMA.
3. Under the low mixing speed, slowly add the mixing water into the mixture. Then mix for 5 minutes using medium speed. During this step, extra attention should be made to examine whether the cementitious materials are agglomerated and stick to the inner wall of the mixer. If so, use appropriate tools to detach the cement block from the inner wall of the mixer and then mix for another 3 minutes.
4. Add the PVA fiber into the mixture under low mixing speed, then switch the mixer to high mixing speed and mix for 5 minutes. The flowability of the mixture may reduce due to the incorporation of the fibers. Then, add

the superplasticizer (water reducer) until it reaches desired flowability. Afterward, add the E5 and mix for another 3 minutes.

For SHCC mixture design, since VMA was incorporated, the fresh mixture may be agglomerated if the mixing is not sufficient. This agglomeration of the cementitious materials will be well-dispersed after the 5 minutes of mixing. However, it should be noted that the agglomerate may stick to the inner wall of the mixer, and the blades of the mixer may not be able to scrape it off the wall. In this case, the issue can be solved by either manually scraping the inner wall of the mixer or changing the mixer.

In this standardized procedure, it is worth noting that the superplasticizer and the E5 were added after the incorporation of the fiber. The reason is that the addition of the VMA aims to improve the fiber distribution by increasing the frictional force, while the superplasticizer and E5 potentially reduce the viscosity and increase the flowability. Therefore, any additives that may counterweigh the effect of the VMA should be added after the PVA fibers have been well mixed.

7.2 Workability and Passing Ability

To evaluate the workability and passing ability of SHCC, the slump flow testing (ASTM C1611) and J-ring testing (ASTM C1621) were performed. The setup and the results of SHCC J-ring testing are shown in Figure 7.1. It can be seen that the fiber dispersion of SHCC is uniform, and no significant fiber clustering was observed. The SHCC successfully passed the J-ring evenly. Table 7.1 reveals the measurement of J-ring testing. The spread range of SHCC is 20.5 inches which is within the range of SCC criteria. The spread speed index, which referred to the time of the SHCC reached 20 inches spread diameter, is 7 seconds, and the results are also in the interval for SCC. The difference between slump flow and J ring flow of SHCC is one inch, which indicates that the fiber would not hinder the matrix from passing the rebar. In summary, SHCC performed excellent workability and passing ability, which is comparable with self-consolidating concrete.

7.3 Layer Structure Design for SHCC-Concrete

In this session, the layered structure beam was designed to investigate the flexural performance of SHCC/Concrete composite with different layer ratios. The dimension of the beam sample is 4" by 4" by 15". It has designed five different configurations of the SHCC/Concrete beam layer, and the SHCC layer varied from 100% (entire SHCC beam) to 0% (entire concrete beam), as Table A.1 presented. Figure 7.2 shows the schematic of SHCC/Concrete beam under the flexural testing. The SHCC was set as the bottom layer, and concrete was cast on top after 45 minutes to ensure the adequate hardness of the SHCC. During the flexural testing, the tension would mainly be resisted by SHCC.

The composite sample is presented in Figure A.15. Figure 7.3 shows the flexural results of different SHCC/Concrete composite beams at the age of 28 days. As can be seen that the modulus of rupture (MOR) raised with the increase of the SHCC layer owing to the excellent tensile and flexural properties of SHCC. The result of the concrete beam is around 570 psi, while the 3"SHCC/1" concrete beam reached 920 psi. Compared with the concrete beam, the incremental increased around 7%

Figure 7.1 Set up and results of SHCC J-ring testing.

TABLE 7.1
Workability results of SHCC compared with SCC criteria

SCC Criteria	SHCC
Spread range: 18 to 30 inches	20.5 in
Spread speed index, T_{20}: 2 to 10 seconds	7 seconds
Difference between slump flow and J ring flow (ASTM C1621)	1 in (no visible blocking)

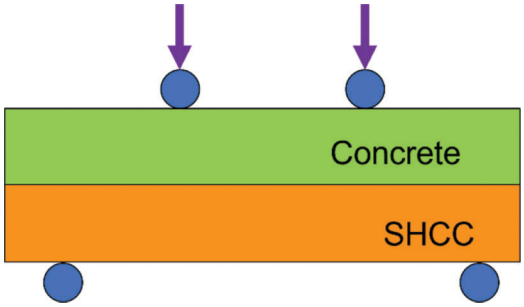

Figure 7.2 Schematic of SHCC/concrete beam.

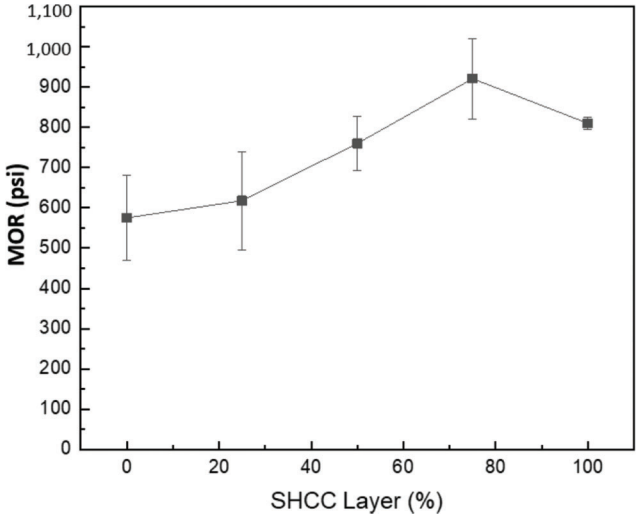

Figure 7.3 The MOR result of SHCC/concrete structure.

for 1" SHCC beam to 60% for 3" SHCC beam. Interestingly, the 100% SHCC beam did not have the highest MOR compared with the layer-structure beam. This might be due to the coarse aggregate interlock of concrete attributes to the resisting of the cracking of SHCC/Concrete composite beam. More testing could be conducted in the future to understand the layer structure behavior and verify the assumption. In conclusion, the SHCC layer can significantly enhance the flexural performance of a large beam structure.

7.4 Summary

In this section, the SHCC samples were prepared from large batch mixing. Based on the large batch mixing, a standardized mixing procedure was proposed for the SHCC. Then, the workability and passing ability of the fresh SHCC mixture were evaluated. Afterwards, the flexural test for the SHCC beam and SHCC/Concrete multilayer composite was conducted at the designed age. The conclusions drawn from this session is listed as follows.

1. During the mixing of the SHCC, agglomeration of the cementitious materials will be well-dispersed after sufficient time of mixing. However, the agglomerate may stick to the inner wall of the mixer, and the blades of the mixer may not be able to scrape it out of the wall. Therefore, this issue should be dealt with by either manually scraping the inner wall of the mixer or changing the mixer.
2. The addition of the VMA in SHCC aims to improve the fiber distribution by increasing the frictional force, while the superplasticizer and E5 potentially reduce the viscosity and increase the flowability. Therefore, any additives that may counterweigh the effect of the VMA should be added after the well-mix of the PVA fibers.
3. From the slump and J-ring testing result, SHCC has excellent workability and passing ability, which is comparable with self-consolidating concrete.
4. The flexural test of the layer-structure beam suggests that the modulus of rupture (MOR) raised with the increase of the percentage of the SHCC layer owing to the excellent tensile and flexural properties of SHCC. Particularly, SHCC and concrete ratio of 3:1 would be the optimal design to reach the excellent flexural performance; however, it was also found that 100% SHCC beam did not have the highest MOR compared with the layer-structure beam. This may be due to the interlocking effect of the coarse aggregate in concrete favors the flexural performance of the multilayer composite.

8. ADVANTAGE OF SHCC DESIGN FOR IN-FIELD APPLICATIONS

8.1 Economic Competitiveness

In this section, a material cost estimation for different mixture designs was compared. The average cost of the raw materials was collected and shown in Table A.12. It is worth noting that the price estimation in this study only includes the cost of the materials, while the unit price of the raw material can be changed. The transportation fee, labor cost, and other cost were not considered.

The estimated cost of the SHCC was compared with the Engineered Cementitious Composite (ECC), Ultra-High Performance Concrete (UHPC) and INDOT-564 concrete. The representative mixture design is shown in Table A.3. The comparison of the cost for different mixture designs is presented in Figure 8.1 and Table 8.1.

It can be seen from the result that compared with the conventional concrete design (INDOT-564), the material cost of the SHCC is higher due to the use of a large volume of cement and the addition of the fibers. As the previous study showed, SHCC exhibited better mechanical performance, including compressive, tensile and flexural behavior. Moreover, the self-healing ability of the SHCC can potentially elongate its service life span, which reduces the cost of the maintenance. When compared with other high performance cementitious composites, the cost of the SHCC is much cheaper and acceptable. The estimated result shows that the cost of the ECC is 1.5–2.0 times higher than the SHCC, while the UPHC is 3.1–12.1 times higher than the SHCC.

8.2 Expected Benefits

In this study, the design of the SHCC materials is developed and evaluated by various testing methods.

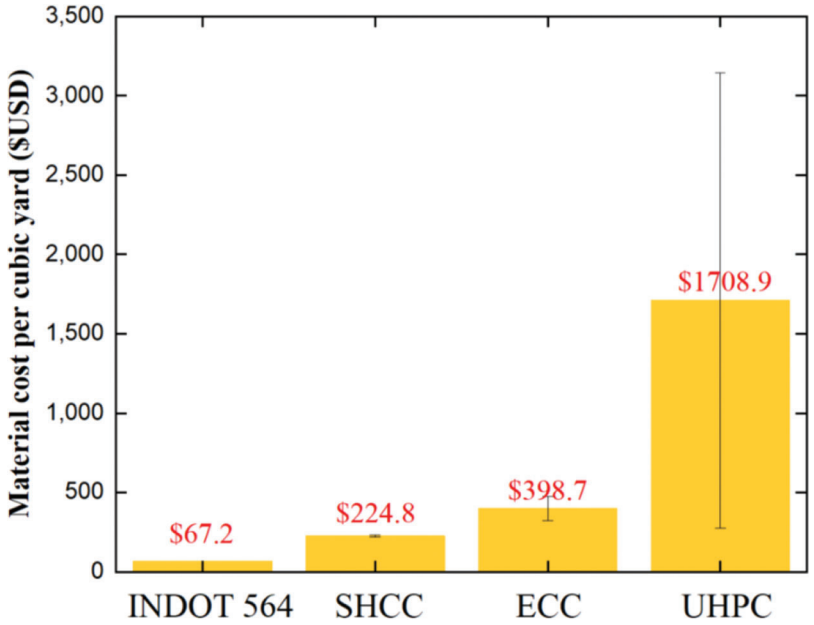

Figure 8.1 Estimated material cost per cubic yard.

TABLE 8.1
Estimated material cost of different mixture designs

	Estimated Price ($/cyd)
INDOT-564 (w/c = 0.42)	67.2
SHCC (w/c = 0.35)	220.9–228.7
ECC (w/c = 0.30)	344.3–453.0
UHPC (w/c = 0.18)	694.0–2,723.9

A comprehensive investigation of the performance of the SHCC was conducted.

The result indicates that SHCC has better ductility, hence favors the application of structures such as bridge deck and link slab that require better flexural and tensile resistance. With the incorporation of the fibers, such as Strux 90/40 or PVA, the material exhibited pseudo-strain-hardening behavior during the loading process. Also, a better mechanical performance was achieved. The bridging effect of the fibers efficiently improved the ductility of the designed cementitious composite, which increased the flexural and tensile strain capacity. In addition, the study of the SHCC/concrete composite shows a better flexural performance of the material when SHCC was set as the bottom layer to sustain tensile stress. This result provides insight on using SHCC to achieve better structure performance while controlling the cost of the material by only partially replacing the convention concrete by SHCC.

The self-healing ability of the SHCC can be used to address the concern of the cracking on the concrete materials. Due to the high volume of cementitious materials, SHCC is capable of healing the cracks by secondary hydration. To further improve the healing efficiency, internal curing agents and nano-silica were used and studied. The incorporation of the internal curing aggregates or the E5-nanosilica can lead to a higher recovery ratio of the sample. In addition, the use of the internal curing method can potentially improve the curing quality by reducing/eliminating the drying shrinkage, while the incorporation of the E5-nanosilica is more convenient compared with internal curing aggregates and favors the strength development.

When used as a patching material, the excellent workability and passing ability of the SHCC meet the requirement of the self-consolidating concrete (SCC), which ensures the good bonding with the old concrete layer and rebar. In addition, this study also noticed an increase in the bonding strength between SHCC and conventional concrete layer when the E5-nanosilica was incorporated, which further made SHCC suitable to be used as a patching material.

8.3 Implementation

The objective of this project is to develop ductile self-healing cementitious composites (SHCC), which can be used in concrete applications especially for link-slab. The SHCC was delivered to INDOT as a reference for the design of concrete materials with ultra-high ductility and self-healing ability that can reduce the need for conventional rehabilitation.

- To ensure the quality of the fiber distribution and the ductility of the SHCC, PVA fiber with short fiber length, high tensile strength, and aspect ratio was chosen. Better mechanical properties and crack width control ability can therefore be expected.
- Internal curing method was applied into the design of the SHCC to further improve the self-healing performance. Internal curing aggregates with high porosity and small pore size, such as zeolite, performed better in the improvement of the healing efficiency. Optimal sand replacing ratio for zeolite is around 15 wt%.

- Superabsorbent polymer (SAP) can effectively seal the crack within a short period; however, it has a negative influence on the mechanical performance of the SHCC.
- Viscosity modifying admixtures (VMA) can effectively improve the fiber distribution and fiber-matrix interface of the SHCC, especially when a higher water to cement ratio is used. The experimental result indicates VMA 450 (binding type) with a dosage of 1% performed the best in SHCC with a water to cement ratio of 0.35, in terms of ductility.
- Addition of the colloidal nanosilica can further improve the mechanical and self-healing performance of the SHCC. The test result suggests 0.6 wt% of cement as the optimal dosage. Also, the bonding strength between the SHCC and conventional concrete layer was increased with the addition of the nanosilica.
- SHCC mixture design with VMA has been proved to possess satisfied workability and passing ability, which is comparable with self-consolidating concrete (SCC).
- The combination of the SHCC with conventional concrete can improve the flexural performance of the beam sample. A higher flexural strength with high modulus of rupture (MOR) can be achieved.

Different strategies for the design of the SHCC can be adopted based on certain applications. For a concrete patching project, it is more desired to have SHCC with a better curing quality and higher bonding strength. Therefore, it is recommended to incorporate the internal curing agent and colloidal nanosilica, which are proven to lead to better curing and bonding performance. A lower PVA fiber content of 1 vol% may be used to reduce the cost. On the other hand, if SHCC is used for a link slab application, ductility and the self-healing ability are favorable. Thus, a higher dosage of the PVA fiber, such as 2 vol% can be used. Internal curing agents such as zeolite can be incorporated to further improve the self-healing performance.

9. FINAL CONCLUSIONS AND RECOMMENDATIONS

This work has conducted an in-depth study on the mechanical properties, self-healing performance, and their underlying mechanism of various types of self-healing cementitious composites (SHCC). Different materials were utilized to incorporated in SHCC for investigation, including different kinds of fiber (PVA, Strux, and other INDOT approved fiber), internal curing agents (zeolite, lightweight aggregate, and super-absorbent polymer), various types of viscosity modifier, and colloidal nanosilica. The pros and cons of each type of SHCC were discussed to provide the comprehensive design concept for engineers on the mixture design of SHCC. The key summary is listed as follows.

- Among the fibers, i.e., PVA fiber and five types of INDOT approved fiber (Strux 90/40, MasterFiber, Fiberforce 650, Tur-Strand SF, MasterFiber Mac Matrix), the SHCC sample with PVA fiber exhibited the highest mechanical properties at 28 days. For compressive strength, the PVA-SHCC performed 10% to 165% higher than others; for tensile strength results, the PVA-SHCC exceeded other sets by 24% to 65%; for flexural strength, the PVA-SHCC behaved 5% to 101% higher than SHCC incorporated with other fibers. Also, based on the results, the crack width control ability of the PVA fiber is better than other fibers in SHCC since PVA fiber has a higher aspect ratio and has a shorter length, which is less prone to entanglement. Thus, PVA fiber can control the propagation of the crack width by generating multiple cracks and potentially increasing the self-healing efficiency.
- In general, the incorporation of internal curing agents in SHCC can enhance the degree of hydration to form more C-S-H gel to strengthen the matrix. The compressive strength results revealed that compared with reference SHCC (w/o internal curing agents), it would have over 15% strength enhancement for the sample with zeolite and 6% improvement for the sample with lightweight aggregate. In addition, internal curing agents were proven to benefit the healing efficiency of SHCC by providing water internally to accelerate the autogenous healing. The internal curing agents with high water absorption rate, finer particle, and small size of pore structure, such as zeolite, is preferable for SHCC on improving the healing performance. On the other hand, the results from SAP samples indicated that SAP could swell inside the crack and efficiency seal the crack within 60 seconds, which can be used as a self-sealing agent in concrete materials.
- The incorporation of the SAP into the cement paste resulted in an increase of the plastic viscosity for over 56% as the dosage of the SAP increased from 0% to 0.24 wt% of cement, which suggest that the incorporation of the SAP may be able to improve the fiber distribution since it may increase the frictional force between fiber and other components of cementitious composite during the mixing process.
- The mechanical tests for the SHCC incorporated with SAP indicate that the incorporation of the SAP particles reduces the 7 days compressive and flexural strength of the sample by over 25% and 20%, respectively. The large voids left by the dried SAP adversely influence the matrix quality. On the other hand, it was also found that with a small dosage of the SAP, the 7 days tensile performance of the SHCC was slightly improved by around 13.8% due to the void created by the SAP could act as flaws which triggered the formation of multiple cracks. However, with a higher dosage of SAP, the tensile strength was decreased as a large number of voids started to adversely affect the performance of the sample. The test result suggests that the incorporation of the SAP may improve the fiber distribution in SHCC, but overall, the mechanical performance was adversely affected by the large void left by the dried SAP.
- Three types of viscosity modify agents were used, including two thickening-type (methenamine based and biphenyl based) and binding types (methylpentane based). The viscosity results indicated that compared with thickening-type VMA, the binding-based VMA could better raise the viscosity of fresh SHCC mortar. The increase of mortar viscosity of SHCC can prevent segregation, improve the interfacial properties between fiber and matrix and fiber distribution. The mechanical strength results indicated that VMA has less impact on flexural strength; however, VMA 450 (binding type) can effectively enhance the ductility of SHCC due to the improvement of interfacial properties.

- Experiments of SHCC with various addition ratios (0%, 0.3%, 0.6%, and 1%) of colloidal nanosilica were conducted, including the mechanical testing and self-healing evaluation. The mechanical results indicated that the incorporation of colloidal nanosilica could significantly improve the strength of SHCC. The mechanical strength of nanosilica based SHCC was higher than reference SHCC of 13% to 27% for compressive strength, 4% to 35% higher for tensile strength, and 7% to 10% higher for flexural strength at 28 days. Specifically, the SHCC with nanosilica additional rate of 0.6% performed the highest compressive strength of over 6,200 psi and tensile strength of around 570 psi. For the ductility, the results indicated that SHCC with 0.3% CNS incorporated presented 188% more ductile than reference SHCC.
- The self-healing evaluation suggests that the SHCC with colloidal nanosilica incorporated presents positive impact for autogenous healing of the pre-cracked sample. Resonant frequency test results indicated that under the wet/dry cycle condition, the RF recovery ratio of nanosilica based SHCC can recover 15% or above for 28 days. The tensile testing revealed that the SHCC sample with E5 CNS can reach higher tensile strength and stiffness retention ratio than reference SHCC sample. Based on the microscope imagine analysis of cracks, all the SHCC showed crack recovery after wet-dry cycles conditions (28 days). Specifically, 0.3% E5 can reach higher than 30% of the recovery of cracks.
- Based on the large size sample preparation, a standardized mixing procedure for the SHCC was proposed. It is suggested that during the mixing, extra attention should be made to check the inner wall of the mixer to ensure any agglomerate of the cementitious materials could be mixed and dispersed by the mixer. In the meanwhile, it is also recommended that any additives that may counterweigh the effect of the VMA, such as superplasticizer and E5, should be added after the well-mix of the PVA fibers.
- From the result of the slump and J-ring testing, SHCC has excellent workability and passing ability, which is comparable with self-consolidating concrete. Then, the SHCC/Concrete multilayer composite were prepared and tested by flexural loading. The result suggests that the modulus of rupture (MOR) increased due to the excellent tensile and flexural properties of SHCC.

In conclusion, this study has conducted extensive experiments to evaluate the mechanical properties and self-healing performance of various designs of SHCC. For the fiber selection, the PVA fiber with great crack width control ability is most favorable to improve the autogenous healing performance. However, INDOT approved fibers such as Strux fiber with the longer length would retain the structure integrity with higher incorporation rate (1%). To control the rheological properties and enhance the interfacial properties between fiber and matrix, the binding type viscosity modifying agents is more favorable. Among the internal curing agent based SHCC, zeolite based SHCC shows better performance than other agents due to the exceptional water absorption capacity and the finer pore size. SAP is capable of absorbing the water and seal the cracks on SHCC within short time; however, it would have a negative impact to decrease the mechanical strength of SHCC. The incorporation of colloidal nanosilica was proven to have positive influence on SHCC on improving the mechanical properties and self-healing ability. Also, a higher bonding strength was achieved with the addition of the nanosilica. For the large batch mixing of the SHCC, a standardized mixing procedure was proposed. It was also found that the SHCC has excellent workability and passing ability, which is comparable with self-consolidating concrete. And the flexural strength of the SHCC/Concrete beam was higher than the strength of the single concrete or the SHCC beam. Nevertheless, the durability properties, such as freeze-thaw properties, Alkali-Silica Reaction (ASR), chloride penetration, abrasion, sulfates attack, and corrosion-related topics, should be investigated. Also, structural member testing (beam, plate and etc.) is recommended to understand the large-scale structural behavior before putting materials into practical structural design.

REFERENCES

Afroughsabet, V., Biolzi, L., & Ozbakkaloglu, T. (2016, March). High-performance fiber-reinforced concrete: A review. *Journal of Materials Science*, *51*(14), 6517–6551.

Akçaoğlu, T., Tokyay, M., & Çelik, T. (2004). Effect of coarse aggregate size and matrix quality on ITZ and failure behavior of concrete under uniaxial compression. *Cement and Concrete Composites*, *26*(6), 633–638.

Bentur, A., Igarashi, S.-I., & Kovler, K. (2001, November). Prevention of autogenous shrinkage in high-strength concrete by internal curing using wet lightweight aggregates. *Cement and Concrete Research*, *31*(11), 1587–1591.

Bentz, D. P. (2007). Internal curing of high-performance blended cement mortars. *ACI Materials Journal*, *104*(4), 408–414.

Bentz, D. P., Hansen, K. K., Madsen, H. D., Vallée, F., & Griesel, E. J. (2001, November). Drying/hydration in cement pastes during curing. *Materials and Structures*, *34*(9), 557–565.

Bentz, D. P., Lura, P., & Roberts, J. W. (2005, February). Mixture proportioning for internal curing. *Concrete International*, *27*(2), 35–40.

Bentz, D. P., & Snyder, K. A. (1999, November). Protected paste volume in concrete: Extension to internal curing using saturated lightweight fine aggregate. *Cement and Concrete Research*, *29*(11), 1863–1867.

Bentz, D. P., & Weiss, W. J. (2011, February 9). *Internal curing: A 2010 state-of-the-art review* (NIST Interagency/Internal Report (NISTIR)–7765). National Institute of Standards and Technology. https://doi.org/10.6028/NIST.IR.7765

Bischoff, P. H. (2003, April). Tension stiffening and cracking of steel fiber-reinforced concrete. *Journal of Materials in Civil Engineering*, *15*(2), 174–182.

Castro, J., Keiser, L., Golias, M., & Weiss, J. (2011). Absorption and desorption properties of fine lightweight aggregate for application to internally cured concrete mixtures. *Cement and Concrete Composites*, *33*(10), 1001–1008.

Cattaneo, S., & Biolzi, L. (2010, September). Assessment of thermal damage in hybrid fiber-reinforced concrete. *Journal of Materials in Civil Engineering*, *22*(9), 836–845.

Chen, W.-F., & Carson, J. L. (1971, December). Stress-strain properties of random wire reinforced concrete. *Journal Proceedings*, *68*(12), 933–936.

Costa, H., Júlio, E., & Lourenço, J. (2012, October). New approach for shrinkage prediction of high-strength lightweight aggregate concrete. *Construction and Building Materials*, *35*, 84–91.

Cusson, D., & Hoogeveen, T. (2007, February). An experimental approach for the analysis of early-age behaviour of high-performance concrete structures under restrained shrinkage. *Cement and Concrete Research*, *37*(2), 200–209.

de la Varga, I., Castro, J., Bentz, D. P., & Weiss, J. (2012, October). Application of internal curing for mixtures containing high volumes of fly ash. *Cement and Concrete Composites*, *34*(9), 1001–1008.

Ding, Y., & Kusterle, W. (2000, October). Compressive stress–strain relationship of steel fibre-reinforced concrete at early age. *Cement and Concrete Research*, *30*(10), 1573–1579.

Dixit, A., Gupta, S., Pang, S. D., & Kua, H. W. (2019, November). Waste Valorisation using biochar for cement replacement and internal curing in ultra-high performance concrete. *Journal of Cleaner Production*, *238*, 117876.

Edvardsen, C. (1999, July). Water permeability and autogenous healing of cracks in concrete. *Innovation in Concrete Structures: Design and Construction* (pp. 473–487). Thomas Telford Publishing.

Eren, Ö., & Celik, T. (1997). Effect of silica fume and steel fibers on some properties of high-strength concrete. *Construction and Building Materials*, *11*(7–8), 373–382.

Feng, J., Su, Y., & Qian, C. (2019, December). Coupled effect of PP fiber, PVA fiber and bacteria on self-healing efficiency of early-age cracks in concrete. *Construction and Building Materials*, *228*, 116810.

Gagné, R., & Argouges, M. (2012, April). A study of the natural self-healing of mortars using air-flow measurements. *Materials and Structures*, *45*(11), 1625–1638.

Ghourchian, S., Wyrzykowski, M., Lura, P., Shekarchi, M., & Ahmadi, B. (2013, March). An investigation on the use of zeolite aggregates for internal curing of concrete. *Construction and Building Materials*, *40*, 135–144.

Hameed, R., Turatsinze, A., Duprat, F., & Sellier, A. (2009, July). Metallic fiber reinforced concrete: Effect of fiber aspect ratio on the flexural properties. *Journal of Engineering and Applied Sciences*, *4*(5), 67–72.

Hasholt, M. T., Jensen, O. M., Kovler, K., & Zhutovsky, S. (2012). Can superabsorent polymers mitigate autogenous shrinkage of internally cured concrete without compromising the strength? *Construction and Building Materials*, *31*, 226–230.

Henkensiefken, R., Bentz, D., Nantung, T., & Weiss, J. (2009a, August). Volume change and cracking in internally cured mixtures made with saturated lightweight aggregate under sealed and unsealed conditions. *Cement and Concrete Composites*, *31*(7), 427–437.

Henkensiefken, R., Castro, J., Bentz, D., Nantung, T., & Weiss, J. (2009b, October). Water absorption in internally cured mortar made with water-filled lightweight aggregate. *Cement and Concrete Research*, *39*(10), 883–892.

Homma, D., Mihashi, H., & Nishiwaki, T. (2009, June). Self-healing capability of fibre reinforced cementitious composites. *Journal of Advanced Concrete Technology*, *7*(2), 217–228.

Huang, H., Ye, G., Qian, C.-X., & Schlangen, E. (2016, February). Self-healing in cementitious materials: Materials, methods and service conditions. *Materials and Design*, *92*, 499–511.

Hung, C.-C., Su, Y.-F., & Hung, H.-H. (2017, July). Impact of natural weathering on medium-term self-healing performance of fiber reinforced cementitious composites with intrinsic crack-width control capability. *Cement and Concrete Composites*, *80*, 200–209.

Hung, C.-C., Su, Y.-F., & Su, Y.-M. (2018). Mechanical properties and self-healing evaluation of strain-hardening cementitious composites with high volumes of hybrid pozzolan materials. *Composites Part B: Engineering*, *133*, 15–25.

Jacobsen, S., Marchand, J., & Hornain, H. (1995, December). SEM observations of the microstructure of frost deteriorated and self-healed concretes. *Cement and Concrete Research*, *25*(8), 1781–1790.

Jensen, O. M., & Hansen, P. F. (2001, April). Water-entrained cement-based materials: I. Principles and theoretical background. *Cement and Concrete Research*, *31*(4), 647–654.

Jensen, O. M., & Hansen, P. F. (2002, June). Water-entrained cement-based materials: II. Experimental observations. *Cement and Concrete Research*, *32*(6), 973–978.

Jiang, Z., Li, W., & Yuan, Z. (2015, March). Influence of mineral additives and environmental conditions on the self-healing capabilities of cementitious materials. *Cement and Concrete Composites*, *57*, 116–127.

Justs, J., Wyrzykowski, M., Bajare, D., & Lura, P. (2015, October). Internal curing by superabsorbent polymers in ultra-high performance concrete. *Cement and Concrete Research*, *76*, 82–90.

Kang, S.-H., Hong, S.-G., & Moon, J. (2018, April). Importance of monovalent ions on water retention capacity of superabsorbent polymer in cement-based solutions. *Cement and Concrete Composites*, *88*, 64–72.

Kaufmann, W., Amin, A., Beck, A., & Lee, M. (2019, May). Shear transfer across cracks in steel fibre reinforced concrete. *Engineering Structures*, *186*, 508–524.

Keskin, S., Keskin, O. K., Anil, O., Şahmaran, M., Alyousif, A., Lachemi, M., Amleh, L., & Ashour, A. (2016, September). Self-healing capability of large-scale engineered cementitious composites beams. *Composites Part B: Engineering*, *101*, 1–13.

Kjeldsen, A. M., Flatt, R. J., & Bergström, L. (2006, July). Relating the molecular structure of comb-type superplasticizers to the compression rheology of MgO suspensions. *Cement and Concrete Research*, *36*(7), 1231–1239.

Köksal, F., Altun, F., Yiğit, İ., & Şahin, Y. (2008, August). Combined effect of silica fume and steel fiber on the mechanical properties of high strength concretes. *Construction and Building Materials*, *22*(8), 1874–1880.

Kong, X., Zhang, Z.-L., & Lu, Z.-C. (2015). Effect of pre-soaked superabsorbent polymer on shrinkage of high-strength concrete. *Materials and Structures*, *48*(9), 2741–2758.

Kou, S. C., Poon, C. S., & Etxeberria, M. (2014, October). Residue strength, water absorption and pore size distributions of recycled aggregate concrete after exposure to elevated temperatures. *Cement and Concrete Composites*, *53*, 73–82.

Kuder, K. G., & Shah, S. P. (2010, February). Processing of high-performance fiber-reinforced cement-based composites. *Construction and Building Materials*, *24*(2), 181–186.

Lau, A., & Anson, M. (2006, September). Effect of high temperatures on high performance steel fibre reinforced concrete. *Cement and Concrete Research*, *36*(9), 1698–1707.

Lee, H. X. D., Wong, H. S., & Buenfeld, N. R. (2018, April). Effect of alkalinity and calcium concentration of pore solution on the swelling and ionic exchange of

superabsorbent polymers in cement paste. *Cement and Concrete Composites*, *88*, 150–164.

Ma, H., Qian, S., & Zhang, Z. (2014, October). Effect of self-healing on water permeability and mechanical property of medium-early-strength engineered cementitious composites. *Construction and Building Materials*, *68*, 92–101.

Ma, X., Liu, J., & Shi, C. (2019). A review on the use of LWA as an internal curing agent of high performance cement-based materials. *Construction and Building Materials*, *218*, 385–393.

Marar, K., Eren, Ö., & Çelik, T. (2001, February). Relationship between impact energy and compression toughness energy of high-strength fiber-reinforced concrete. *Materials Letters*, *47*(4–5), 297–304.

Masum, A. T. M., & Manzur, T. (2019, December). Delaying time to corrosion initiation in concrete using brick aggregate as internal curing medium under adverse curing conditions. *Construction and Building Materials*, *228*, 116772.

Mechtcherine, V., Dudziak, L., Schulze, J., & Staehr, H. (2006, January). Internal curing by super absorbent polymers (SAP)–Effects on material properties of self-compacting fibre-reinforced high performance concrete. *Proceedings of the International RILEM Conference—Volume Changes of Hardening Concrete: Testing and Mitigation* (pp. 87–96).

Mechtcherine, V., Gorges, M., Schroefl, C., Assmann, A., Brameshuber, W., Ribeiro, A. B., Cusson, D., Custódio, J., da Silva, E. F., Ichimiya, K., Igarashi, S.-I., Klemm, A., Kovler, K., de Mendonça Lopes, A. N., Lura, P., Nguyen, V. T., Reinhardt, H.-W., Filho, R. D. T., Weiss, J. . . . Zhutovsky, S. (2014). Effect of internal curing by using superabsorbent polymers (SAP) on autogenous shrinkage and other properties of a high-performance fine-grained concrete: Results of a RILEM round-robin test. *Materials and Structures*, *47*(3), 541–562.

Mechtcherine, V., Snoeck, D., Schröfl, C., De Belie, N., Klemm, A. J., Ichimiya, K., Moon, J., Wyrzykowski, M., Lura, P., Toropovs, N., Assmann, A., Igarashi, S.-I., De La Varga, I., Almeida, F. C. R., Erk, K., Ribeiro, A. B., Custódio, J., Reinhardt, H. W., & Falikman, V. (2018). Testing superabsorbent polymer (SAP) sorption properties prior to implementation in concrete: results of a RILEM Round-Robin Test. *Materials and Structures*, *51*(28), 1–16.

Mihashi, H., & Nishiwaki, T. (2012, May). Development of engineered self-healing and self-repairing concrete-state-of-the-art report. *Journal of Advanced Concrete Technology*, *10*(5), 170–184.

Nishiwaki, T., Koda, M., Yamada, M., Mihashi, H., & Kikuta, T. (2012). Experimental study on self-healing capability of FRCC using different types of synthetic fibers. *Journal of Advanced Concrete Technology*, *10*(6), 195–206.

Noushini, A., Samali, B., & Vessalas, K. (2013, December). Effect of polyvinyl alcohol (PVA) fibre on dynamic and material properties of fibre reinforced concrete. *Construction and Building Materials*, *49*, 374–383. https://doi.org/10.1016/j.conbuildmat.2013.08.035

Paipetis, A., Galiotis, C., Liu, Y. C., & Nairn, J. A. (1999, February). Stress transfer from the matrix to the fibre in a fragmentation test: Raman experiments and analytical modeling. *Journal of Composite Materials*, *33*(4), 377–399.

Paul, Á., & Lopez, M. (2011, July). Assessing lightweight aggregate efficiency for maximizing internal curing performance. *ACI Materials Journal*, *108*(4), 385–393.

Qian, S. Z., Zhou, J., & Schlangen, E. (2010, October). Influence of curing condition and precracking time on the self-healing behavior of engineered cementitious composites. *Cement and Concrete Composites*, *32*(9), 686–693.

Ranade, R., Stults, M. D., Li, V. C., Rushing, T. S., Roth, J., & Heard, W. F. (2011, December 12–14). *Development of high strength high ductility concrete*. 2nd International RILEM Conference on Strain Hardening Cementitious Composites, Rio de Janeiro, Brazil.

Roig-Flores, M., Pirritano, F., Serna Ros, P., & Ferrara, L. (2016, July). Effect of crystalline admixtures on the self-healing capability of early-age concrete studied by means of permeability and crack closing tests. *Construction and Building Materials*, *114*, 447–457. https://doi.org/10.1016/j.conbuildmat.2016.03.196

Şahmaran, M., Lachemi, M., Hossain, K. M., & Li, V. C. (2009, October). Internal curing of engineered cementitious composites for prevention of early age autogenous shrinkage cracking. *Cement and Concrete Research*, *39*(10), 893–901.

Sisomphon, K., Copuroglu, O., & Koenders, E. A. B. (2013, May). Effect of exposure conditions on self healing behavior of strain hardening cementitious composites incorporating various cementitious materials. *Construction and Building Materials*, *42*, 217–224.

Snoeck, D. (2015). *Self-healing and microstructure of cementitious materials with microfibres and superabsorbent polymers* [Doctoral dissertation, Ghent University]. http://hdl.handle.net/1854/LU-7010896

Su, Y.-F., Huang, C., Jeong, H., Nantung, T., Olek, J., Baah, P., & Lu, N. (2020). Autogenous healing performance of internal curing agent-based self-healing cementitious composite. *Cement and Concrete Composites*, *114*, 103825.

Subcommittee C09.64. (2019). *Standard test method for fundamental transverse, longitudinal, and torsional resonant frequencies of concrete specimens* (ASTM C215–19). ASTM International. http://www.astm.org/cgi-bin/resolver.cgi?C215-19

Termkhajornkit, P., Nawa, T., Yamashiro, Y., & Saito, T. (2009, March). Self-healing ability of fly ash–cement systems. *Cement and Concrete Composites*, *31*(3), 195–203.

Tu, W., Zhu, Y., Fang, G., Wang, X., & Zhang, M. (2018). Internal curing of alkali-activated fly ash-slag pastes using superabsorbent polymer. *Cement and Concrete Research*, *116*, 179–190.

Van Tittelboom, K., & De Belie, N. (2013). Self-healing in cementitious materials—A review. *Materials*, *6*, 2182–2217.

Van, V.-T.-A., Rößler, C., Bui, D.-D., & Ludwig, H.-M. (2014, July). Rice husk ash as both pozzolanic admixture and internal curing agent in ultra-high performance concrete. *Cement and Concrete Composites*, *53*, 270–278.

Yang, Y., Lepech, M. D., Yang, E.-H., & Li, V. C. (2009, May). Autogenous healing of engineered cementitious composites under wet–dry cycles. *Cement and Concrete Research*, *39*(5), 382–390.

Yıldırım, G., Keskin, Ö. K., Keskin, S. B., Şahmaran, M., & Lachemi, M. (2015). A review of intrinsic self-healing capability of engineered cementitious composites: Recovery of transport and mechanical properties. *Construction and Building Materials*, *101*(Part 1), 10–21.

Yoo, D.-Y., Kang, S.-T., & Yoon, Y.-S. (2014, August). Effect of fiber length and placement method on flexural behavior, tension-softening curve, and fiber distribution characteristics of UHPFRC. *Construction and Building Materials*, *64*, 67–81.

Yoo, D.-Y., Zi, G., Kang, S.-T., & Yoon, Y.-S. (2015, October). Biaxial flexural behavior of ultra-high-performance fiber-reinforced concrete with different fiber lengths

and placement methods. *Cement and Concrete Composites*, *63*, 51–66.

Zhang, J., Wang, Q., & Zhang, J. (2017, March). Shrinkage of internal cured high strength engineered cementitious composite with pre-wetted sand-like zeolite. *Construction and Building Materials*, *134*, 664–672.

Zhang, J., Zheng, X., & Wang, Q. (2018). Mixture optimization on internally cured high strength engineered cementitious composite with pre-wetted sand-like Zeolite. *Journal of Advanced Concrete Technology*, *16*(9), 485–497.

Zhang, Z., Qian, S., & Ma, H. (2014, February). Investigating mechanical properties and self-healing behavior of microcracked ECC with different volume of fly ash. *Construction and Building Materials*, *52*, 17–23.

Zhu, Q., Barney, C. W., & Erk, K. A. (2015). Effect of ionic crosslinking on the swelling and mechanical response of model superabsorbent polymer hydrogels for internally cured concrete. *Materials and Structures*, *48*(7), 2261–2276.

APPENDIX

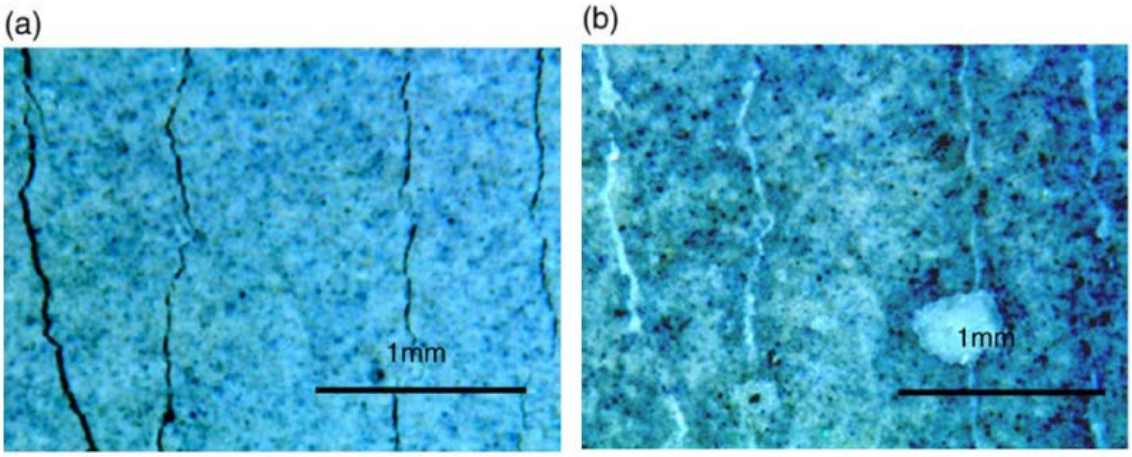

(a) Before self-healing (b) After self-healing

Figure A.1 Microcracks before and after self-healing (Yang et al., 2009).

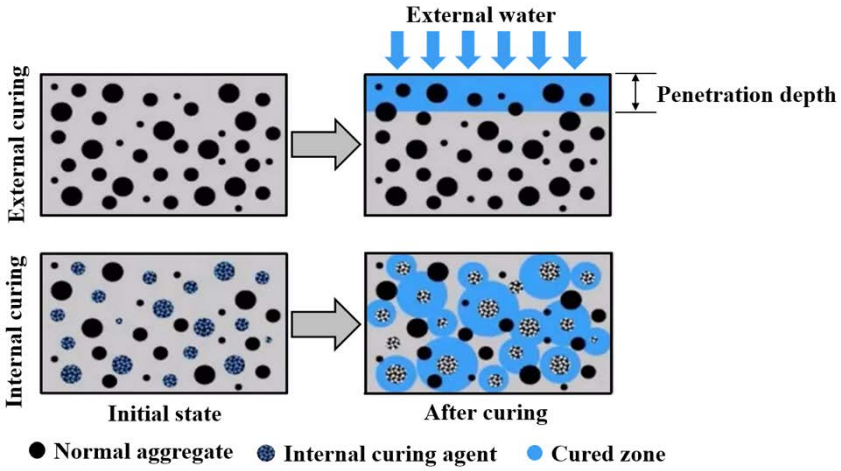

Figure A.2 Conceptual illustration of the differences between external and internal curing.

Figure A.3 Configuration of INDOT approved fibers.

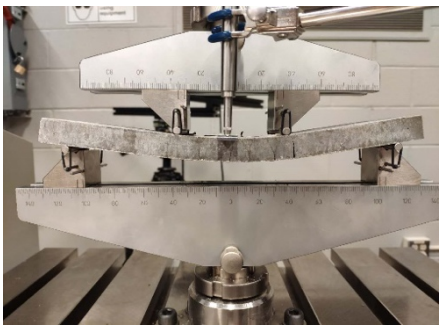

Figure A.4 Test setup for the flexural test.

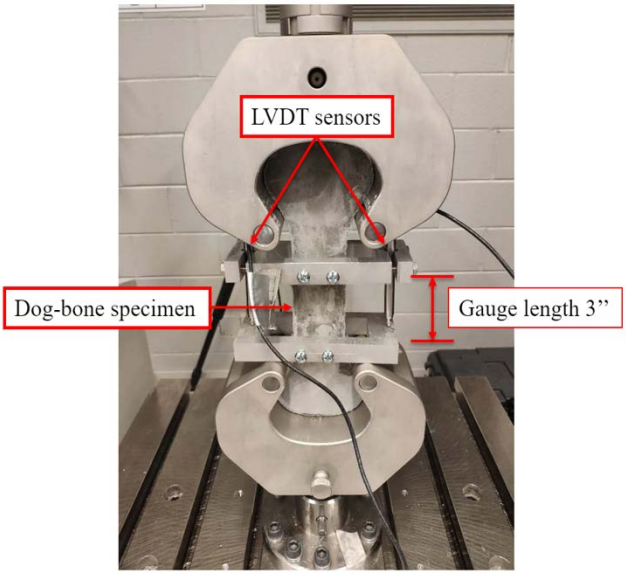

Figure A.5 Test setup for the uniaxial tensile test.

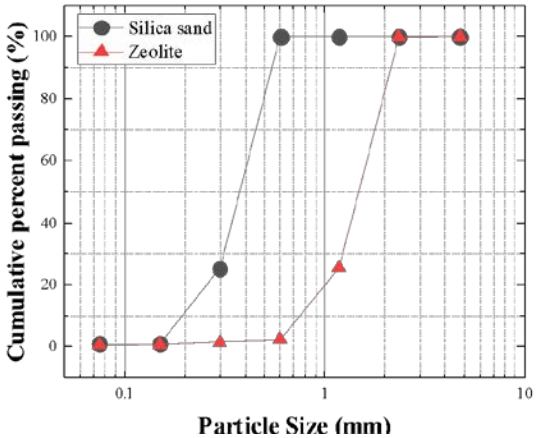

Figure A.6 Particle size distribution of zeolite and silica sand.

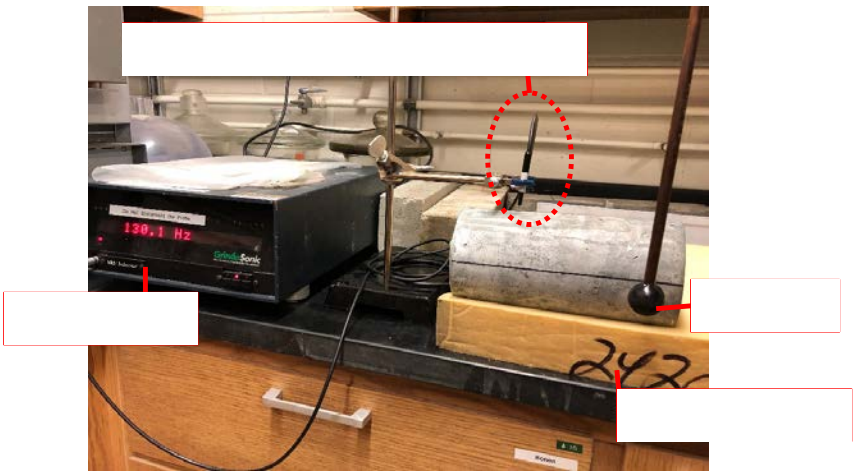

Figure A.7 Setup of resonant frequency test.

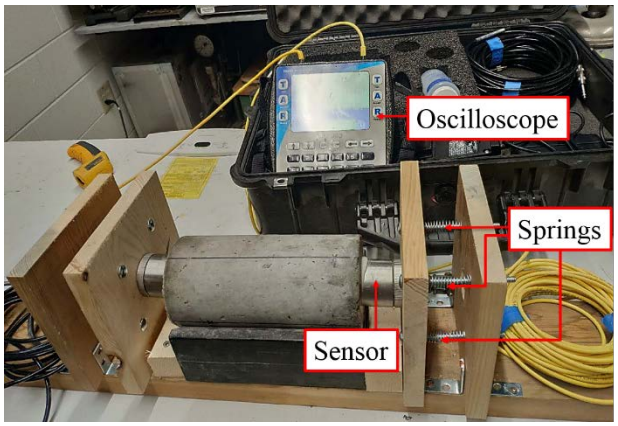

Figure A.8 Setup of ultrasonic velocity test.

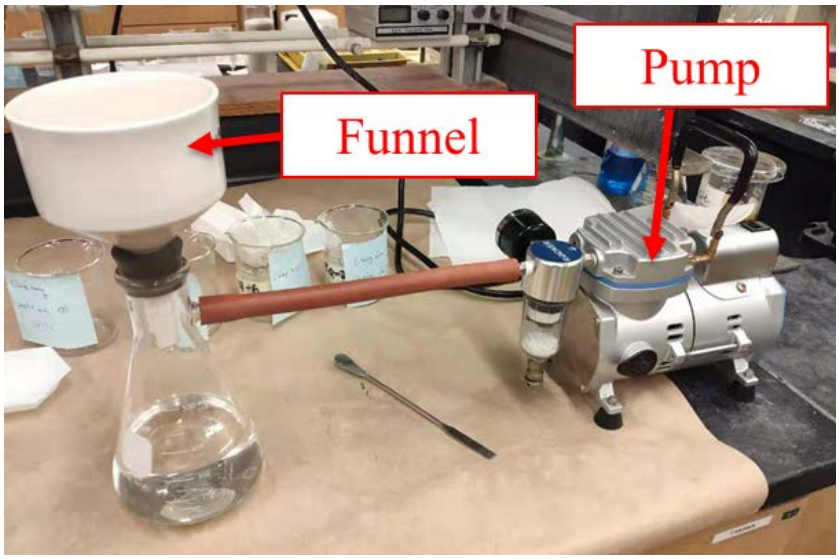

Figure A.9 Experimental setup for filtration test.

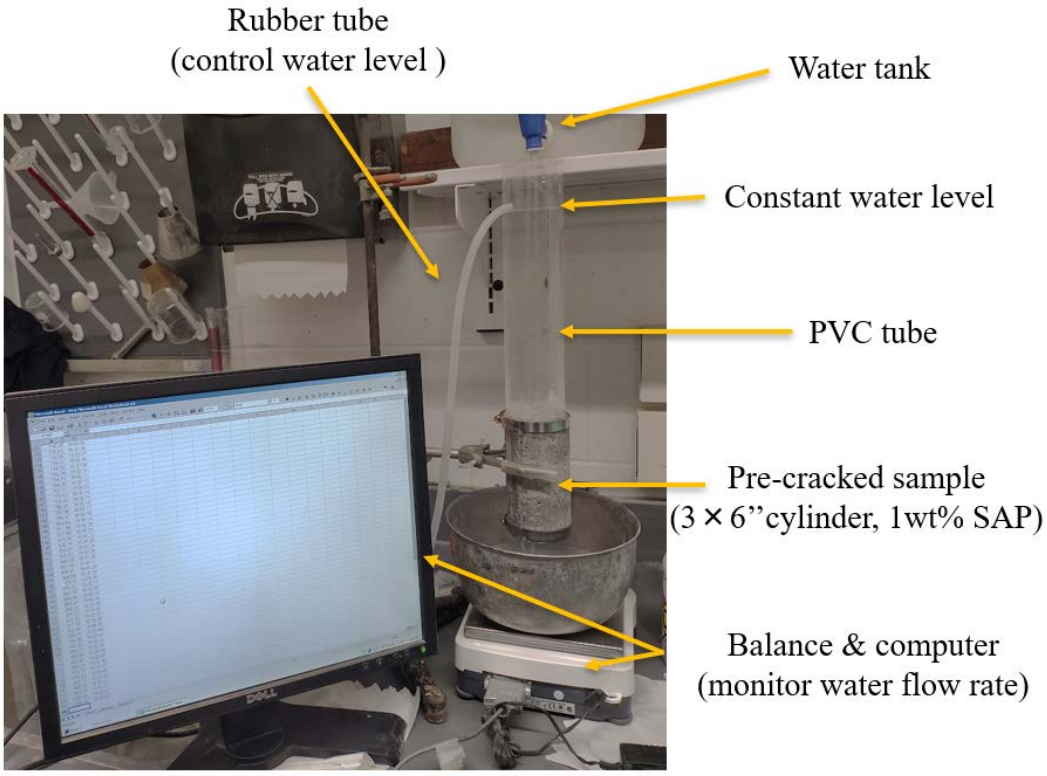

Figure A.10 Experimental setup for water flow test.

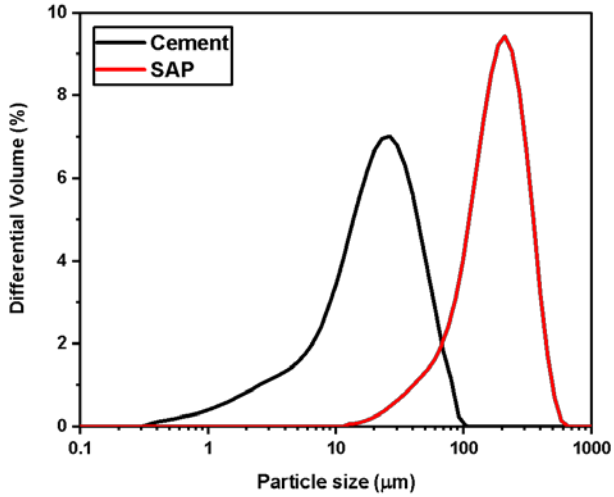

Figure A.11 Particle size distributions of the SAP and cement.

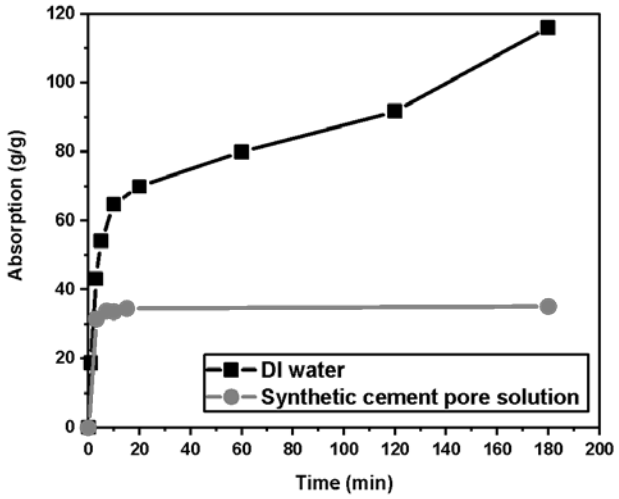

Figure A.12 Absorption behavior of the SAPs in DI water and synthetic cement pore solution.

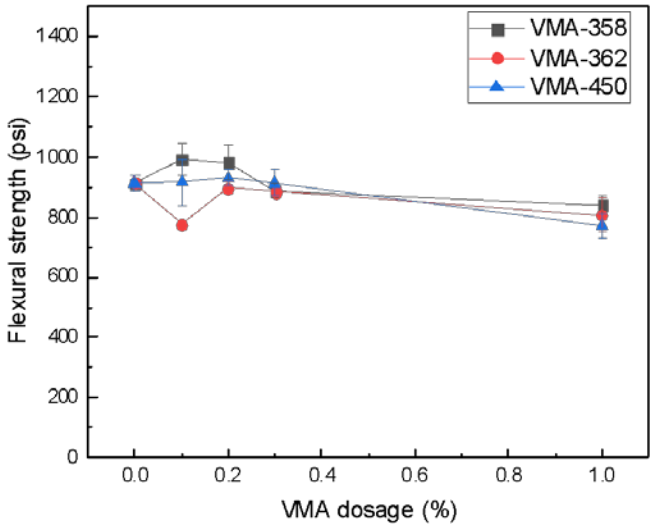

Figure A.13 Results of flexural strength with various configuration of VMA-SHCC with PVA fiber.

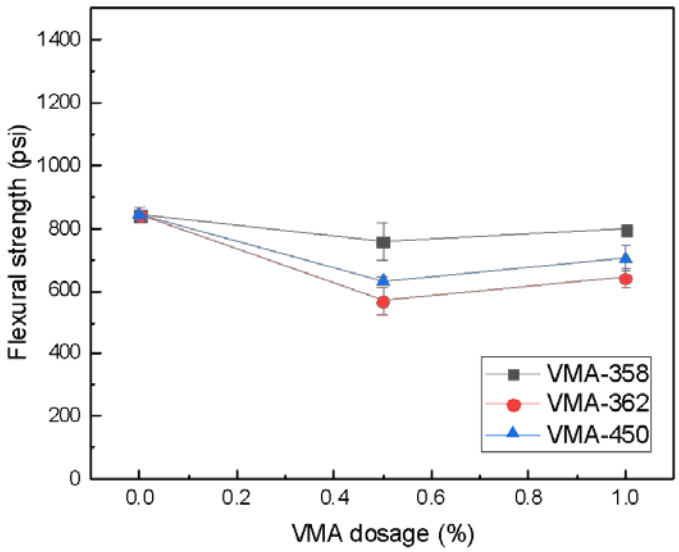

Figure A.14 Results of flexural strength with various configurations of VMA-SHCC with Strux fiber.

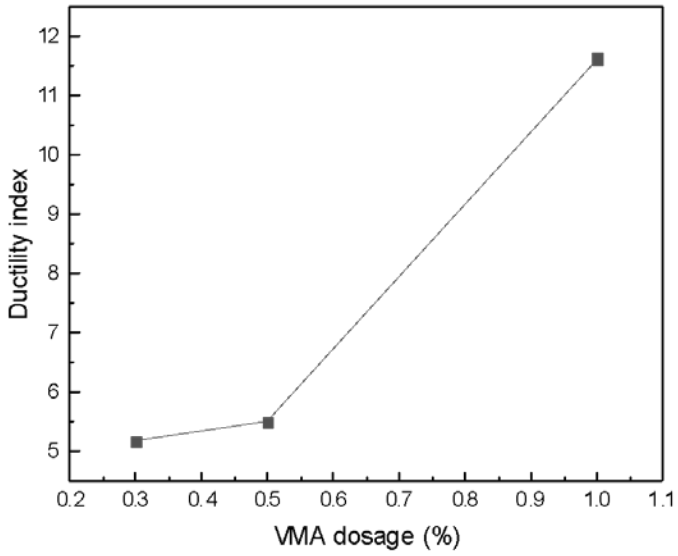

Figure A.15 Ductility index of PVA-SHCC with the various dosage of VMA 450.

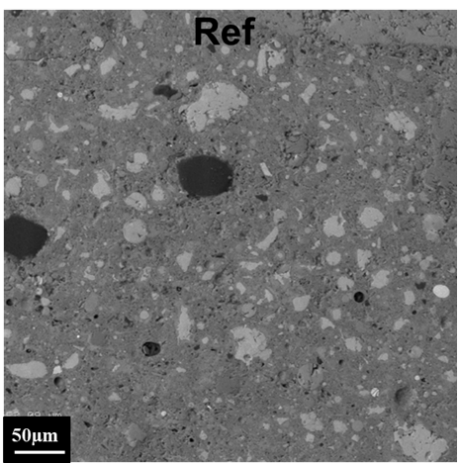

(a) Reference SHCC

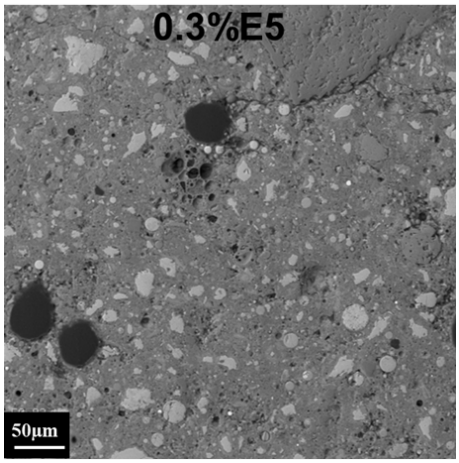

(b) 0.3%E5 SHCC

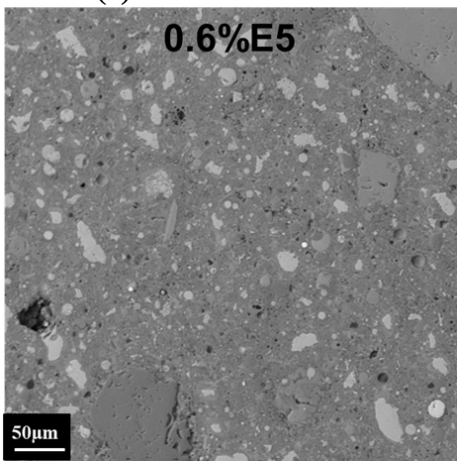

(c) 0.6 % E5 SHCC

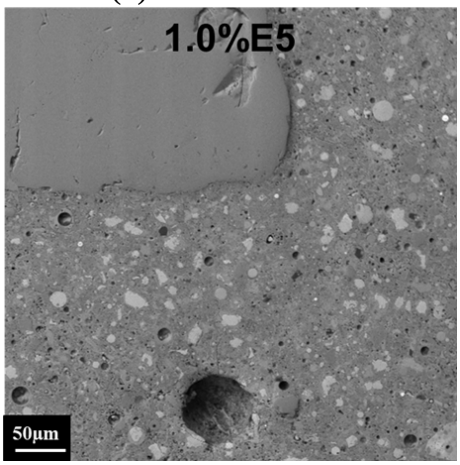

(d) 1% E5 SHCC

Figure A.16 Representative SEM images for SHCC specimens (after 21 W/D cycles).

Figure A.17 SHCC sample and flexural testing.

Table A.1 Material properties of the fibers

Fiber Name	Specific Gravity	Length (In)	Tensile Strength (MPA)	Aspect Ratio
PVA	1.3	0.3	1,600	205
Strux 90/40	0.92	1.55	620	90
Masterfiber Mac Matrix	0.91	2.1	585	70
Fiberforce 650	0.91	1.5	–	100
Tuf-Strand SF	0.92	2	625	74
Forta-Ferro One	0.91	2.25	615	–

Table A.2 Design of different layer structure of SHCC/Concrete beam

SHCC Layer (%)	Layer Structure Configuration
SHCC 100% (SHCC Reference)	SHCC-4″
SHCC 75%	Concrete-1″/SHCC-3″
SHCC 50%	Concrete-2″/SHCC-2″
SHCC 25%	Concrete-3″/SHCC-1″
SHCC 0% (Concrete Reference)	Concrete-4″

Table A.3 Unit price of raw materials

	Type I Cement	Natural Sand	Stone	Fly Ash	Granulated Slag	Silica Sand	Silica Fume	PVA	Steel Fiber
Unit price ($/ton)	~128	~17.5	~21.5	15~40	35–70	50–300	400–1,000	~17,085	2,800–13,300

Note: Table sources: The Aberdeen Group, 1985; Alibaba.com, n.d.; Clayworks Supplies, Inc., n.d.; *Condensed silica fume*, n.d.; FHWA, 2013; HomeAdvisor, n.d.; NYCON, n.d.; Van Oss, 2002; Reference.com, 2020; Statista, n.d.

Table A.4 Mixture designs of different types of concrete materials

	Cement (lb/cyd)	Natural Sand (lb/cyd)	Stone (lb/cyd)	Fly Ash (lb/cyd)	Silica Sand (lb/cyd)	Silica Fume (lb/cyd)	Fiber (vol%)
INDOT-564 (w/c = 0.42)	564	1,344	1800	–	–	–	–
SHCC (w/c = 0.35)	1,241	993	–	620	–	–	1
ECC (w/c = 0.30)	947	–	–	1,136	756	–	2
UHPC (w/c = 0.18)	1,718	–	–	–	1,306	447	2.5

APPENDIX REFERENCES

The Aberdeen Group. (1985). *Fly ash* [PDF file]. https://www.concreteconstruction.net/_view-object?id=00000153-8b9c-dbf3-a177-9fbd58630000

Alibaba.com. (n.d.). *Silica sand price per ton* [Webpage]. https://www.alibaba.com/showroom/silica-sand-price-per-ton.html

Clayworks Supplies, Inc. (n.d.). S*ilica sand bulk pricing–50 lb. bag* [Webpage]. https://clayworkssupplies.com/product/silica-sand-bulk-pricing/

Condensed silica fume. (n.d.). https://www.engr.psu.edu/ce/courses/ce584/concrete/library/materials/Altmaterials/Silica%20Fume.htm

FHWA. (2013, October). *Development of non-proprietary ultra-high performance concrete for use in the highway bridge sector* (Report Publication No. FHWA-HRT-13-100). Federal Highway Administration. https://www.fhwa.dot.gov/publications/research/infrastructure/structures/bridge/13100/index.cfm

HomeAdvisor. (n.d.). *How much does it cost to deliver topsoil, dirt, sand, mulch, or rock?* [Webpage]. https://www.homeadvisor.com/cost/landscape/deliver-soil-mulch-or-rocks/

NYCON. (n.d.). *RMS702* [Webpage]. https://nycon.com/products/rms702

Reference.com. (2020, April 9). *How much does silica sand cost?* https://www.reference.com/science/much-silica-sand-cost-d092088142328ed7

Statista. (n.d.) *Cement prices in the United States from 2010 to 2021* [Webpage]. https://www.statista.com/statistics/219339/us-prices-of-cement/

Van Oss, H. G. (2002). *Slag—Iron and steel* [PDF file]. U.S. Geological Survey Minerals Yearbook. https://s3-us-west-2.amazonaws.com/prd-wret/assets/palladium/production/mineral-pubs/iron-steel-slag/islagmyb02.pdf

About the Joint Transportation Research Program (JTRP)

On March 11, 1937, the Indiana Legislature passed an act which authorized the Indiana State Highway Commission to cooperate with and assist Purdue University in developing the best methods of improving and maintaining the highways of the state and the respective counties thereof. That collaborative effort was called the Joint Highway Research Project (JHRP). In 1997 the collaborative venture was renamed as the Joint Transportation Research Program (JTRP) to reflect the state and national efforts to integrate the management and operation of various transportation modes.

The first studies of JHRP were concerned with Test Road No. 1—evaluation of the weathering characteristics of stabilized materials. After World War II, the JHRP program grew substantially and was regularly producing technical reports. Over 1,600 technical reports are now available, published as part of the JHRP and subsequently JTRP collaborative venture between Purdue University and what is now the Indiana Department of Transportation.

Free online access to all reports is provided through a unique collaboration between JTRP and Purdue Libraries. These are available at http://docs.lib.purdue.edu/jtrp.

Further information about JTRP and its current research program is available at http://www.purdue.edu/jtrp.

About This Report

An open access version of this publication is available online. See the URL in the citation below.

Huang, C., Su, Y.-F., & Lu, N. (2021). *Self-healing cementitious composites (SHCC) with ultrahigh ductility for pavement and bridge construction* (Joint Transportation Research Program Publication No. FHWA/IN/JTRP-2021/36). West Lafayette, IN: Purdue University. https://doi.org/10.5703/1288284317403